BLENDING AND REACTIVE EXTRUSION OF POLYHYDROXYALKANOTES AND NOVEL ALIPHATIC POLYESTER ADDITIVES

by

COURTNEY MARIE KEELER

(Under the Direction of Jason Locklin)

ABSTRACT

Polyhydroxyalkanoates are a class of biodegradable polyester, typically produced by fermentation, that could be a viable replacement to some petroleum-based plastics. This polymer is attractive to research because it is biodegradable, biocompatible, and does not form any microplastics which are harmful to both human health and the environment. PHAs show much promise, but have several factors to overcome including cost, availability, slow nucleation, poor mechanical properties, and aging which decreases PHAs flexibility over time. In this study, the latter two issues are focused on, as several biobased aliphatic polyesters are evaluated as additives to polyhydroxyalkanoates (PHAs) with the goal of increasing flexibility and preventing secondary crystallization. Poly(3-hydroxybutyrate-co-3-hydroxyhexanoate) with 6% and 8% hexanoate are the two PHAs utilized in this project. Blending and reactive extrusion of these PHAs and additives include polylactide, peroxide radical initiator, and novel aliphatic copolyesters synthesized by polycondensation is explored.

INDEX WORDS: Biodegradable, polyhydroxyalkanoates, polyesters, extrusion, polycondensation, tensile testing

# BLENDING AND REACTIVE EXTRUSION OF POLYHYDROXYALKANOTES AND NOVEL ALIPHATIC POLYESTER ADDITIVES

by

**COURTNEY MARIE KEELER** 

BS, University of Montevallo, 2023

A Thesis Submitted to the Graduate Faculty of The University of Georgia in Partial Fulfillment of the Requirements for the Degree

MASTER OF SCIENCE

ATHENS, GEORGIA

2025

© 2025

Courtney Marie Keeler

All Rights Reserved

# BLENDING AND REACTIVE EXTRUSION OF POLYHYDROXYALKANOTES AND NOVEL ALIPHATIC POLYESTER ADDITIVES

by

## **COURTNEY MARIE KEELER**

Major Professor:

Committee:

Jason Locklin

Jeffrey Urbauer

I. Jonathan Amster

Electronic Version Approved:

Ron Walcott Vice Provost for Graduate Education and Dean of the Graduate School The University of Georgia May 2025

#### **DEDICATION**

I would like to take this time to thank all my family and friends who have supported me through my time at UGA. This experience has shaped me in many ways, and I am so grateful for the support system that has surrounded me over the past two years. I especially want to thank both of my parents who raised me into the person that I am today, both of my brothers for teaching many things about life, and both of my sisters-in-law for providing me support and encouragement. I want to thank all of the new friends that I have met here in the program who have both celebrated and commiserated with me. To my best friend from childhood, for checking in on me and being excited for me at every stage. To my fiancé, for supporting me on a daily basis. He has spent countless hours on the phone offering emotional support and keeping me grounded. He is my biggest supporter and continues to encourage me to chase my dreams every day.

Above all, I want to thank God and my church community for supporting my faith throughout this journey. The Lord has used this experience to shape me and give me a new perspective on life that I am grateful for. Leaning on my faith has helped me continue through the hard days, knowing that this is for His glory, and He has my future in His hands.

## **ACKNOWLEDGEMENTS**

I would like to take this opportunity to thank the many mentors who have helped me throughout this program and formed me into a better scientist. My committee members, professors, graduate coordinators, and lab mates have pushed me to become a better academic and trained me in many ways. I especially want to thank my lab mates for training me on countless techniques and instruments and encouraged me when I needed it. Next, I would like to thank the post-doctoral students who have given me so much guidance on various aspects of my projects, especially my mentor Grant. Above all, I want to thank my advisor Dr. Locklin for the countless guidance on my projects over the past year. He has encouraged me and pushed me, forming me into a scientist. He has challenged me and has been a great advisor!

Finally, I want to thank all my funding sources, especially my Graduate School Research and Scholarship Award which allowed me to focus on my research instead of teaching during my first year, a catalyst towards making progress on my projects.

## TABLE OF CONTENTS

		Page
ACKNO	WLEDGEMENTS	V
LIST OF	TABLES	viii
LIST OF	FIGURES	X
СНАРТЕ	ER	
1	Introduction to Polyhydroxyalkanoates and the Plastic Crisis	1
	1.1 Introduction	1
	1.2 Research Goals	8
	1.3 References	12
2	Reactive Extrusion of Polyhydroxyalkanoates and Polylactide to Improve	ve Tensile
	Properties	15
	2.1 Introduction	15
	2.2 Materials and Methods	24
	2.3 Results and Discussion	28
	2.4 Conclusions	47
	2.5 References	48
3	Polyester Synthesis to Understand Structure-Property Relationships	53
	3.1 Introduction	53

	3.2 Materials and Methods56
	3.3 Results and Discussion
	3.4 Conclusions 67
	3.5 References
4	Blending and Reactive Extrusion of Aliphatic Polyesters into Polyhydroxyalkanoates
	to Improve Mechanical Properties
	4.1 Introduction 70
	4.2 Materials and Methods74
	4.3 Results and Discussion
	4.4 Conclusions and Future Directions 94
	4.5 References96
5	Conclusions and future directions
	5.1 Conclusions 98
	5.2 Future Directions99
	5.3 Final Remarks99

## LIST OF TABLES

Page
Table 2.1: Five PLA-PHA blends compounded with 0.2 wt% LP during step 1 of workflow23
Table 2.2: The strain at break and Young's modulus of PHA6 and PHA8 with and without
LP29
Table 2.3: The gel fraction of several PHA samples extruded with various amounts of LP34
Table 2.4: The strain at break of the various PLA-PHA blends extruded into PHA635
Table 2.5: The strain at break of PHA8 and blends and improvement values compared to
control
Table 2.6: Impact testing data of PHA6 and PHA8 before and after REX42
Table 2.7: Concentration of Luperox P in (ppm) and the corresponding peak integration on
GC44
Table 2.8: Summary of residual LP in extruded samples post methanolysis
Table 3.1: List of homopolymers and copolymers synthesized via polycondensation reactions
61
Table 4.1: Six biobased polyesters that are evaluated as PHB-HHx additives72
Table 4.2: The results on different mold temperatures on strain at break
Table 4.3: The results from a small-scale extrusion study testing various polyester additives77
Table 4.4: Tensile testing results of 10, 20, and 30% polyester A loading into PHA678
Table 4.5: Tensile testing of blending vs. reactive extrusion of polyester A in PHA680
Table 4.6: Tensile results of blending and reactive extrusion of polyester B in PHA681

Table 4.7: Tensile results of blending polyester D, E, and F in PHA6	.83
Table 4.8: Tensile data from blending and reactive extrusion of polyesters A and B in PHA8	.87
Table 4.9: Tensile results of 10, 20, and 30 wt% loadings of polyester E in PHA8	.88
Table 4.10: Blending of D, E, and F in PHA8 at 10% loading	.89

## LIST OF FIGURES

Pag
Figure 1.1: Microplastics have been linked to higher rates of cancer in both male and female
humans.
Figure 1.2: Depiction of several copolymers of PHA formed through fermentation
Figure 1.3: Breakdown of the costs associated with PHA production.
Figure 1.4: Graphic of a spherulite.
Figure 1.5: Depiction of the regions of a spherulite, illustrating the crystalline lamella and
amorphous regions that embrittle due to aging
Figure 1.6: Schematic of twin screw extruder.
Figure 1.7: Depiction of the blending of two polymers versus reactive extrusion of two polymers
Figure 2.1: Depiction of the meso-lactide that ring opens to form PLA.
Figure 2.2: Chemical structure of poly(3-hydroxybutyrate-co-3-hydroxyhexanoate)
Figure 2.3: Polylactide reactive extrusion to induce a hardening effect
Figure 2.4: The thermal initiation and homolytic cleavage of tert-butyl peroxybenzoate19
Figure 2.5: Hydrogen abstraction of hydrogen on the backbone of PHA.
Figure 2.6: Blending of PLA into PHA (top) compared to the 2-step extrusion process in which a
pre-compatibilization step is done first (bottom)
Figure 2.7: Workflow depicting two steps of reactive extrusion in the Process 11 and flushing
through the Haake into Minijet injection molder to create tensile samples2

Figure 2.8: Depiction of stress-strain graph obtained from a tensile strength test	22
Figure 2.9: Depiction of PHA blended into PLA with and without the presence of a radical	
initiator2	23
Figure 2.10: Cartoon depiction of step 2 in the extrusion workflow.	24
Figure 2.11: Comparison of the strain at break and Young's modulus of PHA6 and PHA8 with	
and without the presence of LP.	30
Figure 2.12: SSA thermogram overlay of PHA6 control and PHA6 REX samples	31
Figure 2.13: Subtraction of PHA6 control SSA and PHA6, 0.5 wt% LP REX SSA	32
Figure 2.14: SSA thermogram overlay of PHA8 control and PHA8 REX samples	33
Figure 2.15: Visual graphic showing the trend of gel fraction with increasing LP wt%	34
Figure 2.16: Tensile data for PHA6 samples including PHA6 neat, PHA6 REX, PLA blended	
into PHA, and PHA6 with 10% of each of the five formulations from step one	36
Figure 2.17: The aging of PHA6 vs. the aging of 2PHA <sub>8</sub> /8PLA in PHA6 (at 10% abundance)3	37
Figure 2.18: Bar graph displaying strain at break and error of PHA8 control groups and PLA-	
PHA blends in PHA8.	39
Figure 2.19: PHA8 aging vs. 10% PLA REX in PHA8 aging	40
Figure 2.20: The relationship between molecular weight of PHA and abundance of LP during	
extrusion	41
Figure 2.21: The relationship between PLA 4950D molecular weight and concentration of LP in	n
the extruder.	42
Figure 2.22: The effect of reactive extrusion on PHA6 and PHA8 impact strength	43
Figure 2.23: Homolytic cleavage followed by methanolysis of tert-butyl peroxybenzoate	44
Figure 2.24: Standard curve of Lunerox P	45

Figure 3.1: Types of degradation for polymers that are biodegradable	53
Figure 3.2: Esterification and polycondensation scheme for a dicarboxylic acid and di-	
alcohol	55
Figure 3.3: Structures of monomers used for polycondensation polymerization reactions	56
Figure 3.4: The reactor setup for polycondensation.	57
Figure 3.5: The odd-even effect in various polymers.	59
Figure 3.6: Odd-even versus even-even for polybutylene azelate and polybutylene sebacate	60
Figure 3.7: The relationship between carbon length in backbone of diacid monomer and me	lting
point is shown.	63
Figure 3.8: Thermogram overlay of multiple polyesters synthesized	64
Figure 3.9: Melting and cooling DSC curves for three copolyesters	66
Figure 4.1: Structure of poly(3-hydroxybutyrate-co-3-hydroxyhexanoate)	70
Figure 4.2: The workflow for using biobased long chain polyester as additives in PHA	72
Figure 4.3: Monomer components of "polyester A."	78
Figure 4.4: Exploring different loadings of polyester A in PHA6	79
Figure 4.6: Strain at break for polyester A blending and reactive extrusion in PHA6	80
Figure 4.7: Structural components of polyesters B and C.	81
Figure 4.8: Tensile results of blending and reactive extrusion of polyester B in PHA6	82
Figure 4.9: The structural components of polyesters D, E, and F.	83
Figure 4.10: Tensile results of blending polyester D, E, and F in PHA6.	84
Figure 4.11: The aging of PHA6 compared to the aging of 10% A in PHA6 REX	85
Figure 4.12: DSC thermograms for 10% polyester A in PHA6 on day 1 (blue) and day 4	
(green)	86

Figure 4.13: Tensile data from blending and reactive extrusion of polyesters A and B in PHA8.
87
Figure 4.14: Exploring different loadings of polyester E in PHA8
Figure 4.15: Blending of D, E, and F in PHA8 at 10% loading90
Figure 4.16: Aging data of 10% E and 10% A in PHA8 as compared to the control PHA891
Figure 4.17: DSC thermograms of 10% polyester A in PHA8 REX on day 1 (green) and day 7
(blue)91

#### CHAPTER 1

## INTRODUCTION TO POLYHYDROXYALKANOATES AND THE PLASTIC CRISIS

## 1.1 Introduction

The field of polymer chemistry began in the early 1900s when scientists such as Leo Baekeland, Wallace Carothers, Hermann Staudinger, and Stephanie Kwolek began researching synthetic alternatives to natural materials and fibers, such as silk and rubber. Nylon and synthetic polyisoprene are two advances that helped mitigate shortages caused by the world wars in the first half of the 20<sup>th</sup> century. Since then, polymers and plastics have shaped the landscape of the modern world. From sterile medical devices made of plastic, to long lasting tires for vehicular transportation, and high-performance piping to carry fresh water long distances, the current society simply could not continue without the use of plastic. Despite the benefits associated with plastic, there is a negative side that is recently coming to light. From pollution of plastics in the ocean due to the fishing industry (great pacific garbage patch), the impact of microplastics in the soil (agricultural impact), and the bioaccumulation of microplastics in living organisms (cancer, reduced fertility), there are many reasons to support a biocompatible alternative to current petroleum-based polymers.

Although synthetic polymers were not discovered until the 20<sup>th</sup> century, natural polymers such as proteins, polysaccharides, and other macromolecules were discovered in the early 1800s. These natural polymers act as building blocks for life, and many synthetic rubbers are inspired by nature such as synthetic rubber and synthetic ivory (cellulose nitrate). Petroleum-based plastics entered the scene in 1907 with Bakelite, and continued to expand with polyethylene,

polypropylene, and many more that used waste material from the fuel industry. Petroleum based plastics were truly a miracle of science: they were an incredibly cheap material since they were sourced from waste material that could be upcycled into usable materials that were heat resistant, flexible, and strong. The age of plastic took off from there to shape society as we know it, taking over many industries such as the textile industry (nylon, polyesters), medical industry (joint replacement, syringes, medical tubing), and commodity industry (shopping bags, food packaging, home decorations). It was only until much after the plastic boom that humans noticed negative environmental and biological effects. Many applications of plastics are single use, meaning minutes after being used, they are tossed into landfills or littered into the environment. Not only do these materials take hundreds of years to break down, but they also leach microplastics in the process, as well as any additives such as plasticizers that can cause detrimental ecological impact.

## 1.1.1 Microplastics

Microplastics are defined by the EPA as plastics that have eroded in size down to five millimeters to one nanometer in size. Although microplastics are physically smaller in size, they still maintain their high molecular weight, indicating that they are not degrading overtime.

Microplastics are problematic not only to wildlife but also studies have been to show detrimental effects to human health. Microplastics are associated with decreased fertility and higher rates of cancer. 2

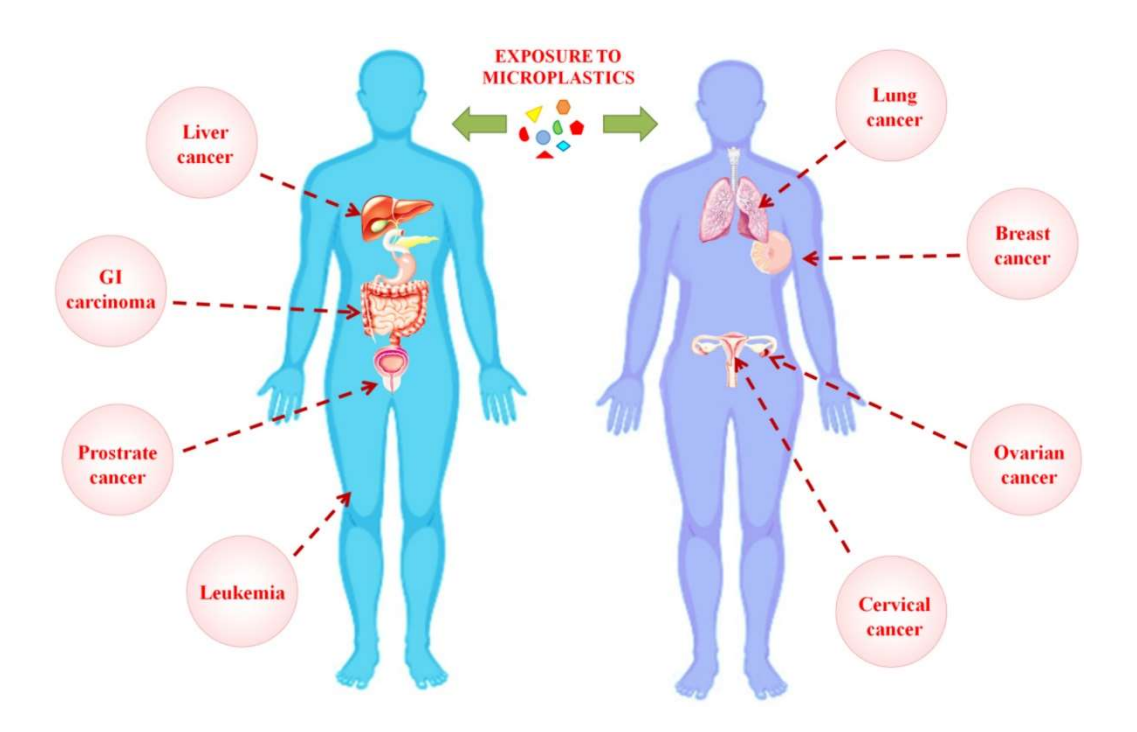


Figure 1.1 Microplastics have been linked to higher rates of cancer in both male and female humans.<sup>2</sup>

The concern of microplastic leaching is not only affecting the environment but also directly affecting humans because of the uptake of microplastics in the soil, it being found in drinking water, and it being found in human tissue. Higher rates of cancer have been noted in many studies, and fertility is also being negatively affected.<sup>2, 3</sup> Pollution of plastics has become a major issue as well as seen with the Great Pacific Garbage Patch, and landfills are starting to fill up in major cities.<sup>4</sup> With all of these problems with petroleum-based plastics, it is physically not possible for our current society to simply stop using them all together. Recycling is a well-intentioned idea, but not efficient enough to combat these issues. Mechanical recycling is too expensive, and the plastic produced at the end of the process is of a lower grade and must be used for a different application.<sup>5</sup> Chemical recycling is slightly more promising due to its ability to return to pure monomer, but it is once again costly and not feasible for many plastics, especially copolymers and blends.<sup>5</sup> These issues could slowly kill the planet as we know it until

evolution can develop some sort of enzyme to adapt against these persistent plastics in the environment.

## 1.1.2 Biobased Polymers

Keeping these issues in mind, let's turn our attention to biobased polymers as an alternative to petroleum-based polymers. Biobased polymers are defined as polymers harvested from biological sources (fermentation) or polymers synthesized from monomers derived from biobased sources. These biopolymers have a tall order to fill – not only will they need to compete with an incredibly inexpensive material, but petroleum-based plastics also have great physical properties, heat tolerance and solvent resistance. These properties are difficult to replicate as seen in the current biopolymer alternatives on the market. Polylactide (PLA) is one example of a biobased polymer currently available on a commercial scale. PLA can be produced through either fermentation or through synthetic polymerization of either ring opening of lactide, or polycondensation of lactic acid. The resulting polymer is fully biobased, however cannot biodegrade in ambient conditions. PLA is industrially compostable, meaning elevated temperatures and proper tumbling of the compost must be done to promote degradation, and it can also be chemically recycled.<sup>8</sup> This is much better than discarding these products in the landfill, and either way it still decreases the volume of plastics in the system being produced from petroleum. Currently on the market there are companies producing PLA based single use products such as plastic cutlery and take out containers, and it is also seen as a biobased garden tarp for agriculture uses. Despite this, PLA tends to be more expensive and is quite brittle. Additionally, it is only industrially compostable rather than home compostable or biodegradable. PBAT, poly(butylene adipate-co-terephthalate) is another biobased polymer on the market that is used for flexible films for food packaging and biodegradable grocery bags. 9 Once again, PBAT

is industrially compostable, which is a step in the right direction, however it is still desirable to obtain a material that is home compostable and biodegradable in the environment including soil and marine.

This brings the discussion to polyhydroxyalkanoates (PHAs). PHAs are a class of polyesters that are usually formed through the fermentation of microorganisms. <sup>10</sup> Under the right conditions and with genetic modification, these microorganisms can produce a high molecular weight polyester that can be harvested from cells and processed. Genetically manipulating the bacteria and changing the feedstock in the fermentation reactors can induce copolymers to form. Usually, PHB (polyhydroxybutyrate) is the dominant polymer, but by manipulating genetics and feed stock, copolymers can form, having drastically different properties than PHB. <sup>11</sup> These copolymers are desirable due to lower crystallinity and brittleness, yielding more flexible products. The ratio of these copolymers can be varied to induce a change in the physical

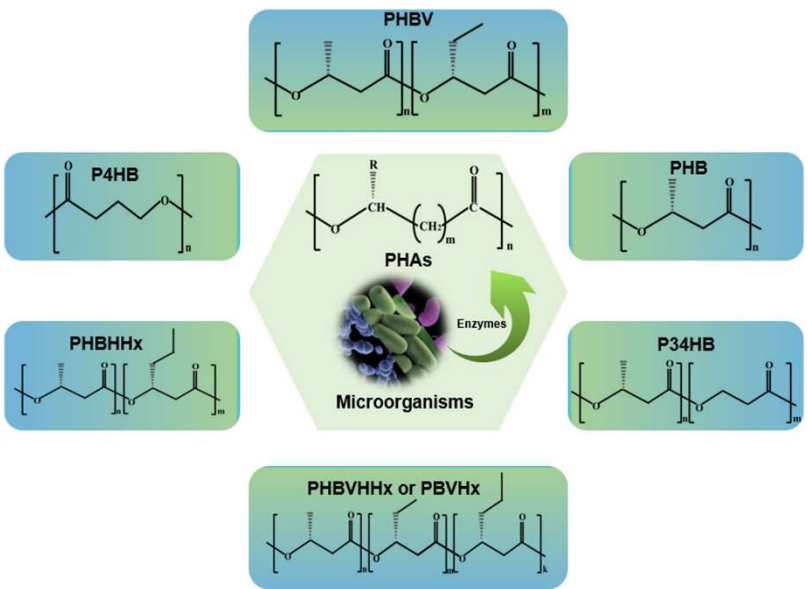


Figure 1.2. Depiction of several copolymers of PHA formed through fermentation. 12

properties of the final polymer. Furthermore, PHAs are completely biodegradable and home compostable. With all the positives of PHA, why is it not commonly and abundantly found commercially? The main hinderances to PHA include high cost, slow crystallization and nucleation, poor mechanical properties, and aging overtime.<sup>13</sup>

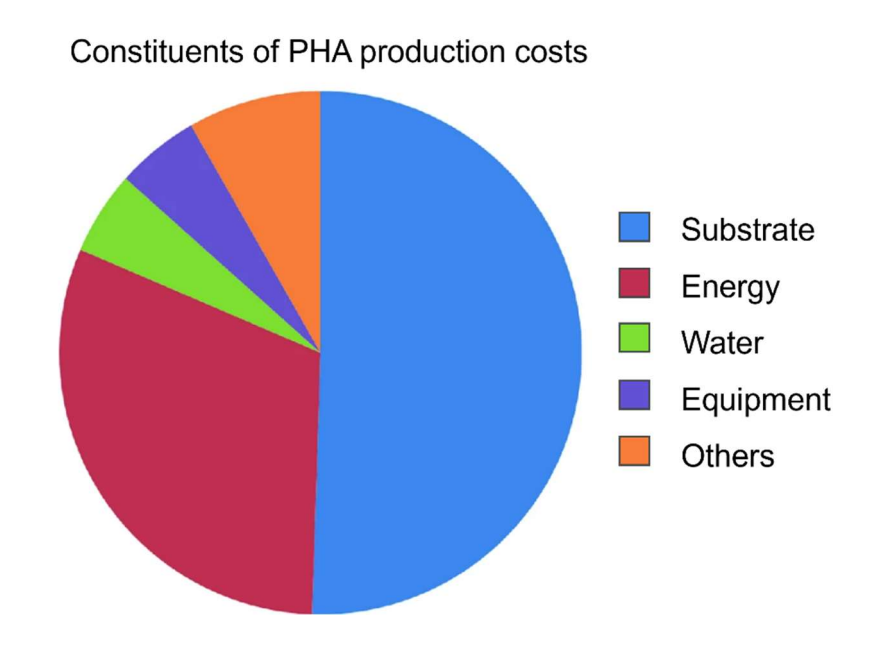


Figure 1.3. Breakdown of the costs associated with PHA production. 14

As seen in figure 1.3, a huge amount of money is invested in generating and genetically modifying microorganism substrates. In addition to this, there is a large amount of energy required to keep the reactors at the ideal temperature for fermentation. Not to mention the costs of the fermentation reactors and the cost of the feedstock.

## 1.1.3 Areas of Improvement

Slow crystallization and poor nucleation are two additional issues that hinder PHA from being a viable commercial alternative to petroleum-based plastics. In an industrial setting, polymers must be able to crystallize in molds quickly, usually in a matter of millisecond, to make many products per minute and turn a profit. PHA has slow and broad crystallization that hinders

its ability to be industrially viable without additives such as nucleating agents. <sup>15</sup> Nucleating agents increase the speed at which spherulites form and decrease the size of the spherulites, improving the crystallization of PHA. <sup>15</sup> Polymers crystallize differently than small molecules. Rather than a single unit cell crystal, polymers crystallize outwards from a single crystal nucleus in a spherulitic fashion. These spherulites contain crystalline regions and amorphous regions, giving polymers their unique properties.

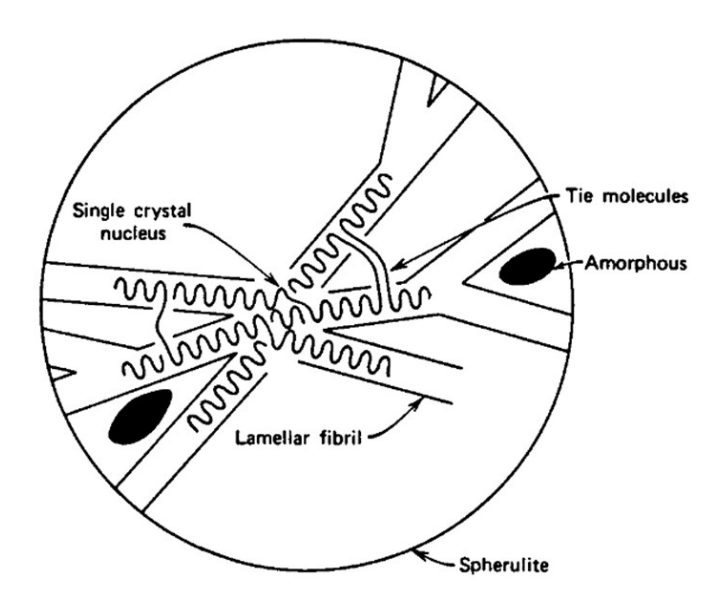


Figure 1.4. Graphic of a spherulite. 16

In addition to poor crystallization and high costs, PHA has issues with mechanical performance and aging overtime. PHA is known to be brittle and becomes even more brittle overtime due to secondary crystallization. Secondary crystallization is a process in which the amorphous regions of the spherulite begin to rearrange into a more crystalline formation, leading to embrittlement.

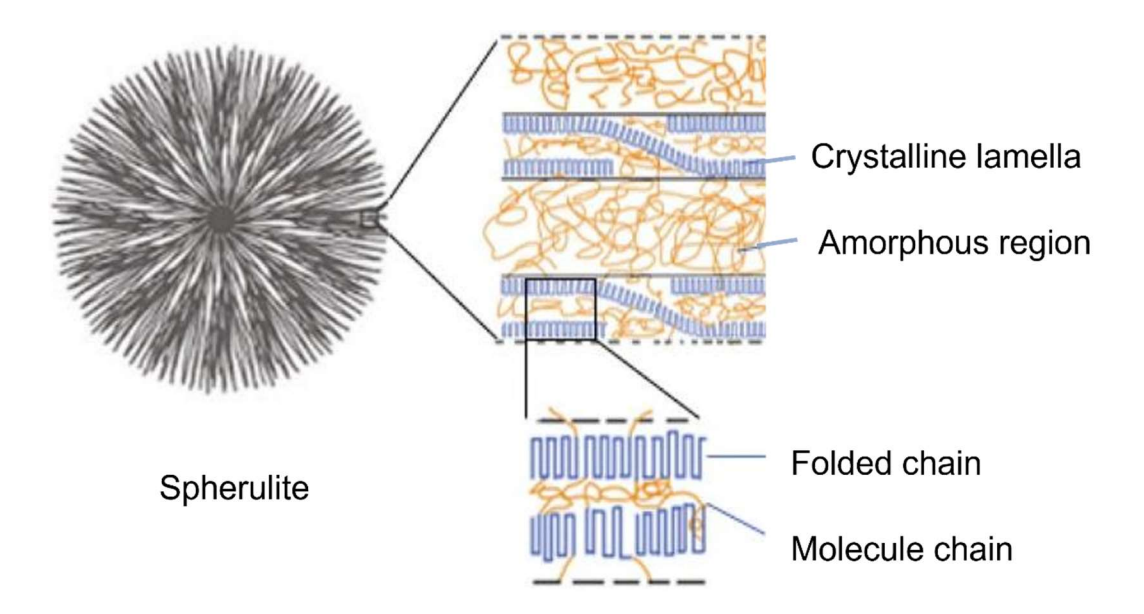


Figure 1.5. Depiction of the regions of a spherulite, illustrating the crystalline lamella and amorphous regions that embrittle due to aging.<sup>17</sup>

This is problematic due to the decrease in mechanical properties that this brings about. This influences the shelf-life and stability of properties.

## 1.2 Research Goals

This document aims to improve two of the issues with PHA that has been laid out in the above: improve the poor mechanical properties of PHA and mitigate the negative effects of aging. This is done by blending and reactive extrusion of poly(3-hydroxybutyrate-co-3-hydroxyhexanoate) with various additives such as a radical initiator and several aliphatic biobased polyesters. Extrusion is the process in which polymer material, either resins, pellets, or powders, are melted, sheared through screws, and comes out a die.<sup>18</sup>

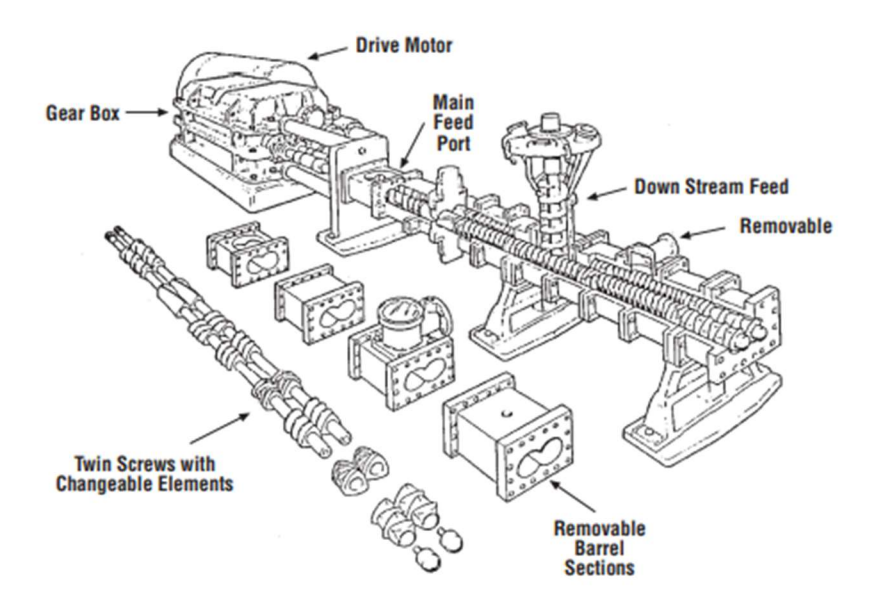


Figure 1.6. Schematic of twin screw extruder. 19

Extrusion is an effective way to blend multiple polymers to create a cohesive and thoroughly mixed plastic. Reactive extrusion is a technique in which the extruder is viewed as a reactor vessel rather than just a machine to process material. In reactive extrusion, post polymerization modifications, grafting, and crosslinking can be done through the addition of radical initiators. <sup>18</sup> Radical initiators can scavenge radicals from the backbone of a polymer, leading to an opportunity for crosslinking to occur between two radicals on the backbone meeting and forming a covalent bond. Reactive extrusion can also compatibilize two polymers and form a more cohesive blend, as shown in figure 1.7.

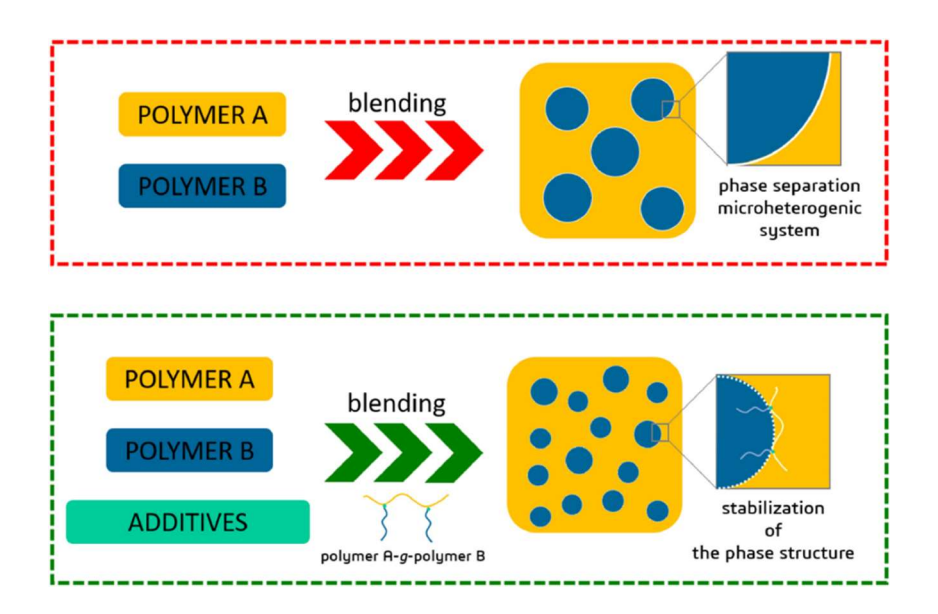


Figure 1.7. Depiction of the blending of two polymers versus reactive extrusion of two polymers. The above figure shows that compatibilizing two polymers, although they may be immiscible, can stabilize the interphase structure. This could lower the energy difference between the two phases of polymers, leading to a polymer with better properties.

Although there are multiple areas for polyhydroxyalkanoate improvement, this document focuses on the poor mechanical properties and the aging issues. These problems are tackled with reactive extrusion of PHA using the radical initiator tert-butyl peroxybenzoate, with the goal of lightly crosslinking the PHA to improve mechanical properties. Reactive extrusion of PHA is also done in the presence of PLA via a two-step extrusion process in an effort to compatibilize the two polyesters, leading to better properties than simple blending. In addition to studies of PHA and PLA reactive extrusion, other biobased polyester additives that are synthesized inhouse are assessed as PHA additives to improve flexibility. These polyester additives are synthesized through a bulk polycondensation process and vary from simple polyesters to more complex copolymers. The synthesized polymers are characterized by NMR to determine copolymerization ratios, DSC to determine thermal properties, and some undergo extrusion and

injection molding to access tensile properties. From this library of polyesters, a select group is evaluated as PHA additives in both blending and reactive extrusion studies.

#### 1.3 References

- (1) Service, N. O. *What are microplastics*. National Oceanic and Atmospheric Administration, <a href="https://oceanservice.noaa.gov/facts/microplastics.html">https://oceanservice.noaa.gov/facts/microplastics.html</a> (accessed 2025.
- (2) Goswami, S.; Adhikary, S.; Bhattacharya, S.; Agarwal, R.; Ganguly, A.; Nanda, S.; Rajak, P. The alarming link between environmental microplastics and health hazards with special emphasis on cancer. *Life Sciences* **2024/10/15**, *355*. DOI: 10.1016/j.lfs.2024.122937.
- (3) Lebreton, L.; Slat, B.; Ferrari, F.; Sainte-Rose, B.; Aitken, J.; Marthouse, R.; Hajbane, S.; Cunsolo, S.; Schwarz, A.; Levivier, A.; et al. Evidence that the Great Pacific Garbage Patch is rapidly accumulating plastic. *Scientific Reports 2018 8:1* **2018-03-22**, *8* (1). DOI: 10.1038/s41598-018-22939-w.
- (4) Siddiqua, A.; Hahladakis, J. N.; Al-Attiya, W. A. K. A. An overview of the environmental pollution and health effects associated with waste landfilling and open dumping. *Environmental Science and Pollution Research International* **2022 Jul 1**, *29* (39). DOI: 10.1007/s11356-022-21578-z.
- (5) Schyns, Z. O. G.; Shaver, M. P. Mechanical Recycling of Packaging Plastics: A Review. *Macromolecular Rapid Communications* **2021/02/01**, *42* (3). DOI: 10.1002/marc.202000415.
- (6) Bio-Based Polymer an overview | ScienceDirect Topics. *Encyclopedia of Renewable and Sustainable Materials* **2020**. DOI: 10.1016/B978-0-12-803581-8.11521-8.
- (7) Oksiuta, Z.; Jalbrzykowski, M.; Mystkowska, J.; Romanczuk, E.; Osiecki, T. Mechanical and Thermal Properties of Polylactide (PLA) Composites Modified with Mg, Fe, and Polyethylene (PE) Additives. *Polymers* **2020 Dec 9**, *12* (12). DOI: 10.3390/polym12122939.

- (8) McGuire, T. M.; Buchard, A.; Williams, C. Chemical Recycling of Commercial Poly(l-lactic acid) to l-Lactide Using a High-Performance Sn(II)/Alcohol Catalyst System. *Journal of the American Chemical Society* **September 1, 2023**, *145* (36). DOI: 10.1021/jacs.3c05863.
- (9) Jian, J.; Xiangbin, Z.; Xianbo, H. An overview on synthesis, properties and applications of poly(butylene-adipate-co-terephthalate)–PBAT. *Advanced Industrial and Engineering Polymer Research* **2020/01/01**, *3* (1). DOI: 10.1016/j.aiepr.2020.01.001.
- (10) Zytner, P.; Zytner, P.; Kumar, D.; Kumar, D.; Elsayed, A.; Elsayed, A.; Mohanty, A.; Mohanty, A.; Ramarao, B. V.; et al. A review on polyhydroxyalkanoate (PHA) production through the use of lignocellulosic biomass. *RSC Sustainability* **2023/11/30**, *I* (9). DOI: 10.1039/D3SU00126A.
- (11) Chandra, R.; Thakor, A.; Mekonnen, T. H.; Charles, T. C.; Lee, H.-S. Production of polyhydroxyalkanoate (PHA) copolymer from food waste using mixed culture for carboxylate production and Pseudomonas putida for PHA synthesis. *Journal of Environmental Management* **2023/06/15**, *336*. DOI: 10.1016/j.jenvman.2023.117650.
- (12) Liu, J.; Zhou, Z.; Li, H.; Yang, X.; Wang, Z.; Xiao, J.; Wei, D.-X. Current status and challenges in the application of microbial PHA particles. *Particulogy* **2024/04/01**, *87*. DOI: 10.1016/j.partic.2023.08.011.
- (13) S, C.; B, Y.; RD, T.; P, D. A review on production of polyhydroxyalkanoate (PHA) biopolyesters by thermophilic microbes using waste feedstocks PubMed. *Bioresource technology* **2021 Dec**, *341*. DOI: 10.1016/j.biortech.2021.125900.
- (14) Gahlawat, G. Challenges in PHAs Production at Mass Scale. *SpringerBriefs in Molecular Science* **2019**. DOI: 10.1007/978-3-030-33897-8\_3.

- (15) Bledsoe, J. C.; Crane, G. H.; Locklin, J. J. Beyond Lattice Matching: The Role of Hydrogen Bonding in Epitaxial Nucleation of Poly(hydroxyalkanoates) by Methylxanthines. *ACS Applied Polymer Materials* **April 13, 2023**, *5* (5). DOI: 10.1021/acsapm.3c00494.
- (16) Harwood, H. J. Principles of polymerization(Odian, George). *Journal of Chemical Education* **1971**, *48* (11), A734. DOI: 10.1021/ed048pA734.1.
- (17) Wang, A.; Chen, C.; Liao, L.; Qian, J.; Yuan, F.-G.; Zhang, N.; Wang, A.; Chen, C.; Liao, L.; Qian, J.; et al. Enhanced β-Phase in Direct Ink Writing PVDF Thin Films by Intercalation of Graphene. *Journal of Inorganic and Organometallic Polymers and Materials 2019 30:5* **2019-09-27**, *30* (5). DOI: 10.1007/s10904-019-01310-0.
- (18) Lambla, M. Reactive Extrusion. *Rheological Fundamentals of Polymer Processing* **1995**. DOI: 10.1007/978-94-015-8571-2 20.
- (19) John Goff, T. W. *The Dynisco Extrusion Processors Handbook*; DeLaney, D., Ed.; Vol. 2nd edition; Dynisco, 1983.

#### CHAPTER 2

# REACTIVE EXTRUDION OF POLYHYDROXYALKANOATES AND POLYLACTIDE TO IMPROVE TENSILE PROPERTIES

## 2.1 Introduction

The introduction chapter of this thesis displayed the environmental dangers of petroleumbased plastics and the issues with current biobased alternatives. Between the increasing size of the Great Pacific Garbage Patch to the health and environmental concerns of microplastics, finding biodegradable alternatives are a necessary area of research. 1-4 This sets the scene for the motivation behind the research contained in this chapter: to improve the current bio-based and biodegradable alternatives to current petroleum-based polymers, specifically using PHA and PLA. These biobased alternatives tend to have poor mechanical and thermal properties, increased costs of production, and oftentimes age. 5, 6 Improving poor mechanical properties and decreasing the effect of aging is the main goal of the research in this chapter. The two biobased polymers that are explored in this chapter include PLA, polylactide, and PHA, polyhydroxyalkanoate. Polylactide can be formed through either fermentation, or through ring opening polymerization of lactide.<sup>7,8</sup> The PLA used in this study is an amorphous grade sourced from the company NatureWorks with the code 4950D. This PLA is made from the ring opening of meso-lactide, meaning it has both L and D chirality, decreasing the crystallinity of this grade compared to one with all L or all D configurations<sup>9</sup>.

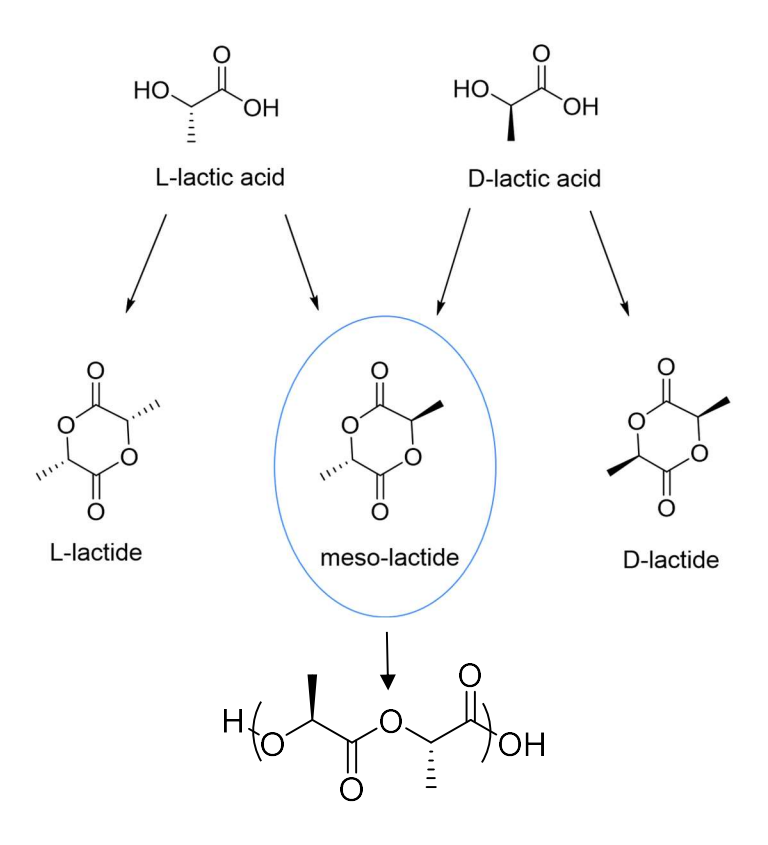


Figure 2.1 Depiction of the meso-lactide that ring opens to form PLA.

Polyhydroxyalkanoates, abbreviated PHAs, are a class of fully biobased and biodegradable polyesters that can be formed through fermentation. <sup>10</sup> It is also possible for PHA to be produced through biosynthetic pathways using unconventional feedstocks. <sup>11</sup> The microorganisms that are used to produce PHA can be genetically modified to tune the properties of the final polymer. <sup>12</sup> Different copolymers can be formed through a combination of different feed ratios and genetic engineering. Polyhydroxybutyrate, PHB, is a very brittle polyester, so typically it can be copolymerized to make it more flexible. <sup>13</sup> Poly(3-hydroxybutyrate-co-3-hydroxyhexanoate) is a copolymer of butyric acid and hexanoic acid and will be explored throughout this project, and can be abbreviated PHB-HHx. This copolymer is known to be more flexible than PHB and is therefore a desirable PHA to research. <sup>14</sup> Two batches of PHA are used in this project named "PHA6" and "PHA8," and have 6% and 8% hexanoate respectively, as quantified by NMR. These two PHA copolymers are explored throughout this document to

understand how different additives affect the mechanical properties of PHA. These PHAs are the same copolymer poly(3-hydroxybutyrate-co-3-hydroxyhexanoate) with different ratios of hexanoate.

Poly(3-hydroxybutyrate-*co*-3-hydroxyhexanoate)

Figure 2.2 Chemical structure of poly(3-hydroxybutyrate-co-3-hydroxyhexanoate).

These two PHAs will be named PHA6 and PHA8 indicating 6% hexanoic acid, 94% butyric acid, and 8% hexanoate, 92% butyrate. The butyrate portion of the copolymer tends to be more brittle and crystalline and therefore is usually copolymerized to make it more flexible. 13 Although these two PHA polyesters seem very similar, they have very different mechanical properties. PHA8 has lower crystallinity due to the hexanoate, leading to slightly slower crystallization and worse secondary crystallization (aging) as compared to PHA6. Aging, as described in the introduction chapter, is the slow, secondary crystallization of PHA that causes embrittlement and degradation of mechanical properties. 15, 16 These characteristics support that PHA8 is more flexible than PHA6. When the two polyesters are extruded and tensile tested, the strain at break, a measurement of how far a polymer sample can stretch before breaking, is 3.5 times higher for PHA8 as compared to PHA6. This is beneficial for applications that require a more flexible polymer. More research needs to be done to fully understand why this is the case.

These two copolymers of PHA are formed through fermentation, a process with many variables that are difficult to control<sup>17</sup>. Between the feed ratios, genetic manipulation of the

substrate, and downstream processing, it can be difficult to get consistent properties of the PHA across different batches after harvesting, but can be accomplished through careful control of the reactors. With this in mind, the research in this project focuses specifically on the two batches of PHA obtained from the reactors at Whitehall, GA, and may not be generalized to other PHA batches, potentially even ones with the same hexanoate content due to other factors such as cell debris content. PHA6 is a very clean polymer with around 1% cell debris content, and PHA8 has modest cell debris content of about 3%, as confirmed with Soxhlet extraction.

PLA is very brittle, having a low elongation at break of around 2-7%, and a high Young's modulus of around 1-3 GPa, depending on the grade, meaning it requires a high amount of force to deform the polymer.<sup>19</sup> These properties could help increase the strength of PHB-HHx, which has a moderate Young's Modulus of 0.7-1 GPa, depending on the copolymer ratios.<sup>20</sup> Blending of PHA and PLA will be compared to a two-step reactive extrusion process, and testing of these formulations is done by extrusion, injection molding, tensile testing, and differential scanning calorimetry.

## 2.1.1 Reactive Extrusion

Reactive extrusion, commonly abbreviated as REX, is the process of chemically reacting a polymer while it processes through an extruder to either crosslink, graft, or perform a post-polymerization modification.<sup>21</sup> Reactive extrusion has been shown in PLA to enhance the strain at break and induce a hardening effect.<sup>22</sup>

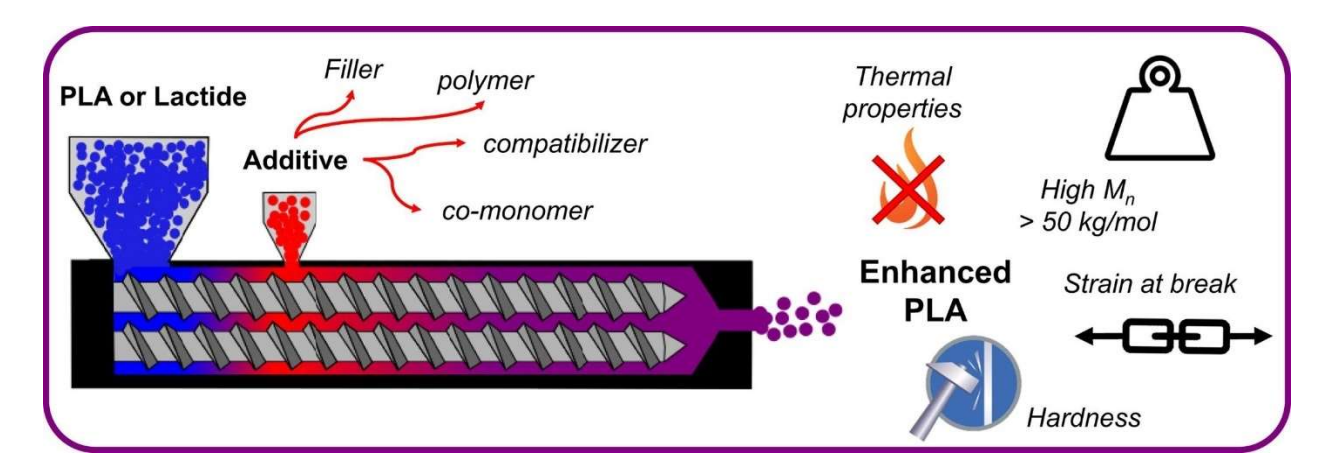


Figure 2.3. Polylactide reactive extrusion to induce a hardening effect. <sup>22</sup>

These chemical reactions are typically brought on by a radical initiator such as benzoyl and dicumyl peroxides.<sup>23</sup> Under heat, peroxides undergo homolytic cleavage, generating two radicals which can subsequently attack double bonds or carbonyls on the polymer chain.

Figure 2.4. The thermal initiation and homolytic cleavage of tert-butyl peroxybenzoate.

This can lead to new bond formation, forming a stronger and tougher polymer, as two radicals on the backbone of a polymer such as PHA, terminate by meeting each other and forming new covalent bonds.

Figure 2.5. Hydrogen abstraction of hydrogen on the backbone of PHA.

The energy required to break a covalent bond is magnitudes higher than the energy required to break intermolecular forces, making for a stronger polymer. Although reactive extrusion can drastically improve the properties of some polymers, there are concerns with the technique due to leftover peroxides not being fully consumed due to their half-life decomposition. Quantifying the residual peroxide concentration is important for degradation testing and FDA regulation. Residual peroxide could be toxic to the microbes in the soil, hindering the biodegradation of the plastic, and active radical species cannot be present in plastics for use in food packaging. Later in this chapter, a novel technique for quantifying residual tert-butyl peroxybenzoate is explored.

## 2.1.2 Experimental Design

In this project, reactive extrusion is used in attempts to induce light crosslinking and improve the compatibility of PHA and PLA blending. When two polymers are blended, there are distinct interphase separation that can cause voids in the mechanical strength.<sup>24</sup> Using a radical initiator such as LP can stabilize the phase structure between the immiscible domains, leading to a stronger polymer.

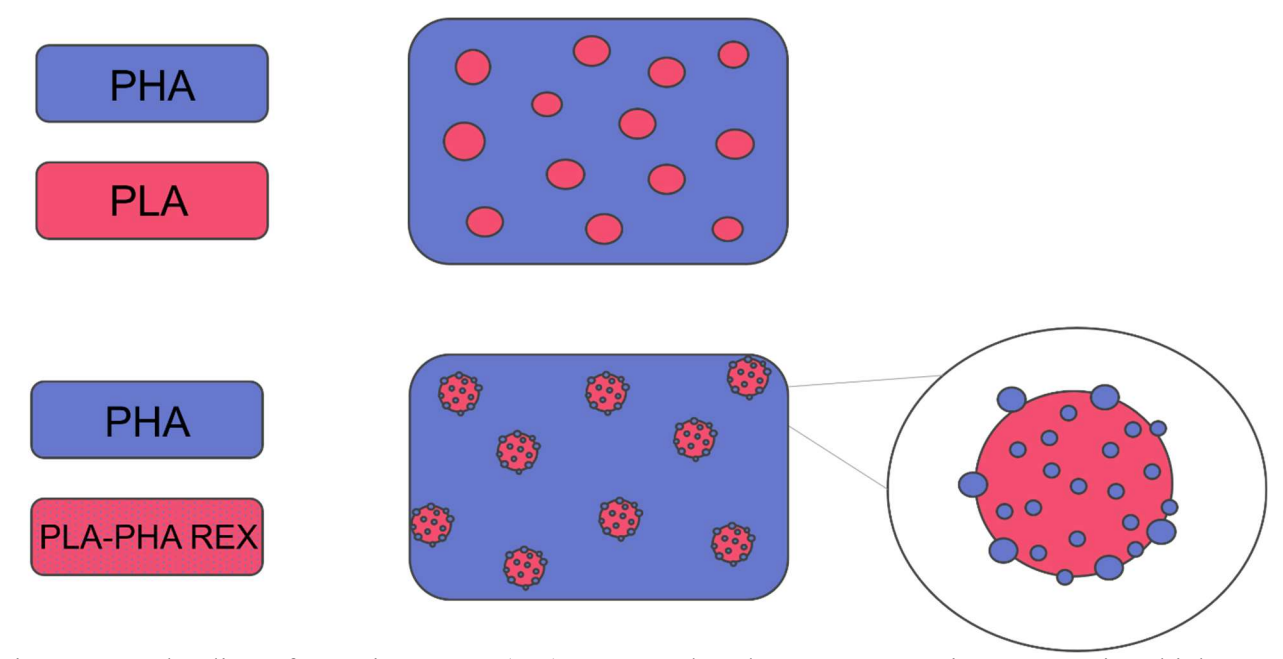


Figure 2.6. Blending of PLA into PHA (top) compared to the 2-step extrusion process in which a pre-compatibilization step is done first (bottom).

This project aims to prove through mechanical data that a pre-compatibilization step improves the strain at break as compared to simple blending of PHA and PLA.

The inspiration for this project is to improve the mechanical properties of PHA by adding PLA and tert-butyl peroxybenzoate to the extrusion process. The workflow occurs in a two-step extrusion process, depicted in figure 2.6. The workflow includes a "pre-compatibilization" step in which PHA and PLA are incorporated together via a reactive extrusion step, followed by an additional reactive extrusion step in which the "pre-compatibilized" PLA in extruded into PHA in a 1 to 9 ratio.



Figure 2.7 Workflow depicting two steps of reactive extrusion in the Process 11 and flushing through the Haake into Minijet injection molder to create tensile samples.<sup>25</sup>

Finally, these samples are injection molded, and mechanical properties are observed through tensile testing. Although many properties can be gleamed from a stress-strain graph, such as Young's modulus (slope of the stress over strain of the linear portion of the graph), yield strength (point at which permanent deformation has occurred), and ultimate stress (stress value at breaking point), the element that will be observed most closely in this study in the strain at break.

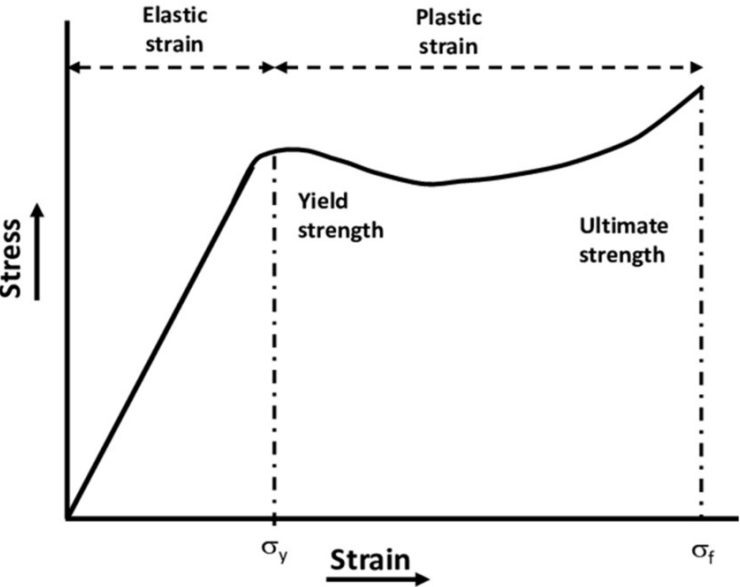


Figure 2.8 Depiction of stress-strain graph obtained from a tensile strength test. <sup>26</sup>

The strain at break is the distance that a dog bone tensile bar can stretch before completely breaking. This number is reported in a unit of length measurement but can also be reported in relation to the original length of the specimen. For example, 100% elongation corresponds to a sample that doubled its length before breaking. For the purposes of this document, all strain at break data is reported in a percentage of the original sample length.

Aging of PHA is a prevalent issue that causes embrittlement and loss of flexibility over time.

This is a major drawback due to the loss of mechanical properties, and issues with shelf life in an

application setting. Aging can be quantified by measuring the decrease in the strain at break overtime, or by measuring the change in crystallinity through DSC.

The process of extrusion follows the 4-step workflow depicted in figure 2.7. PLA and PHA undergo a pre-compatibilization step by reactive extrusion with LP to form a PLA dominant blend. There are 5 different blends that are made, all with 0.2 wt% LP:

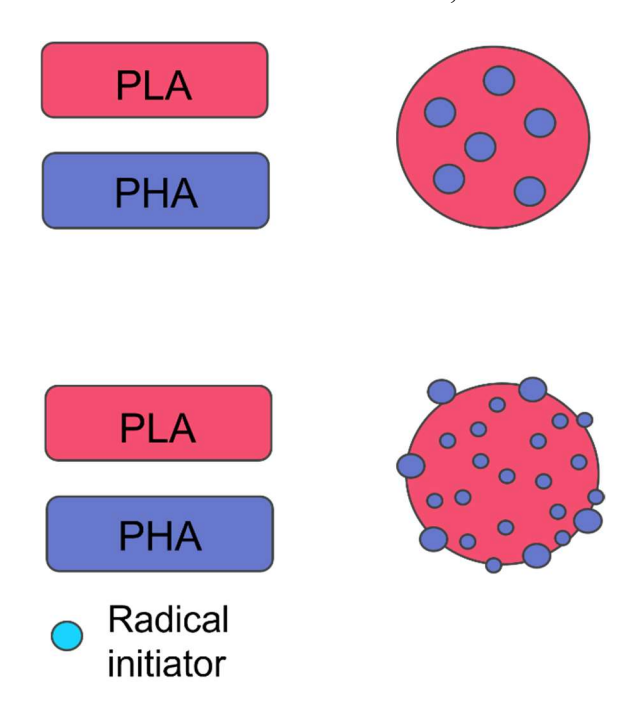


Figure 2.9. Depiction of PHA blended into PLA with and without the presence of a radical initiator.

Table 2.1. Five PLA-PHA blends compounded with 0.2 wt% LP during step 1 of workflow.

PLA
1PHA <sub>6</sub> /9PLA
2PHA <sub>6</sub> /8PLA
1PHA <sub>8</sub> /9PLA
2PHA <sub>8</sub> /8PLA

Next, the PLA/PHA blends undergo a second reactive extrusion step into PHA by adding 10% of extrudate 1 into 90% PHA in the presence of 0.2 wt% LP.

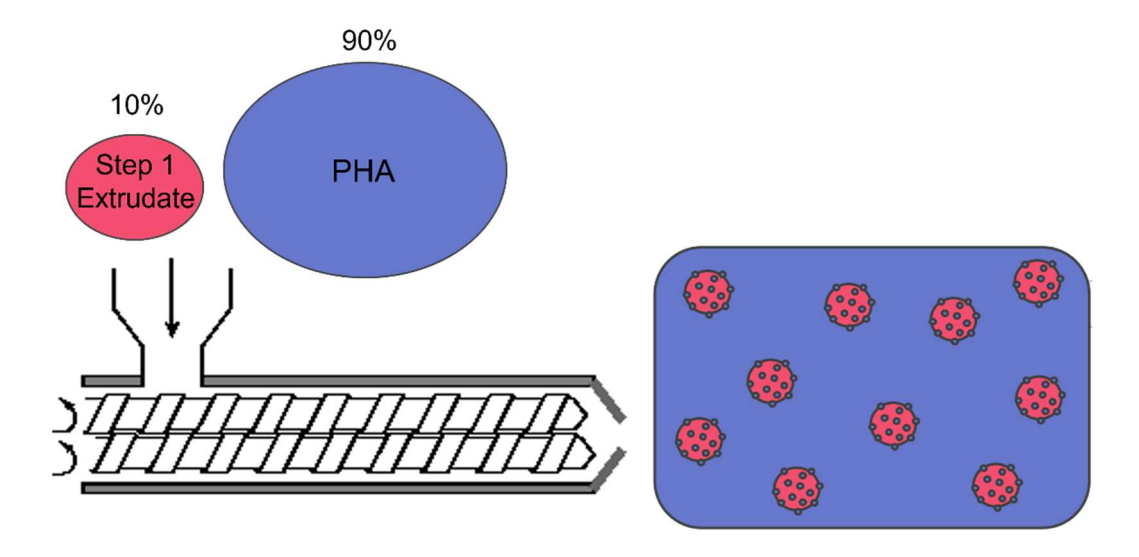


Figure 2.10. Cartoon depiction of step 2 in the extrusion workflow.

These samples were then cut and flushed through the Haake and injected into the MiniJet Injection Molder to form the ASTM Type 5 dog bone. Tensile testing was then conducted on the Shimadzu tensile tester, pulled at a rate of 10 mm/min to collect strain at break data.

# 2.2 Materials and Methods:

#### 2.2.1 Materials:

The materials used include poly(3-hydroxybutyrate-co-3-hydroxyhexanoate) with 6% hexanoate, named PHA6, and poly(3-hydroxybutyrate-co-3-hydroxyhexanoate) with 8% hexanoate, named PHA8, sourced from the New Materials Institute of the University of Georgia bioreactors. Polylactide, PLA 4950D sourced from NatureWorks, and tert-butyl peroxybenzoate, trade-named Luperox P® from Sigma Aldrich.

Equipment for extrusion Thermo Scientific Process 11 extruder, Thermo Scientific Haake extruder, Thermo Scientific Minijet injection molder. Bruker 600 MHz NMR to determine copolymer ratios of the two PHAs, a Hewitt Packard gas chromatography and GC-MS to detect

and quantify residual peroxide concentration, a TA instruments differential scanning calorimeter (DSC) to determine thermal properties and percent crystallinity of PHA, Malvern GPC to determine molecular weight of samples. Shimadzu tensile tester and an Instron impact tester for mechanical properties.

# 2.2.2 Peroxide Masterbatch Preparation

In order to perform reactive extrusion, the peroxide initiator must be evenly distributed throughout the sample using a masterbatch. Individual masterbatches were formed for each type of PHA. 10g. of PHA powder was suspended in acetone in a 250 mL round bottom flask. 0.4 g of Luperox P was added to the suspension, sonicated, and the acetone was rotovaped off. The resulting powder was placed under reduced pressure overnight to remove any remaining solvent. The final PHA masterbatch which contained 4 wt% peroxide, ready to be used for extrusion, and stored in the freezer to prevent loss of initiator.

#### 2.2.3 Extrusion Procedure

In step one of the extrusion workflow, PLA was the dominant polymer, with PHA6 and PHA8 being incorporated in either 0, 10, or 20 wt%, in the presence of 0.2 wt% peroxide initiator. The Process 11 was set to 180 °C at all temperature zones, due to this being the ideal extrusion temperature for this grade of PLA. The PLA was cryo-milled to form a fine powder that could more easily disperse with the PHA. ~20g. of material was weighed out, thoroughly mixed in a coffee grinder, and hand-fed into the Process 11 extruder, with a screw speed of 50 rpm. This corresponded to around 5 minutes of resonance time.

In step two of the extrusion workflow, 10 wt% of extrudate from step one was mixed into PHA6 and PHA8 in the presence of 0.2 wt% peroxide initiator. The Process 11 was set to 150 °C at all temperature zones, due to this being the ideal extrusion temperature for PHA. The

extrudate from step one was finely cut up and ~35g. of sample was weighed out, mixed in a coffee grinder, and hand fed into the extruder with screw speed 100 rpm. The corresponded to around 2.5 minutes of resonance time.

Lastly, the extrudate from step two was cut up and flushed through the Haake extruder without cycling at a temperature of 150 °C and screw speed of 100 rpm. The cylinder of the Haake Minijet injection molder was set to 150 °C and the ASTM Type V mold was set to 70 °C. 2.2.4 Mechanical and Thermal Properties

Tensile testing was done on a Shimadzu AGS-X tensile tester where the type V dog bones were pulled at a rate of 10 mm/min. Samples were aged for 2 days prior to testing, and another sample was tested on day 8. Thermal properties, including percent crystallinity, glass transition temperature, and cold crystallization peaks, were collected using a TA instruments Discovery 250 differential scanning calorimeter. Samples were taken from the side of the tensile bar measuring between 4-7 mg. of material, and aluminum reference pans were used. Samples were equilibrated at room temperature and then heated to 180 °C at a rate of 10 °C/min. Next, they were cooled at 10 °C/min to -20 °C in order to observe glass transition temperature. Lastly, samples were heated once again to 200 °C and cooled to 0 °C to observe any nucleation above that temperature. Percent crystallinity was obtained by the software using equation 1, in which  $\Delta$ H is the specific enthalpy of fusion of the sample, calculated by the software as the area of the melting endotherm,  $\Delta$ H<sub>c</sub> is the theoretical enthalpy of fusion for a 100% crystalline polymer, which is 146 J/g for PHB, and  $\Phi$  is the weight fraction of the sample.

$$X_c(\%) = \frac{\Delta H}{\Delta H_c * \phi} * 100 \tag{1}$$

2.2.5 GPC

Gel permeation chromatography was done using a Malvern \_\_ GPC with liquid phase chloroform to determine molecular weight of PHA samples before and after REX. Samples were measured out in a 1 mg/mL of HPLC grade chloroform, given sufficient time to dissolve, and filtered through a 0.23 µm syringe filter. The software compares the elution time of the sample to the polystyrene calibration standards to estimate molecular weight.

# 2.2.6 Gel Content

Gel fraction to determine the extent of crosslinking of REX samples was done according to ASTM standard D2765. A sample of 1000 mg. dried polymer was placed into a "tea bag" shaped mesh container with 120 mesh pore size. Using metal wire, up to 3 samples were suspended into a 500 mL round bottom flask filled chloroform. A reflux condenser was placed onto the flask, and the apparatus refluxed on a heating mantle for 24 hours. Next, the samples were removed from the solvent and dried in a vacuum oven for 12-24 hours to ensure they are fully dried. The original mass and the final mass are plugged into equations 2 and 3 to yield the solvent extraction percentage and the gel fraction respectively. W1 is the mass of the empty bag unstapled, W2 is the mass of the sample in the bag, with the top unstapled W3 is the mass of the sample inside of the mesh bag after stapling shut, and W4 is the mass of the sample in enclosed mesh bad post extraction.

$$\frac{(W3-W4)}{(W2-W1)} * 100 = solvent \ extraction \%$$
 (2)

$$100 - solvent \ extraction \% = gel \ content$$
 (3)

#### 2.2.7 NMR

The Bruker 600 MHz nuclear magnetic resonance instrument was used to quantify the copolymer ratios of PHA. A sample of 10 mg of PHA/mL of deuterated chloroform was prepared and allowed to dissolve overnight. The instrument was used under the appropriate

conditions per instrument training guidelines. Spectrograms were processed using Mnova software.

## 2.2.8 GC and GC-MS Methanolysis

Methanolysis was done using 10 mg of polymer sample, 150 μL of concentrated sulfuric acid, 1 mL of HPLC grade chloroform, and 850 μL of methanol in a glass tube, vortexed and refluxed at 100 °C for 2.5 hrs. The solution was worked up with 1 mL of deionized water, and the chloroform layer was extracted and placed in a GC vial. A Hewit Packard gas chromatography instrument was used with standard FAME method.

#### 2.2.9 Soxhlet Extraction

Soxhlet extraction of PHA6 and PHA8 was done to determine the amount of cell debris left over from downstream processing in the samples. Cellulose thimbles were dried in a vacuum oven to remove moisture, and a mass was quickly obtained. 1 g. of PHA was measured into the thimble. The thimbles were placed in a Soxhlet extractor attached to a 250 mL round bottom flask, and a reflux condenser. The round bottom flask was filled with chloroform and the entire apparatus was refluxed for 24 hrs on a heating mantle. The cellulose thimble was then drained and dried overnight in a vacuum oven. A new measurement was obtained, and leftover mass was attributed to residual cell debris. The PHA6 was found to have ~1 wt% cell debris and the PHA8 was found to have ~3 wt% cell debris.

#### 2.3 Results and Discussion:

# 2.3.1 Mold Temperature Study

To begin this extrusion project, a small-scale experiment was conducted to determine the optimal mold temperature for injection molding. Previous studies from our lab on PHA extrusion and injection molding indicate conflicting results between 40 °C mold and 70 °C mold

temperatures. Therefore, both mold temperatures were used, and the better result was used through the rest of the projects. In three samples tested, 70 °C mold temperature yields higher strain at break, and produces less brittle, more ductile polymers, so this temperature is used throughout the project. The higher temperature allows the chains to fold in a more favorable manner that can better dissipate the force of the tensile test.

# 2.3.2 Effect of Radical Initiator on PHA

Using the extrusion conditions laid out in the methods section, the effect of introducing the radical initiator, Luperox P (abbreviated LP), into PHA6 and PHA8 with reactive extrusion is shown in the tensile data below.

Table 2.2. The strain at break and Young's modulus of PHA6 and PHA8 with and without LP

Sample	Strain at Break	Young's Modulus
РНА6	38.5%	0.825 GPa
PHA8	130%	0.743 GPa
PHA6-0.2LP	63.4% (1.6 X)	0.776 GPa
PHA8-0.2LP	231% (1.7 X)	0.647 GPa

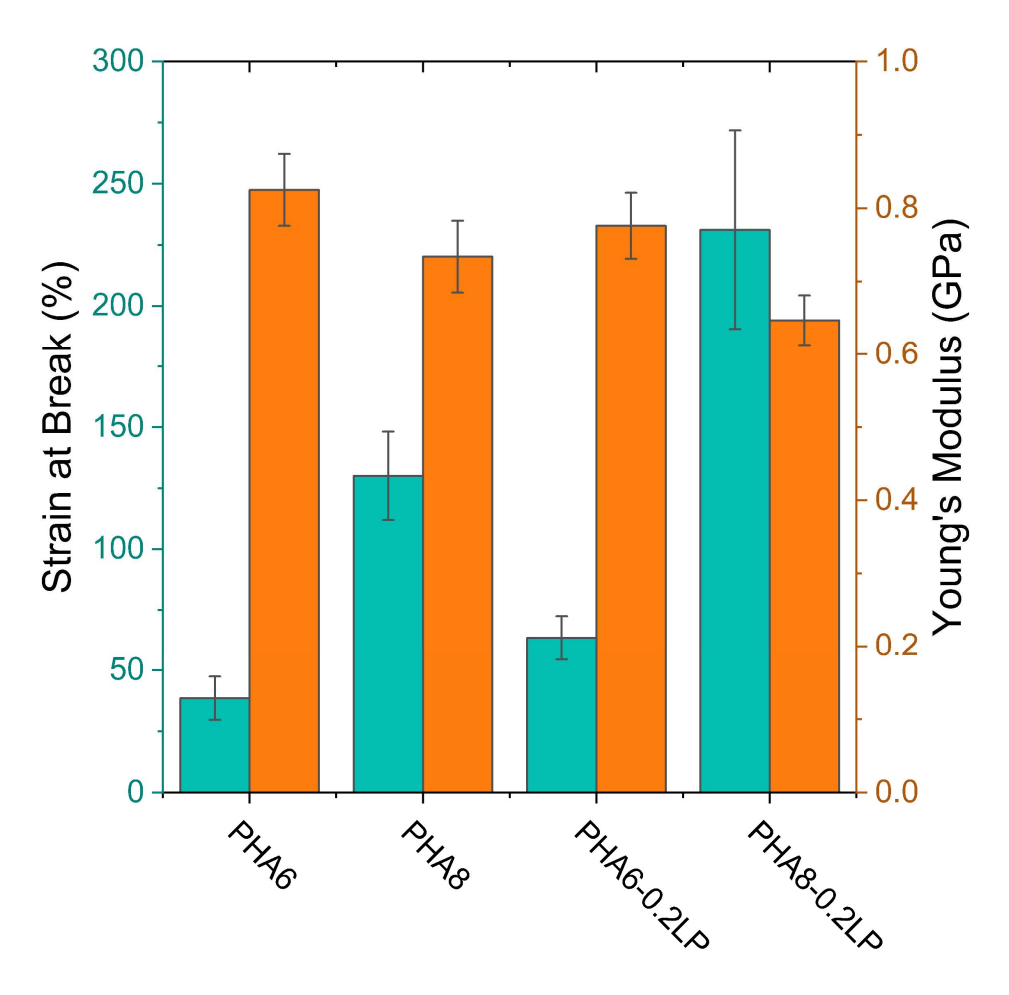


Figure 2.11. Comparison of the strain at break and Young's modulus of PHA6 and PHA8 with and without the presence of LP

It is clear from the above data that there is a significant improvement in the strain at break and a decrease in Young's modulus when PHA is extruded in the presence of 0.2 wt% LP. Without any peroxide initiator present during extrusion, PHA6 exhibits a strain at break of 39%, while PHA8 exhibits a strain at break of 130%. Although there is only 2% more hexanoate copolymer in PHA8, it is significantly more flexible as shown by the increase in the strain at break and lowering of the Young's modulus. When peroxide initiator is introduced into the extruder at a 0.2 wt% loading, there is 1.7 times increase in the strain at break for both PHA6 and PHA8. This could suggest light crosslinking which was hypothesized in the introduction section. Young's Modulus had little to no decrease in the REX samples as compared to the neat PHA6

and PHA8. This means that there is a notable increase in the strain at break without compromising on the strength of the material. To further investigate why PHA exhibits an improvement in tensile properties in the presence of Luperox P radical initiator, a small-scale experiment was done to test the extent of cross linking.

# 2.3.3 Crystallinity and REX

Differential scanning calorimetry is done to evaluate if reactive extrusion influences the crystallinity of PHA6 and PHA8. A special method called SSA is used in which many steps of heating and cooling are done in 10 °C increments, and a master curve is obtained. This method deconvolutes a broad melting curve since regions of the polymer that are excluded from crystalline lamella melt first, and more crystalline and tightly packed chains that are part of the crystalline lamella melt at a higher temperature.

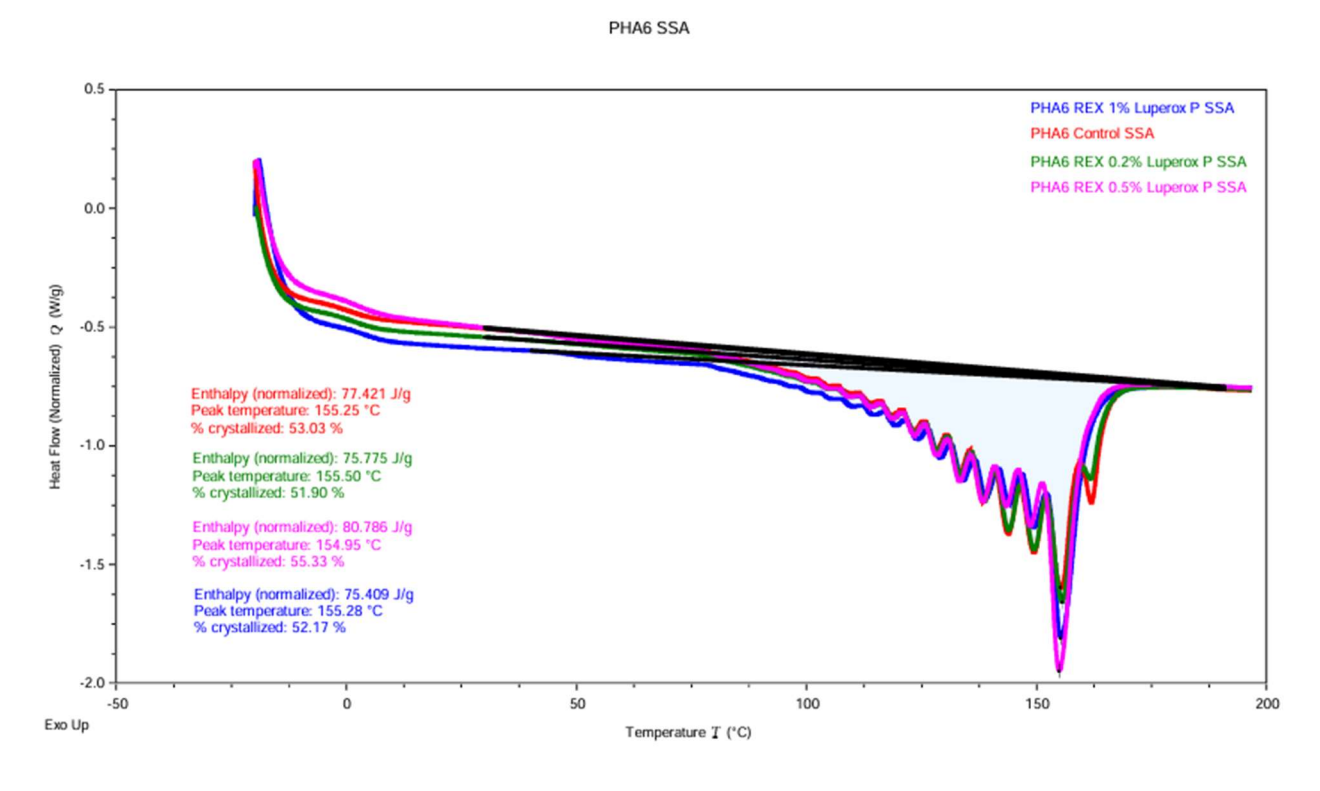


Figure 2.12. SSA thermogram overlay of PHA6 control and PHA6 REX samples.

As shown in the above figure, although the overall percent crystallized, as calculated from the enthalpy integration, does not follow a clear trend, it is interesting to note that the distribution of the melting curve changes.

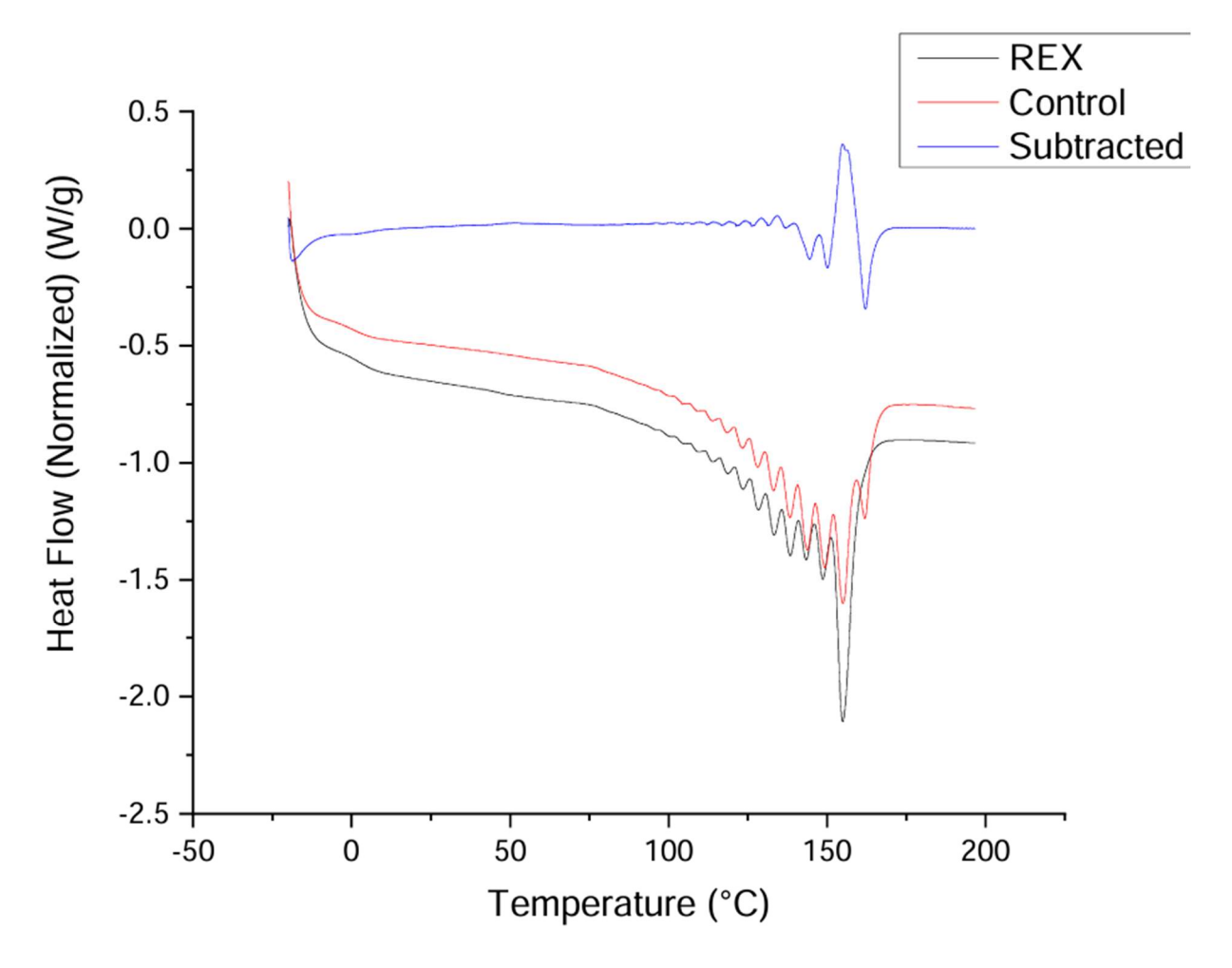


Figure 2.13. Subtraction of PHA6 control SSA and PHA6, 0.5 wt% LP REX SSA.

There is a disappearance of the highest melting peak implies that there is less order in the reactive extrusion sample, corroborated by the improvement in the strain at break of REX samples. SSA was also conducted for PHA8 and various amounts of radical initiator.

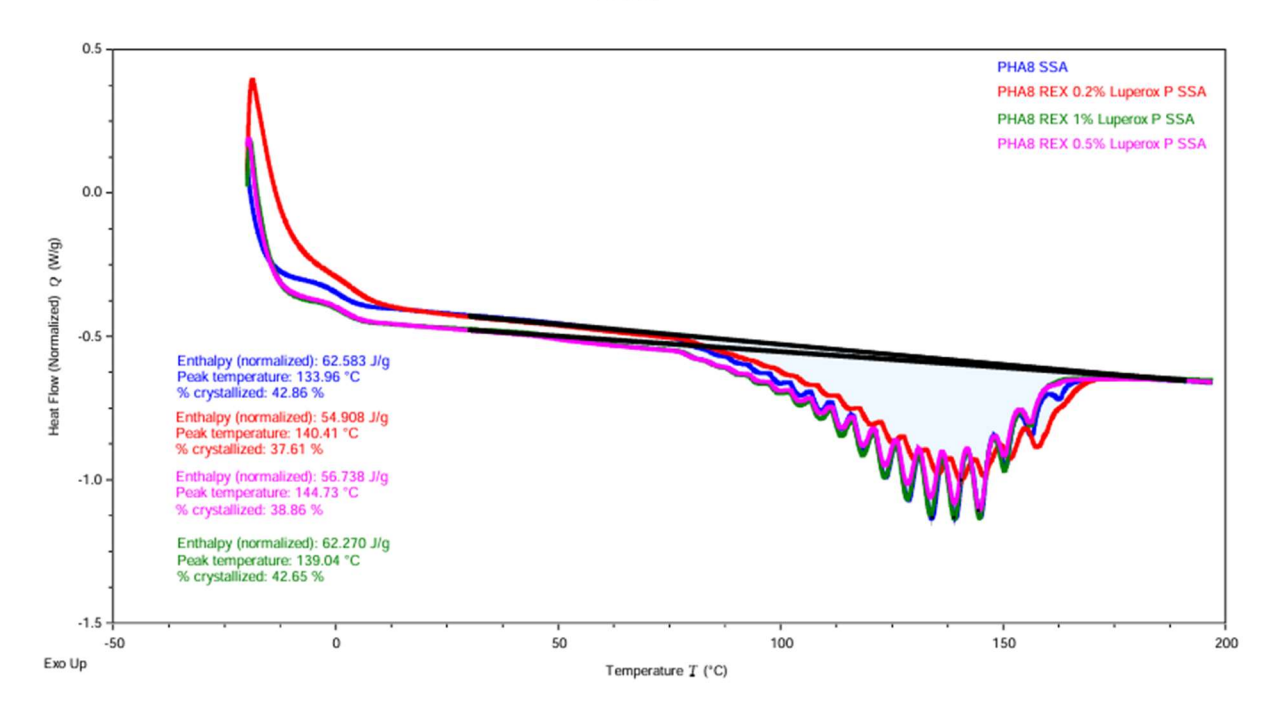


Figure 2.14. SSA thermogram overlay of PHA8 control and PHA8 REX samples.

In the case of PHA8 there is a large decrease in crystallinity once Luperox P is introduced to the extrusion process. Once again, there is a decrease in the highest melting peak, and an increase in the lower melting peaks. The PHA8, 0.2% LP (red line) displays interesting traits that must be further studied. The second highest melting peak has a higher integration than expected, and this is not fully understood at this time.

# 2.3.4 Evidence of Crosslinking

In a gel content experiment, crosslinked parts of the polymer are resistant to solvation and will remain behind in the enclosed mesh bag, and soluble sections of the polymer pass through the mesh and dissolve in the bulk solvent. Therefore, remaining mass after chloroform reflux is the gel fraction. A large value for the gel content corresponds to a high degree of crosslinking. Table 2.3 shows the gel fraction for each extruded sample with the indicated weight percent of LP.

Table 2.3. The gel fraction of several PHA samples extruded with various amounts of LP.

Sample	Weight %	Gel
Sample	Luperox P	Fraction
	0	0.15
	0.2	0.52
РНА6	0.5	43.54
	1	20.71
	3	17.187
	0	1.17
PHA8	0.2	12.85
	0.5	68.92
	1	30.23

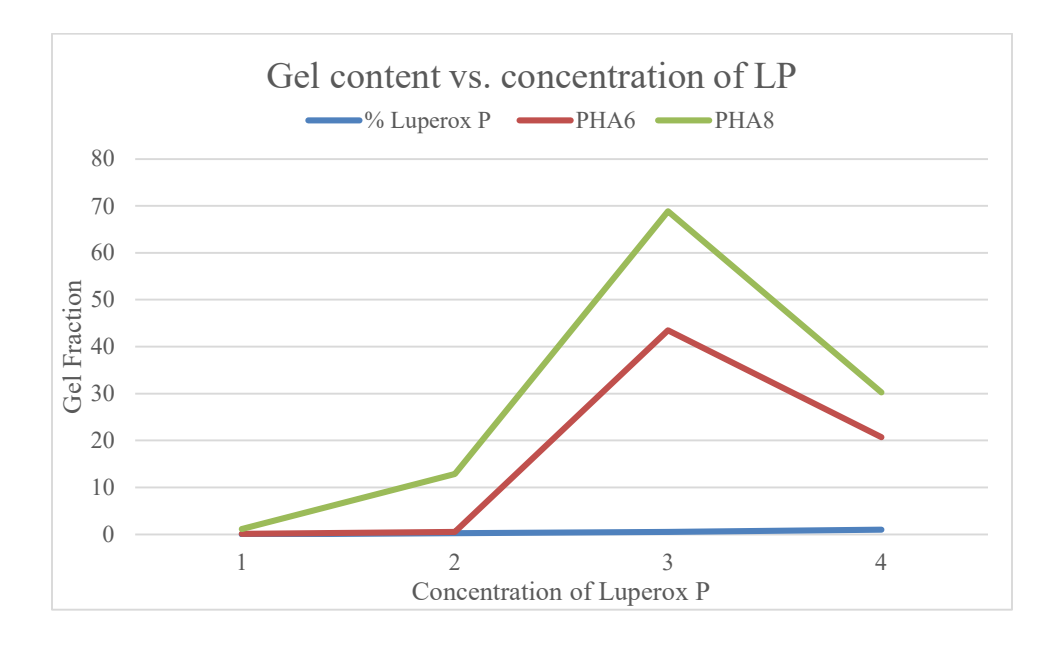


Figure 2.15. Visual graphic showing the trend of gel fraction with increasing LP wt%.

Based on the data, PHA8 has much higher gel content than PHA6, potentially indicating that PHA8 is more reactive to REX, leading to more covalent crosslinks. This could be due to the higher amount of hexanoate in PHA8. PHA with a higher amount of propyl groups from the hexanoate may have a greater reactivity towards the peroxide initiator, leading to more crosslinking and higher gel content. Interestingly for both PHA samples, 0.5 wt% of LP yielded the highest gel fraction.

# 2.3.5 Two Step Extrusion

Moving forward into the effect of PLA blended into PHA in the presence of LP, figure 9 below shows the impact of the 2-step extrusion process on the PHA-PLA REX samples. Recall from the above table 2.1 that the 5 PLA-PHA formulations extruded in step 1 are then incorporated into PHA in a 1 to 9 ratio in the presence of LP.

Table 2.4. The strain at break of the various PLA-PHA blends extruded into PHA6.

Sample	Strain at Break	Improvement
PHA6-Neat	38.5%	-
PHA6-REX	63.4%	1.6 X
PLA-blend	30.3%	-
PLA-REX	167%	4.3 X
1PHA <sub>6</sub> /9PLA	195%	5 X
2PHA <sub>6</sub> /8PLA	39.3%	-
1PHA <sub>8</sub> /9PLA	166%	4.3 X
2PHA <sub>8</sub> /8PLA	158%	4.1 X

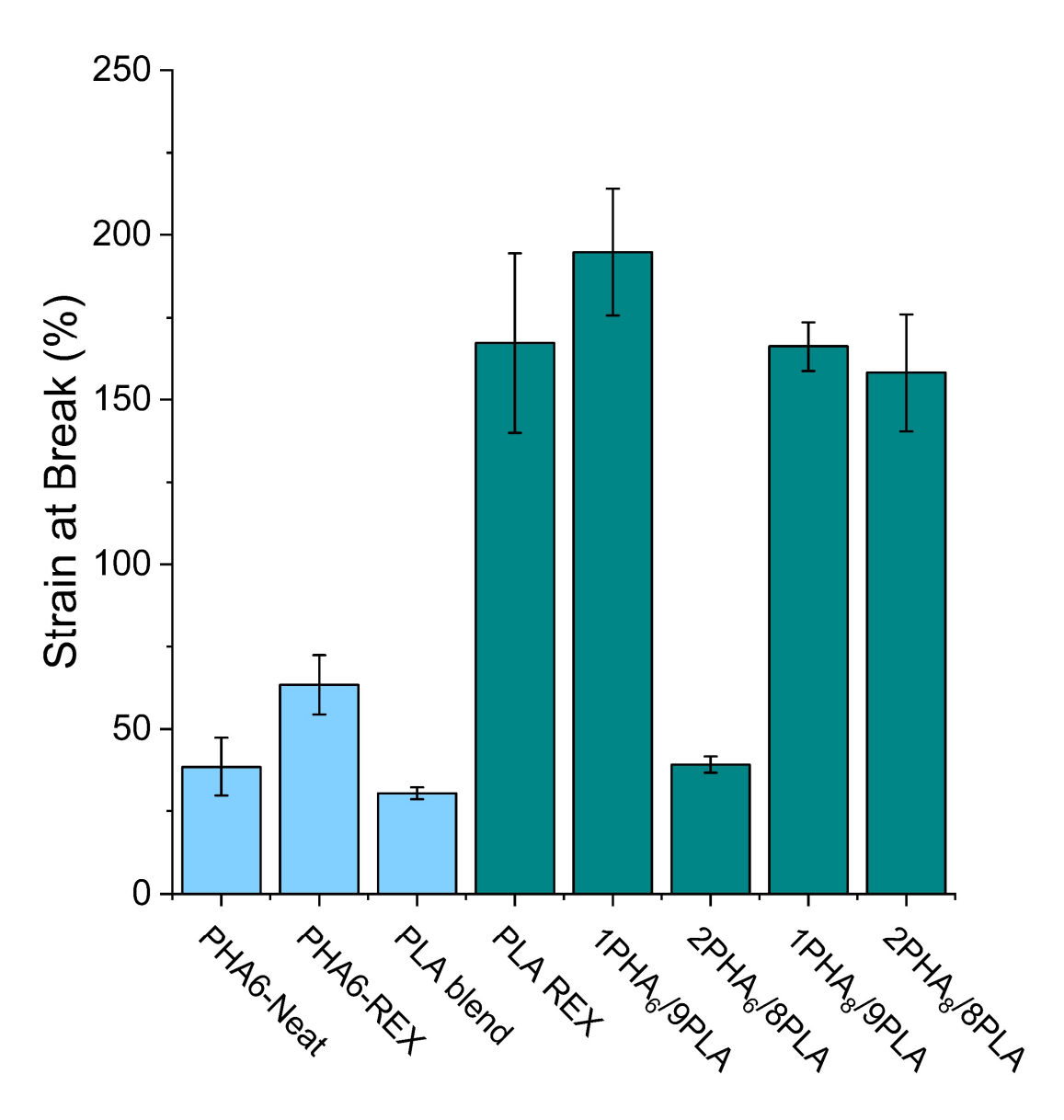


Figure 2.16. Tensile data for PHA6 samples including PHA6 neat, PHA6 REX, PLA blended into PHA, and PHA6 with 10% of each of the five formulations from step one.

The PHA6-neat sample has a strain at break of 38.5%, this is improved by a factor of 1.6 when extruded in the presence of the radical initiator, LP. When PLA is blended into PHA6 in a 10% abundance, the results show no improvement to the strain at break as compared to the control PHA6 sample. However, when PLA undergoes the pre-compatibilization step with LP, and then extruded with PHA6 in a 10% abundance, the strain at break is enhanced by a factor of 4.3. These results suggest that pre-compatibilization allows the PLA to interact with the PHA in a

constructive manner, leading to significant improvement to the mechanical properties. This improvement is expanded upon in the case of 1PHA<sub>6</sub>/9PLA. When this formulation is introduced to PHA6 and LP in a 10% abundance, 5 times increase in the strain at break is observed. This result supports the hypothesis that pre-compatibilization may be improving the compatibility of the two polymers, leading to a final product with more desirable properties. The other formulations performed similarly with a 4.3 times improvement and 4.1 times improvement for 1PHA<sub>8</sub>/9PLA and 2PHA<sub>8</sub>/8PLA respectively into PHA6 in the presence of LP. The one outlier seen in the data is 2PHA<sub>6</sub>/8PLA, which has the same strain at break as the PHA6 control.

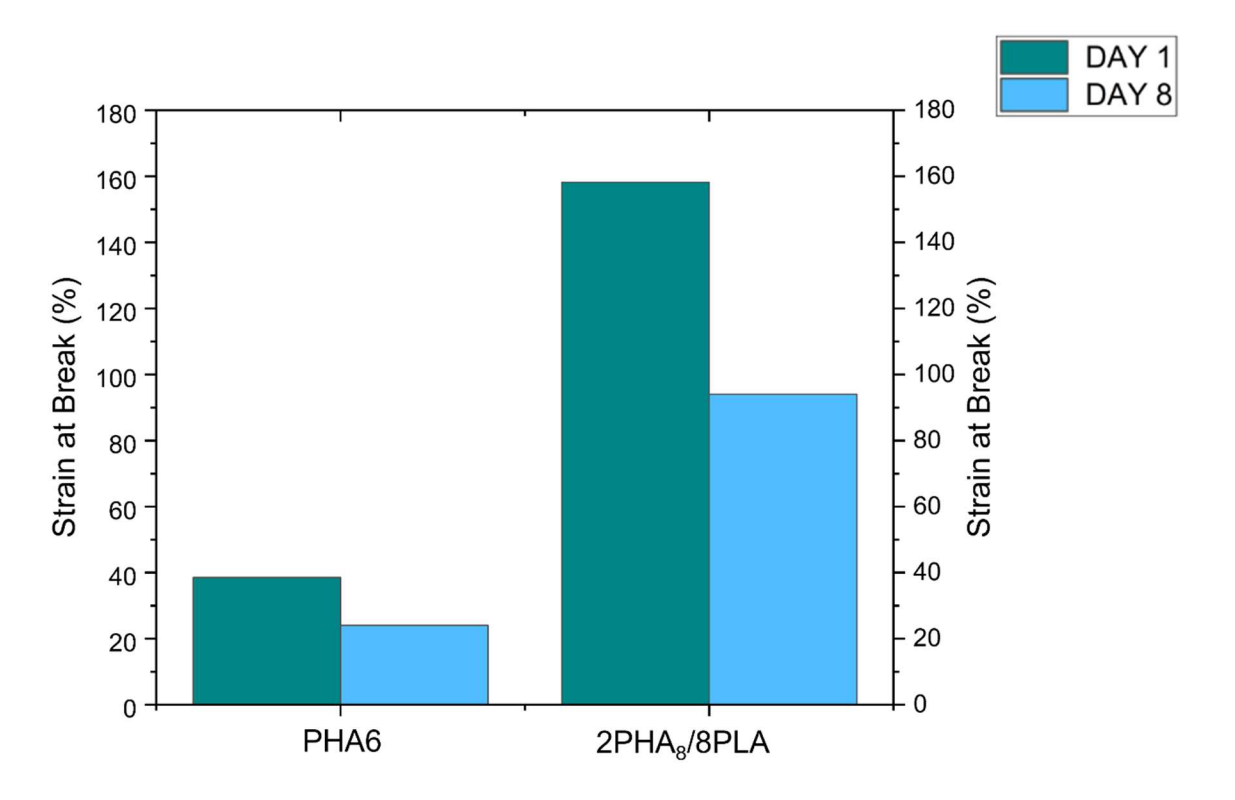


Figure 2.17. The aging of PHA6 vs. the aging of 2PHA<sub>8</sub>/8PLA in PHA6 (at 10% abundance). Neat PHA6 has a reduction in the strain at break by 30% within one week of extrusion. In the case of 2PHA<sub>8</sub>/8PLA extruded in PHA6 at a 10% abundance, the strain at break reduced by 40% within one week of extrusion. This indicates that although this blend overall improves the strain at break, it does not appear to improve the aging issues associated with PHA.

The same process as above was completed with PHA8, and the strain at break results are shown in table 2.4 and figure 2.15.

Table 2.5. The strain at break of PHA8 and blends and improvement values compared to control.

РНА	Strain at Break	Improvement
PHA8-Neat	130%	-
PHA8 REX	231%	1.8 X
PLA Blend	172%	1.3 X
PLA REX	253%	1.9 X
1PHA <sub>6</sub> /9PLA	198%	1.5 X
2PHA <sub>6</sub> /8PLA	174%	1.3 X
1PHA <sub>8</sub> /9PLA	130%	-
2PHA <sub>8</sub> /8PLA	239%	1.8 X

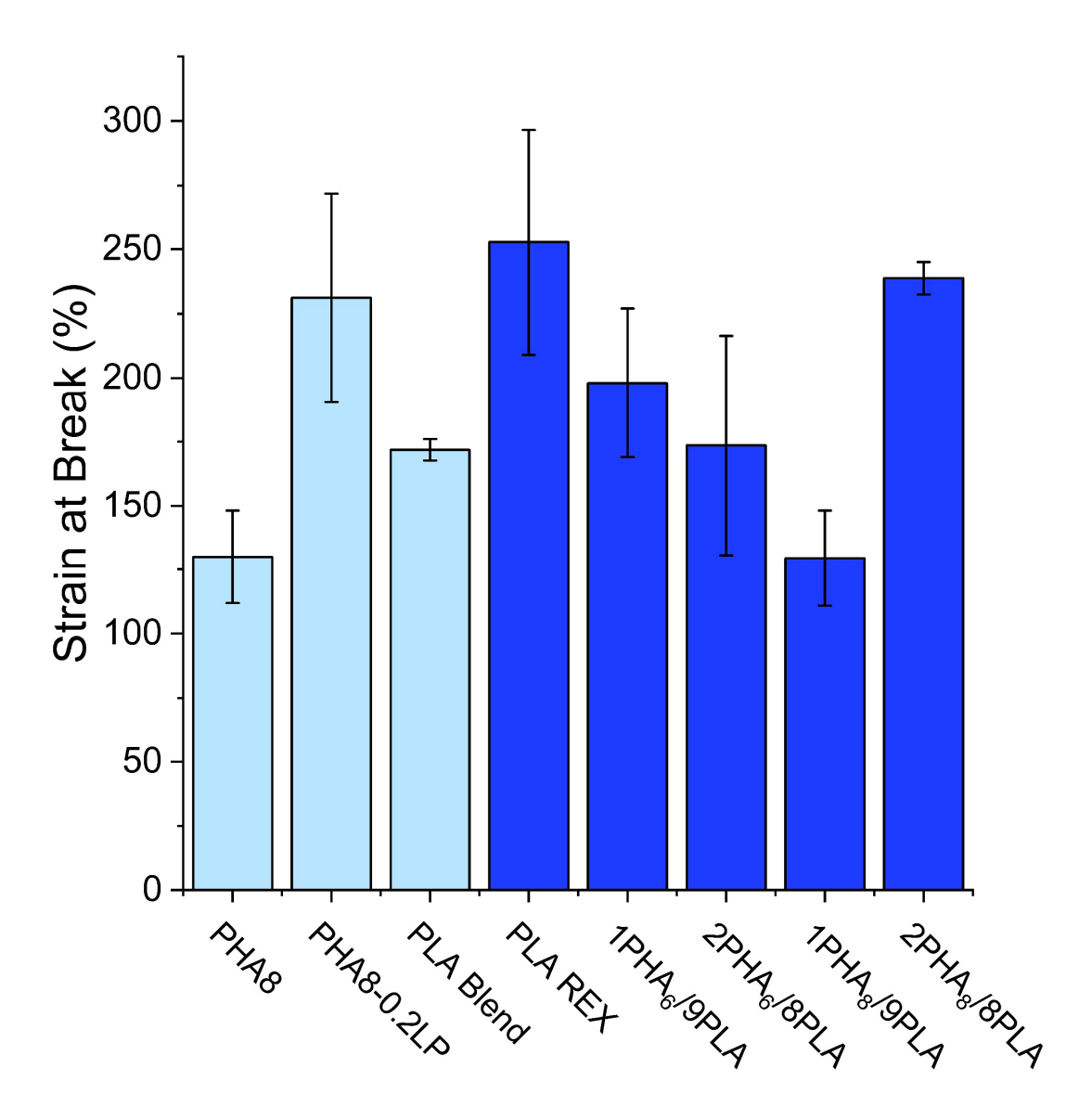


Figure 2.18. Bar graph displaying strain at break and error of PHA8 control groups and PLA-PHA blends in PHA8.

PHA8 control has a strain at break of 130%, and this is improved by a factor of 1.8 when extruded in the presence of 0.2 wt% LP. Blending PLA into PHA8 in a 10% ratio leads to a meager 1.3 times improvement without the presence of LP. However, when the PLA *underwent* the pre-compatibilization step and then blended into PHA8 in the presence of LP, the strain at break increases to 253%, almost double the improvement compared to the control. The other formulations show improvements between 1.3 and 1.8 X, except for 1PHA8/9PLA, which

demonstrated similar properties to the control PHA8. This is possibly due to poor mixing or some other phenomenon yet to be uncovered.

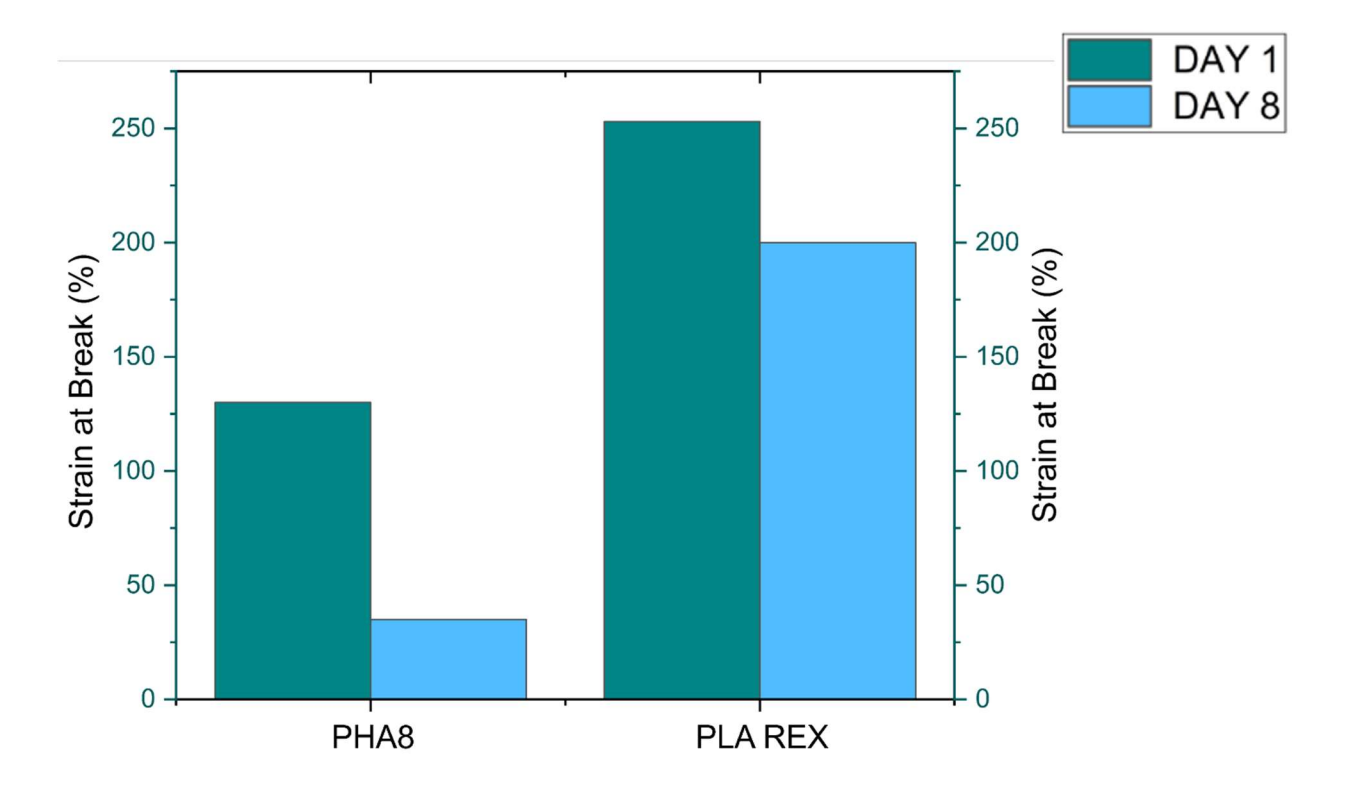


Figure 2.19. PHA8 aging vs. 10% PLA REX in PHA8 aging.

The control PHA8 ages aggressively with a 70% reduction in strain at break over 1 week. However, when 10% PLA-REX is introduced to PHA8 in the presence of LP, the reduction in strain at break is only 15%. Although this is far from an absence of aging, it is a significant improvement towards solving the aging phenomenon that plagues PHA.

# 2.3.6 Molecular Weight Considerations

Above a certain concentration of radical initiator, more bonds may break than are built, potentially degrading the molecular weight. A study was conducted to determine molecular weight change with extrusion and REX using the Malvern GPC. Gel Permeation Chromatography (GPC) is a technique in which a sample is dissolved in a solvent such as chloroform, filtered through a syringe filter, injected into the liquid chromatography system,

travels through the silica column, and is detected by the RI detector. The software then compares the elution time of the polymer to the calibration curve of the reference, which in this case is polystyrene. High molecular weight fragments elute faster because larger sized fractions have less opportunity to interact with the material in the column, whereas the smaller radius fractions can become caught in the column and interact with the silica gel, causing them to elute later. Higher molecular weight polymers have a larger radius of gyration and elute faster than lower molecular weight polymers.

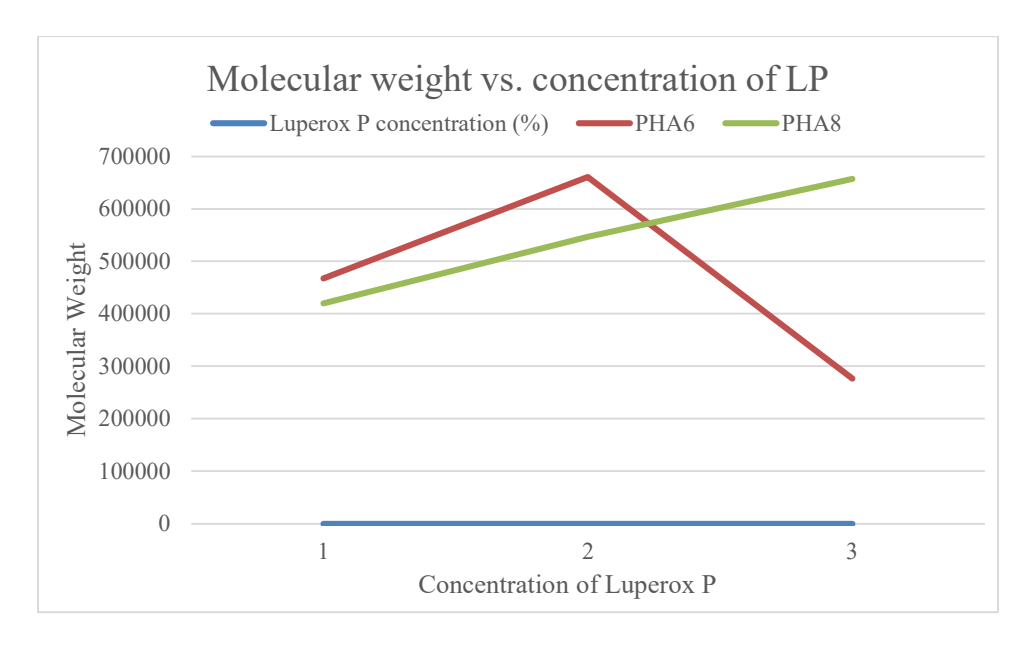


Figure 2.20. The relationship between molecular weight of PHA and abundance of LP during extrusion.

As Luperox P concentration increases, the molecular weight increases for PHA8, but for PHA6, 1 wt% LP shows a decrease in the molecular weight. This confirms the information eluded from the gel fraction data. High concentration of Luperox P breaks down molecular weight in PHA6, leading to a much lower gel fraction than the PHA8.

PLA 4950D was also studied to determine if REX caused a change in molecular weight. Once again, the Malvern GPC was used to understand fluctuations in  $M_{\rm w}$ , and the findings agree that 1 wt% LP will degrade molecular weight.

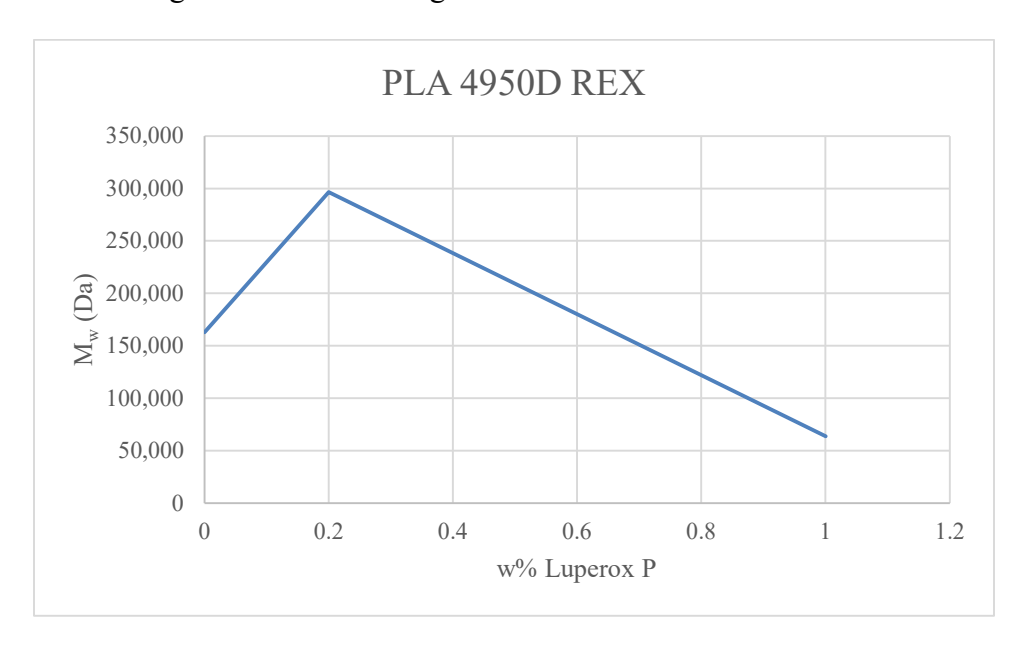


Figure 2.21. The relationship between PLA 4950D molecular weight and concentration of LP in the extruder.

The graph above shows that an increase in molecular weight is seen when 0.2 wt% Luperox P, but then a drastic decrease is seen when 1 wt% Luperox P is used. Too much radical initiator can begin to break bonds therefore decreasing the overall  $M_w$ .

# 2.3.7 Impact Testing

Another mechanical testing method is used to determine if these reactive extrusions samples have an improvement on impact modification.

Table 2.6. Impact testing data of PHA6 and PHA8 before and after REX.

Sample	Depth	Width	Break	Strength 1	Strength 2	Break
	(mm)	(mm)	( <b>J</b> )	(kJ/m^2)	(J/m)	Type
PHA6 Avg	10.19	3.09	0.0548	1.74083	17.7390	Hinge

PHA8 Avg	10.13	3.07	0.0807	2.595933	26.0313	Hinge
PHA6 0.2% LupP	10.14	3.087	0.0731	2.33783	23.7104	complete
PHA8 0.2% LupP	10.16	3.1	0.0910	2.89371	29.3823	complete
PHA6 0.5% LupP	10.15	3.07	0.0844	2.71185	27.4857	complete
95% PHA6, 5%	10.16	3.065	0.0659	2.119745	21.52545	complete
(PHA6, 1% LupP)						

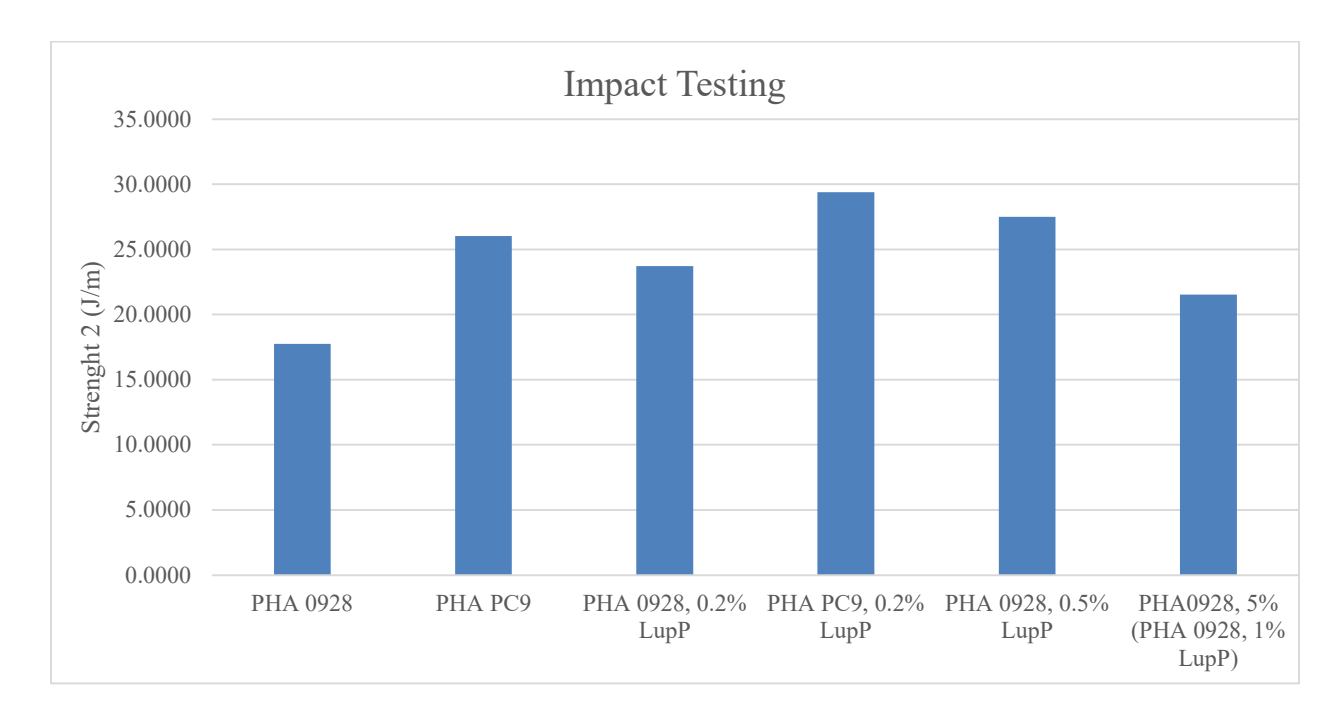


Figure 2.22. The effect of reactive extrusion on PHA6 and PHA8 impact strength. As witnessed in the above table and graph, there does not appear to be a noticeable trend correlating reactive extrusion of PHA6 and PHA8 and impact strength.

# 2.3.8 Analytical Method Development

Analytical method development is done determine leftover Luperox P concentration in extruded samples. A standard curve of Luperox P concentrations that undergo the methanolysis process described in the methods section above. Methnaolysis is a process in which Fischer

esterification is done, and the heat allows for homolytic cleavage of the peroxide. After methanolysis is complete, the chloroform layer is extracted and injected into the GC-MS instrument. The compound of interest is methyl benzoate, mz = 136 g/mol, and elutes at the 8-minute mark.

Figure 2.23. Homolytic cleavage followed by methanolysis of tert-butyl peroxybenzoate.

The standard curve is complete with several concentrations by beginning with a stock solution of 250 ppm and then diluted in ½ increments from 250ppm-7ppm. These samples go through the methanolysis process and are injected into the GC instrument, and the peak of interest are integrated. The integrated values correspond to the original concentration and a standard curve can be constructed. The plot is set with y-intercept equal to zero.

Table 2.7. Concentration of Luperox P in (ppm) and the corresponding peak integration on GC

Conc. LupP (ppm)	Integration Area
200	16818.4
100	6275.4
125	9081.1
62.5	5814.7
50	3899.8

44

31.25	2932.2
15.625	1481.6
7.8125	643.174

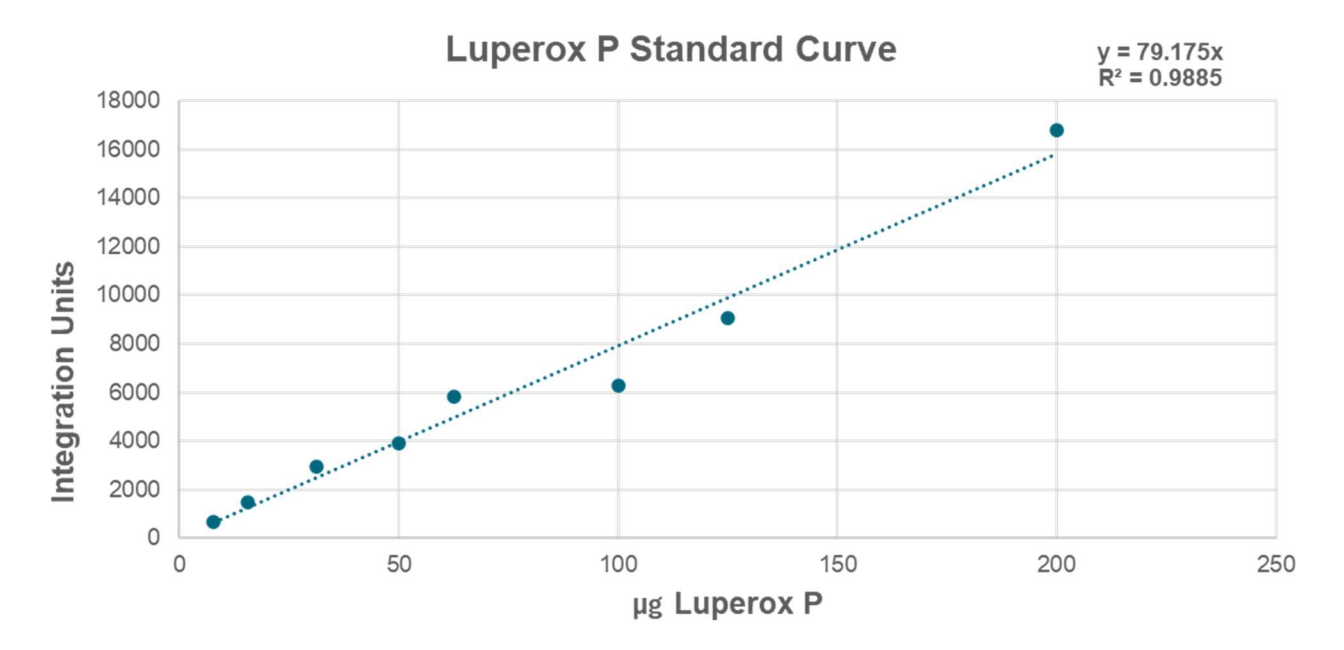


Figure 2.24 Standard curve of Luperox P.

Samples of PHA that have undergone reactive extrusion are then dissolved, subjected to methanolysis, and the peak at 8 minutes is integrated. The integration value is inserted into the standard curve equation to determine the exact concentration of Luperox P leftover in the PHA samples. It is important to know if there is a high amount of residual peroxide because it is toxic and its degradation products include benzene, which is a carcinogen. Although t-butyl perbenzoate was found to be only mildly toxic, localized to the site of dermal contact, it is still unclear if it is linked to cancer.<sup>27, 28</sup>

This standard curve was then used to determine residual concentration of Luperox P in various reactive extrusion samples. These samples include PHA6 and PHA8 extruded with PLA. Due to the very low concentration of LP anticipated to be left behind in these extruded samples,

the polymers were dissolved in a 10x abundance, to enhance the peaks, a lead to more accurate integration values. The increase in sample size from 10 mg. to 100 mg. means that the concentration of Luperox P calculated from the standard curve is divided by a factor of 10 to account for this concentration increase. The methanolysis process works by breaking down the polymer into monomer through acid hydrolysis, and then any carboxylic acid groups then undergo Fisher esterification. After the reflux time of 2.5 hours, the samples are cooled, and an aqueous workup is. The chloroform layer is then placed into a GC autosampler vial, and the standard Fame method is run with a HP GC instrument under Helium gas. The intensity of the methyl benzoate peak of interest is low, but the signal to noise ratio allows for accurate integration. The limit of detection for the instrument for this compound is 7 ppm. Using the line of best fit from the standard curve, the integration of the peak at 8 minutes was plugged into "y," and "x" is solved for.

Table 2.8. Summary of residual LP in extruded samples post methanolysis.

Sample Name	Residual Peroxide (ppm)	% consumed	% remaining
PHA6, 0.2% LP	218.38	89.08	10.92
PHA8 0.2% LP	216.78	89.16	10.84
PHA6, 0.5% LP	1625.22	67.50	32.50
PHA8, 0.5% LP	365.92	92.68	7.32
10% 1PHA <sub>8</sub> /9PLA, 90% <b>PHA6</b> , 0.2% LP	391.17	80.44	19.56
10% 1PHA <sub>8</sub> /9PLA, 90% <b>PHA8</b> , 0.2% LP	134.52	93.27	6.73

As a general trend, there is a higher amount of leftover Luperox P in the PHA6 samples as opposed to the PHA8 samples, potentially indicating that the PHA8 is more reactive towards

REX because more LP was consumed by the PHA8 samples under the same extrusion conditions.

#### 2.4 Conclusions

The findings in this project suggest that utilizing a two-step extrusion technique helps compatibilze PHB-HHx and PLA, leading to a more flexible polymer. Strain at break, quantified through tensile testing, was improved by over 400% when 10% of a PLA-PHA blend was reactively extruded into PHA in the presence of the radical initiator, tert-butyl peroxybenzoate. The two-step extrusion approach was found to be five times more effective than simple blending of PHA and PLA, and much more effective than a one-step reactive extrusion. Utilizing the precompatibilization step leads to much better tensile properties, leading to a sample that is PHB-HHx dominant (90 wt%) and 5 times more flexible than neat PHB-HHx. Future directions of this project include biodegradation testing. Since PLA is only industrially compostable while PHA is home compostable, respirometry studies must be done to determine is the incorporation of PLA hinders the biodegradation of PHA. Additionally, the residual tert-butyl peroxybenzoate could cause issues with degradation as the radical peroxide could be toxic to the microorganisms in the soil.

The goal of this project was to improve the strain at break of PHB-HHx by using PLA and a radical initiator, and this goal was achieved. However, the limitations of this study include many variables that can be difficult to control when it comes to reactive extrusion. Resonance time in the extruder will highly influence the extent of new bond formation, and this resonance time can be difficult to control, even in a small academic setting. More work needs to be done to control the resonance time and therefore have more consistent results across samples.

#### 2.5 References

- (1) Lebreton, L.; Slat, B.; Ferrari, F.; Sainte-Rose, B.; Aitken, J.; Marthouse, R.; Hajbane, S.; Cunsolo, S.; Schwarz, A.; Levivier, A.; et al. Evidence that the Great Pacific Garbage Patch is rapidly accumulating plastic. *Scientific Reports 2018 8:1* **2018-03-22**, *8* (1). DOI: 10.1038/s41598-018-22939-w.
- (2) Kozlov, M. Your brain is full of microplastics: are they harming you? *Nature 2025 638:8050* **2025-02-11**, *638* (8050). DOI: 10.1038/d41586-025-00405-8.
- (3) Sajjad, M.; Huang, Q.; Khan, S.; Khan, M. A.; Liu, Y.; Wang, J.; Lian, F.; Wang, Q.; Guo, G. Microplastics in the soil environment: A critical review. *Environmental Technology & Innovation* **2022/08/01**, *27*. DOI: 10.1016/j.eti.2022.102408.
- (4) Rosenboom, J.-G.; Langer, R.; Traverso, G.; Rosenboom, J.-G.; Langer, R.; Traverso, G. Bioplastics for a circular economy. *Nature Reviews Materials 2022 7:2* **2022-01-20**, *7* (2). DOI: 10.1038/s41578-021-00407-8.
- (5) Enumo, A.; Gross, I. P.; Saatkamp, R. H.; Pires, A. T. N.; Parize, A. L. Evaluation of mechanical, thermal and morphological properties of PLA films plasticized with maleic acid and its propyl ester derivatives. *Polymer Testing* **2020/08/01**, *88*. DOI: 10.1016/j.polymertesting.2020.106552.
- (6) Chavez, B. A.; Raghavan, V.; Tartakovsky, B. A comparative analysis of biopolymer production by microbial and bioelectrochemical technologies. *RSC Advances* 2022 Jun 1, 12 (25). DOI: 10.1039/d1ra08796g.
- (7) Widjaja, T.; Hendrianie, N.; Nurkhamidah, S.; Altway, A.; Yusuf, B.; F, F.; Alifatul, A.; Pahlevi, A. Poly lactic acid production using the ring opening polymerization (ROP) method

- using Lewis acid surfactant combined iron (Fe) catalyst (Fe(DS)3). *Heliyon* **2023 Jul 7**, *9* (8). DOI: 10.1016/j.heliyon.2023.e17985.
- (8) Swetha, T. A.; Ananthi, V.; Bora, A.; Sengottuvelan, N.; Ponnuchamy, K.; Muthusamy, G.; Arun, A. A review on biodegradable polylactic acid (PLA) production from fermentative food waste Its applications and degradation. *International Journal of Biological Macromolecules* **2023/04/15**, *234*. DOI: 10.1016/j.ijbiomac.2023.123703.
- (9) Hador, R.; Shuster, M.; Venditto, V.; Kol, M. Stereogradient Poly(Lactic Acid) from meso-Lactide/L-Lactide Mixtures. *Angewandte Chemie International Edition* **2022/10/04**, *61* (40). DOI: 10.1002/anie.202207652.
- (10) Zytner, P.; Zytner, P.; Kumar, D.; Kumar, D.; Elsayed, A.; Elsayed, A.; Mohanty, A.; Mohanty, A.; Ramarao, B. V.; et al. A review on polyhydroxyalkanoate (PHA) production through the use of lignocellulosic biomass. *RSC Sustainability* **2023/11/30**, *1* (9). DOI: 10.1039/D3SU00126A.
- (11) Agnew, D. E.; Pfleger, B. F. Synthetic biology strategies for synthesizing polyhydroxyalkanoates from unrelated carbon sources. *Chemical engineering science* **2012 Dec 19**, *103*. DOI: 10.1016/j.ces.2012.12.023.
- (12) Chacón, M.; Wongsirichot, P.; Winterburn, J.; Dixon, N. Genetic and process engineering for polyhydroxyalkanoate production from pre- and post-consumer food waste. *Current Opinion in Biotechnology* **2024/02/01**, *85*. DOI: 10.1016/j.copbio.2023.103024.
- (13) McAdam, B.; Fournet, M. B.; McDonald, P.; Mojicevic, M. Production of Polyhydroxybutyrate (PHB) and Factors Impacting Its Chemical and Mechanical Characteristics. *Polymers* **2020 Dec 4**, *12* (12). DOI: 10.3390/polym12122908.

- (14) Tang, H. J.; Neoh, S. Z.; Sudesh, K. Frontiers | A review on poly(3-hydroxybutyrate-co-3-hydroxyhexanoate) [P(3HB-co-3HHx)] and genetic modifications that affect its production. Frontiers in Bioengineering and Biotechnology 2022/12/05, 10. DOI: 10.3389/fbioe.2022.1057067.
- (15) Fabra, M. J.; Sánchez, G.; López-Rubio, A.; Lagaron, J. M. Microbiological and ageing performance of polyhydroxyalkanoate-based multilayer structures of interest in food packaging. LWT - Food Science and Technology 2014/12/01, 59 (2). DOI: 10.1016/j.lwt.2014.07.021.
- (16) Srubar, W. V.; Wright, Z. C.; Tsui, A.; Michel, A. T.; Billington, S. L.; Frank, C. W. Characterizing the effects of ambient aging on the mechanical and physical properties of two commercially available bacterial thermoplastics. *Polymer Degradation and Stability* **2012**/**10**/**01**, 97 (10). DOI: 10.1016/j.polymdegradstab.2012.04.011.
- (17) Chandra, R.; Thakor, A.; Mekonnen, T. H.; Charles, T. C.; Lee, H.-S. Production of polyhydroxyalkanoate (PHA) copolymer from food waste using mixed culture for carboxylate production and Pseudomonas putida for PHA synthesis. *Journal of Environmental Management* **2023/06/15**, *336*. DOI: 10.1016/j.jenvman.2023.117650.
- (18) Werker, A.; Bengtsson, S.; Korving, L.; Hjort, M.; Anterrieu, S.; Alexandersson, T.;

  Johansson, P.; Karlsson, A.; Karabegovic, L.; Magnusson, P.; et al. Consistent production of high quality PHA using activated sludge harvested from full scale municipal wastewater treatment PHARIO. *Water Science and Technology* 2018/12/28, 78 (11). DOI: 10.2166/wst.2018.502.

  (19) Oksiuta, Z.; Jalbrzykowski, M.; Mystkowska, J.; Romanczuk, E.; Osiecki, T. Mechanical and Thermal Properties of Polylactide (PLA) Composites Modified with Mg, Fe, and Polyethylene (PE) Additives. *Polymers* 2020 Dec 9, 12 (12). DOI: 10.3390/polym12122939.

- (20) Vanheusden, C.; Samyn, P.; Goderis, B.; Hamid, M.; Reddy, N.; Ethirajan, A.; Peeters, R.; Buntinx, M.; Vanheusden, C.; Samyn, P.; et al. Extrusion and Injection Molding of Poly(3-Hydroxybutyrate-co-3-Hydroxyhexanoate) (PHBHHx): Influence of Processing Conditions on Mechanical Properties and Microstructure. *Polymers 2021, Vol. 13, Page 4012* **2021-11-20**, *13* (22). DOI: 10.3390/polym13224012.
- (21) Lambla, M. Reactive Extrusion. *Rheological Fundamentals of Polymer Processing* **1995**. DOI: 10.1007/978-94-015-8571-2 20.
- (22) Augé, M.-O.; Roncucci, D.; Bourbigot, S.; Bonnet, F.; Gaan, S.; Fontaine, G. Recent advances on reactive extrusion of Poly(lactic acid). *European Polymer Journal* **2023/02/07**, *184*. DOI: 10.1016/j.eurpolymj.2022.111727.
- (23) Phiri, M. M.; Phiri, M. J.; Formela, K.; Wang, S.; Hlangothi, S. P. Grafting and reactive extrusion technologies for compatibilization of ground tyre rubber composites: Compounding, properties, and applications. *Journal of Cleaner Production* **2022/10/01**, *369*. DOI: 10.1016/j.jclepro.2022.133084.
- (24) Mississippi, U. o. S. *Miscible Polymer Blends*. 2005. https://www.pslc.ws/mactest/blend.htm (accessed 2025.
- (25) Fisher, T. <a href="https://www.thermofisher.com/order/catalog/product/567-7600">https://www.thermofisher.com/order/catalog/product/567-7600</a> (accessed.
- (26) Alasfar, R. H.; Ahzi, S.; Barth, N.; Kochkodan, V.; Khraisheh, M.; Koç, M.; Alasfar, R. H.; Ahzi, S.; Barth, N.; Kochkodan, V.; et al. A Review on the Modeling of the Elastic Modulus and Yield Stress of Polymers and Polymer Nanocomposites: Effect of Temperature, Loading Rate and Porosity. *Polymers 2022, Vol. 14, Page 360* **2022-01-18**, *14* (3). DOI: 10.3390/polym14030360.

- (27) Matthews, H. B. NTP Technical Report on Toxicity Studies of t-butyl perbenzoate. *NIH Publication No. 92-3134* **1992**, (No. 92-3134), 23. (accessed 3/19/2025).
- (28) Health, N. J. D. o. Hazardous Substance Fact Sheet; 2000.

https://nj.gov/health/eoh/rtkweb/documents/fs/1794.pdf (accessed 3/19/2025).

#### CHAPTER 3

# POLYESTER SYNTHESIS TO UNDERSTAND STRUCTURE-PROPERTY RELATIONSHIPS

# 3.1 Introduction

Polyesters are a common class of polymers that have the potential to be biodegradable and biocompatible. Biodegradability is dependent on many factors including chemical structure, molecular weight, crystallinity, and the environment the polymer is exposed to.<sup>2</sup>

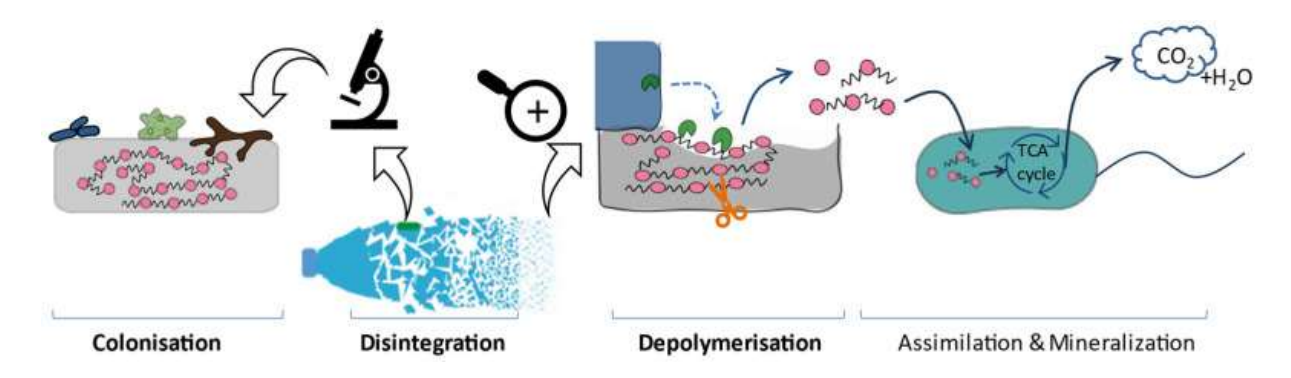


Figure 3.1. Types of degradation for polymers that are biodegradable.<sup>2</sup>

Not all polyesters are biodegradable, however polyesters can be hydrolyzed back into monomers, leading to a viable chemical recycling option.<sup>2</sup> Additionally, monomers can be sources from either biological or renewable sources, especially the dialcohol component. This is desirable because even if the polymer formed is not biodegradable, monomers sourced from renewable resources. For example, 2,3-butanediol is a natural metabolite formed from bacterial fermentation using a variety of renewable carbon sources such as xylose, glucose, and corn.<sup>3</sup> Sourcing monomers from natural makes them more likely to biodegrade because enzymes may already be present in nature that can biodegrade the polymer. Keeping these factors in mind, this

project aims to explore polycondensation polymerization to form various copolymers from potentially biobased monomers.

## 3.1.1 Polymer Chain Length and Melting Temperature

It is common for longer chain polyesters to have higher melting points due to tighter and more dense packing. These polymers have elevated T<sub>g</sub> values as well due to the tighter packing restricting segmental motion.<sup>4</sup> However, this is not always the case, as polybutylene succinate displays higher melting point and crystallinity than both polybutylene azelate and polybutylene sebacate, even though the latter two polymers have a longer carbon chain length.<sup>5</sup> This may be in part due to the fact that both the diacid and diol contain the same number of carbons (4) in polybutylene succinate, allowing for tighter packing. Due to the higher crystallinity and melting temperature, polybutylene succinate shows the slowest rate of potential biodegradation of the three polyesters describe in the study.<sup>5</sup>

Although a sacrifice could be made on biodegrading with high melting points, different applications of the polymers will require different melting points. For example, if a polymer is to be used in packaging and needs to be stored in a refrigerator or freezer, the melting point and Tg need to be tuned so that it does not become too glassy and brittle under those low temperatures. Likewise, if a plastic is to be used in an outdoor setting, such as a handle on a shovel, it needs to be able to withstand elevated temperatures without melting in the hand or losing its properties. Therefore, it is important to continue researching structure-property relationships. This chapter dives deep into the structure-property relationships of a small library of polyesters including several copolymers with up to 4 different diacids in one formulation, and up to 2 different diols in one formulation. Several diacids and diols are polymerized using bulk polycondensation and properties such as melting temperature, crystallinity, and tensile properties are measured.

Figure 3.2. Esterification and polycondensation scheme for a dicarboxylic acid and di-alcohol.

Step growth polymerization is a polymerization technique that is sometimes referred to as polycondensation due to reactions producing a by-product such as water or methanol that needs to be removed to drive the reaction forward. Polycondensation reactions are desirable because they can be done in bulk, without solvent, making it a greener process. However, step growth polymerization is astronomically slower than their counterpart reaction—chain growth polymerization. Chain growth polymerization, also called radical polymerization, is a very fast and exothermic process in which molecular weight is built very quickly. These reactions typically require solvents to disperse heat and allow for mixing despite high viscosity early in the reaction. Transesterification must occur before the melt polycondensation step, leading to a completely random copolymer.

# 3.1.2 Research Aims

In this chapter, potentially biobased, commercially available monomers are polymerized through polycondensation to yield polyesters with varying crystallinities. Crystallinity is directly related to thermal properties. Structure character relationships are evaluated using differential scanning calorimetry (DSC) to understand the effect of carbon chain length of the monomers on crystallinity, glass transition temperature, and melting temperature of the polymer. Tensile testing is conducted on a select few to assess Young's modulus and strain at break properties.

#### 3.2 Materials and Methods:

#### 3.2.1 Materials

The dicarboxylic acid monomers used include succinic acid (4C), glutaric acid (5C), adipic acid (6C), suberic acid (8C), azelaic acid (9C), 98% pure sourced from Ambeed, sebacic acid (10C), 98% pure sourced from Ambeed, and itaconic acid. The diols used include 1,3-propanediol (3C), 1,3-butanediol (4C), 1,4-butanediol (4C), 1,5-pentanediol (5C), 1,8-octanediol (8C). There was one AB monomer used that has one carboxylic acid group and one alcohol group, capable of forming a homopolymer with itself. (S) 2-hydroxypropanoic acid, sourced from Ambeed. zirconium t-butoxide in butanol sourced from Ambeed.

Figure 3.3. Structures of monomers used for polycondensation polymerization reactions.

#### 3.2.2 Polycondensation Setup

The reaction set-up included one 250 mL 3-neck round bottom flask, one short path condenser, one 100 mL catch flask, one mechanical stirrer with metal rod and metal blade, one stirrer vacuum adaptor, one Schlenk line, one vacuum pump (Welch). Cold water flowed through the condenser, and a methanol/dry ice trap was used to prevent volatiles from entering the

vacuum pump. To control temperature, a heating mantle and J-Kem with temperature probe were used to hold temperatures and conduct a temperature ramp.



Figure 3.4. The reactor setup for polycondensation.

# 3.2.3 Polycondensation Procedure

Reactions were typically done at 1 mol. scale, between 120 - 150 g. of starting material. 5 mol% excess diol was used. The reactions began with vacuum-nitrogen backfill done twice once reactants melted, followed by a 15 °C/hr. ramp to 180 °C, and mechanically stirred under N<sub>2</sub> gas for 12 hrs. Pressure on the system was reduced pressure to 100-200 millitorr for 1.5-2 hrs., driving off excess water to prevent poisoning of the catalyst. The zirconium tert-butoxide catalyst was next added in 0.5 mol% abundance, and temperature was increased to 200 °C. After the polymer built enough viscosity, the temperature was increased to 210 °C, to help lower viscosity and promote efficient stirring. Once the polymer became difficult to stir due to its high viscosity and exhibited the Weissenberg Effect, a phenomenon in which the polymer creeps up the stir rod, the reaction was finished.

#### 3.2.4 GPC

Molecular weight was obtained using a Shimadzu Prominence UFLC GPC, using HPLC-grade chloroform as the mobile phase. Polyester samples are dissolved in HPLC grade chloroform in 2 mg/mL concentrations, filtered through a 0.22 µm PTFE syringe filter, and injected into the column using the autosampler. The reference for the calibration curve is polystyrene.

#### 3.2.5 NMR

Bruker 600 MHz NMR was used to confirm copolymer ratios. Samples were dissolved in deuterated chloroform in 10 mg/mL concentrations.

# 3.2.6 Thermal Characterization

TA instruments Discovery 250 differential scanning calorimeter used transition temperatures and enthalpy values. Samples were equilibrated at -80 °C, heat ramped 10 °C/min to 150 °C, then cooled 10 °C/min to -20 °C. For tensile bar samples, samples were equilibrated at 23 °C, ramped 10 °C/min to 150 °C, then cooled 10 °C/min to -80 °C, then heated a second time to 150 °C.

# 3.2.7 Extrusion

Thermo Scientific Haake extruder and Thermo Scientific Minijet injection molder was used form ASTM type V dog bones for tensile testing.

# 3.2.8 Mechanical Properties

Shimadzu AGS-X tensile tester was used to pull ASTM type V dog bones at a rate of 10 mm/min. Samples were aged 1-2 days before testing and tested again between 7-8 days post injection molding.

#### 3.3 Results and Discussion:

# 3.3.1 Odd-Even Characteristics

Polymers can demonstrate either an even-even or odd-even effect depending on the number of carbons present in both monomers.<sup>9</sup> For example, if both a diol and diacid have an even number of carbons, the resulting polymer has even-even characteristics.<sup>5, 10</sup> However, if one of the two monomer possesses an odd number, interesting characteristics arise. Instead of a linear correlation between increasing carbon chain length and increasing crystallinity and melting temperature, there is a dip when it comes to odd-even polymers.<sup>9</sup>

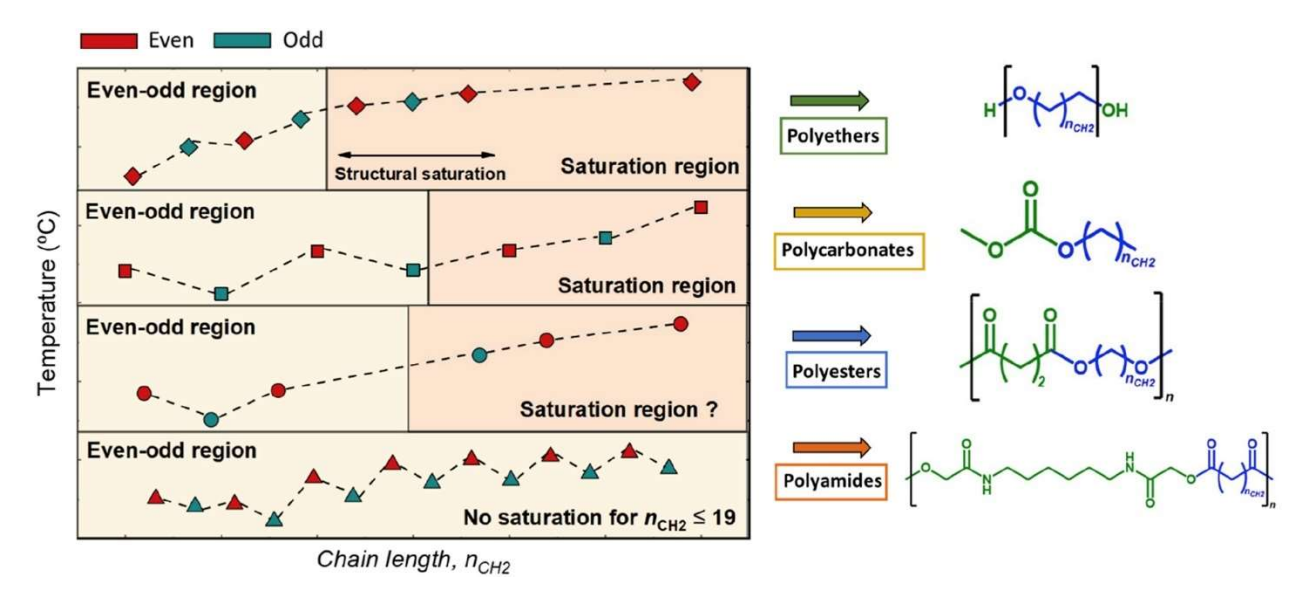


Figure 3.5. The odd-even effect in various polymers.<sup>9</sup>

For even-even polyesters, every other carbonyl is pointing in the same direction, and the dipole moment that creates a partial positive on the carbonyl carbon and a partial negative on the oxygen draw the chains closer together, increasing crystallinity, and therefore increasing  $T_g$  and  $T_m$ . The chains can pack tighter together when the carbonyl alternates "up" and "down," leading to a higher melting point. In figure 3.6 below, the polycondensation of azelaic acid (9C) with 1,4-butanediol (4C) is compared to sebacic acid (10C) and 1,4-butanediol.

polybutylene azelate

$$HO \longrightarrow OH \longrightarrow HO \longrightarrow OH \longrightarrow OH$$

Figure 3.6. Odd-even versus even-even for polybutylene azelate and polybutylene sebacate.

In both cases, the partial negative on the carbonyl oxygens attract the partial positive on the carbonyl carbon, leading to London Dispersion intermolecular forces. However, these forces are stronger and lead to tighter packing in the case of sebacic acid and 1,4-butanediol since the carbonyls point in alternating directions, sterically allowed for closer chain interaction. This is evidenced by a 20 °C higher melting temperature for polybutylene sebacate as compared to polybutylene azelate.

# 3.3.2 Copolymers

The copolymers are formed by bulk polycondensation polymerization with 5 mol% excess diol to promote full conversion and to compensate if any diol is prematurely distilled over. Sufficient vacuum pressure is prioritized by utilizing a surplus of vacuum grease, to ensure the water is driven off and the reaction proceeds forward. The catalyst used is zirconium t-butoxide in butanol at a concentration of 0.5 mol%. This catalyst was chosen because of its approval for use in food-grade polymers and has been shown to work well with these reactions.

A variety of diacids and diols are used to form the polyesters and have either an odd number of carbons in the backbone, or an even number of carbons. 23 distinct polyesters were synthesized

and characterized, with many of them copolymers. The copolymers produced are shown below in table 3.1. Tensile testing is shown for some of the semi-crystalline polymers.

Table 3.1. List of homopolymers and copolymers synthesized via polycondensation reactions polymerized with Zirconium tert-butoxide catalyst in 0.005 mol eq. abundance.

Polyester or Copolyester	Characterization	T <sub>m</sub> or T <sub>g</sub>	Tc	Molecular Weight (Da)	Tensile Properties:
0.25 mol eq. succinic acid, 0.25 mol eq. glutaric acid, 0.25 mol eq. azelaic acid, 0.25 mol eq. azelaic acid, 0.25 mol eq. sebacic acid, 1.05 mol eq. 1,4-butanediol	Waxy, semi- crystalline	28.16 °C	9.5 °C	120,997	1,000%
0.25 mol eq. azelaic, 0.25 mol eq. sebacic, 0.50 mol eq. glutaric, 1.05 mol eq. 1,4-BDO	Semi-crystalline	29.1 °C	10.5 °C	127,524	500%
Sebacic acid, 1,4- butanediol	Semi-crystalline	66.59 °C	45.83 °C	54,139	7%
Sebacic acid, 1,8-octanediol	Semi-crystalline	71.31 °C	54.56 °C	83,000	5%
Azelaic acid, 1,5- pentanediol	Semi-crystalline	49.8 °C	28.9 °C	73,220	40%
0.25 mol eq. succinic acid, 0.25 mol eq. glutaric acid, 0.25 mol eq. azelaic acid, 0.25 mol eq. azelaic acid, 0.25 mol eq. sebacic acid, 1.05 mol eq. 1,4-butanediol, 0.01 mol eq. itaconic acid	Semi-crystalline	27.4 °C	9.7 °C	26,009	40%
1 mol eq. azelaic acid, 1 mol eq. lactic acid, 1.05 mol eq. 1,4-butanediol	Low-melting semi-crystalline	12.27 °C	-33.13 °C	80,143	-
1 mol eq. sebacic acid, 1 mol eq. lactic acid, 1.05 mol eq. 1,4-butanediol	Low-melting semi-crystalline	36 °C	9 °C	73,928	-

0.25 mol eq. sebacic acid, 0.75 mol eq. glutaric acid, 0.5 mol eq. 1,3-propanediol, 0.5 mol eq. 1,4-butanediol	Amorphous	-59.77 °C	N/A	68,589	-
Adipic acid, 1,3-BDO	Amorphous	-48.54 °C	N/A	70,000	-
Adipic acid, 1,4-BDO	Semi-crystalline	49 °C	30 °C	65,589	-
1.0 mol eq. azelaic acid, 1.05 mol eq. 1,3-BDO	Amorphous	-55 °C	N/A	70,501	-
1.0 mol eq. azelaic acid, 1.05 mol eq. 1,4-BDO	Semi-crystalline	49 °C	25 °C	132,724	-
0.125 mol eq. sebacic, 0.125 mol eq. azelaic acid, 0.75 mol eq. glutaric acid, 0.25 mol eq. 1,3-PDO, 0.75 mol eq. 1,4-BDO	Amorphous	-61 °C	N/A	62,349	-
0.50 mol eq. glutaric, 0.50 sebacic mol eq., 1.05 mol eq. 1,4-BDO	Semi-crystalline	43.3 °C	24.2 °C	71,486	-
1 mol eq. sebacic acid, 1.05 mol eq. 1,4-BDO, 0.01 mol eq. itaconic acid	Semi-crystalline	72 °C	53 °C	73,464	-
1 mol eq. sebacic acid, 1.05 mol eq. 1,4-BDO, 0.02 mol eq. itaconic acid	Semi-crystalline	72 °C	53 °C	103,021	-
0.25 mol eq. sebacic, 0.75 mol eq. glutaric, 1.05 mol eq. 1,4-BDO	Semi-crystalline	35.2 °C	9.9 °C	30,681	-
<ul><li>0.25 mol eq. sebacic,</li><li>0.75 mol eq. glutaric,</li><li>1.05 mol eq. 1,3-PDO</li></ul>	Semi-crystalline	27. 6 °C	N/A	32,816	-
<ul><li>0.25 mol eq. azelaic,</li><li>0.75 mol eq. glutaric,</li><li>1.05 mol eq. 1,4-BDO</li></ul>	Semi-crystalline	23.8 °C	-3.3 °C	45,062	-
0.50 mol eq. azelaic, 0.50 mol eq. glutaric, 1.05 mol eq. 1,4-BDO	Semi-crystalline	29.7 °C	9.6 °C	80,486	-
Suberic acid, 1,8-octanediol	Semi-crystalline	66.9 °C	50 °C	80,000	-
Suberic acid, 1,4-BDO	Semi-crystalline	55.3 °C	30 °C	138,000	-

If both the diacid and diol have the same number of carbons, there will be a very ordered structure in which every carbonyl is matched perfectly with another carbonyl, increasing crystallinity. When the diacid and diol do not have the same number of carbons in the backbone, there will not be a perfect 1:1 match between every carbonyl, leading to more disorder. This is further exacerbated when one monomer has an even number of carbons and the other has an odd number of carbons. Now, instead of every carbonyl lining up, it may be every other, or once every three that line up. Therefore, there are less frequent dipole-dipole interactions between carbonyls, thus decreasing crystallinity,  $T_g$ , and  $T_m$ . In this work, the even-odd polymers tend to be fully amorphous, so a melting temperature is not observed, while the odd-odd and even-even polyesters are semi-crystalline. Expanding on this idea, it is generally observed throughout this project that the odd-odd polymers have a lower  $T_m$  than the even-even, and the even-odd have the lowest  $T_m$ , sometimes not having one due to being completely amorphous.

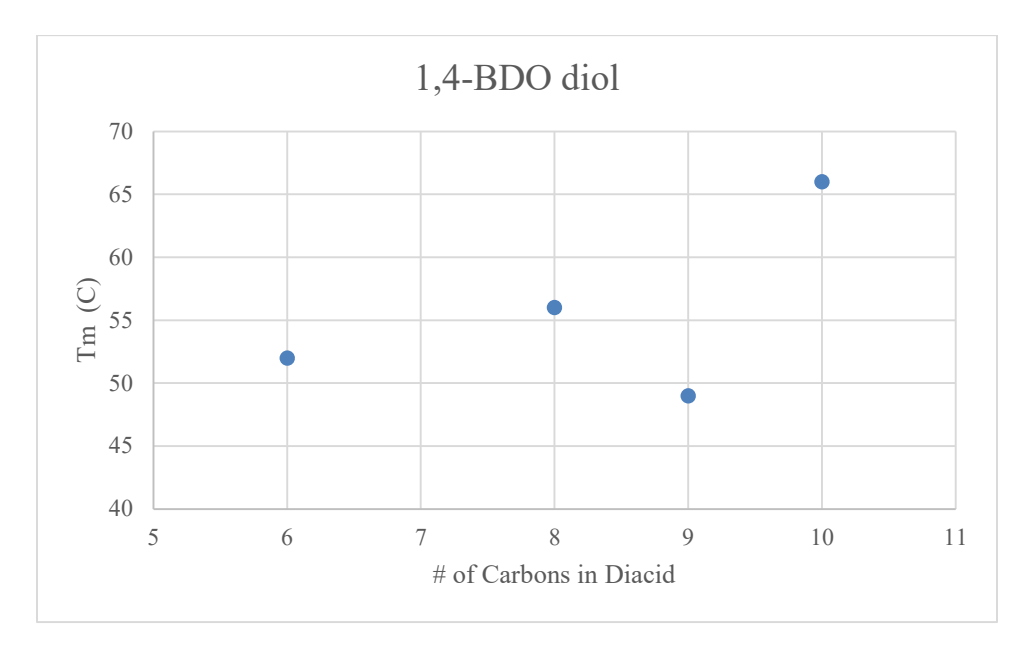


Figure 3.7. The relationship between carbon length in backbone of diacid monomer and melting point is shown.

As shown in the above graph showing experimental data, increasing the carbon chain length of the diacid monomer increases the melting temperature in a linear fashion for the even diacids. However, this linear trend falters in the case of the odd carbon number diacid. When azelaic acid (9C) is polymerized with 1,4-butanediol (4C), the melting temperature is 49 °C, which is even lower than adipic acid (6C) polymerized with 1,4-butanediol (4C), which has a melting point of 52 °C. In contrast, suberic acid (8C) and sebacic acid (10C) have much higher melting points of 56 °C and 66 °C respectively. This trend is similar for odd-odd polyesters. There is a linear increase in melting temperature with increasing carbon chain among odd-odd polyesters, but overall, there are lower melting temperatures than even-even polyesters.

The figure below is a summary of melting endotherms of various polymers synthesized in this study.

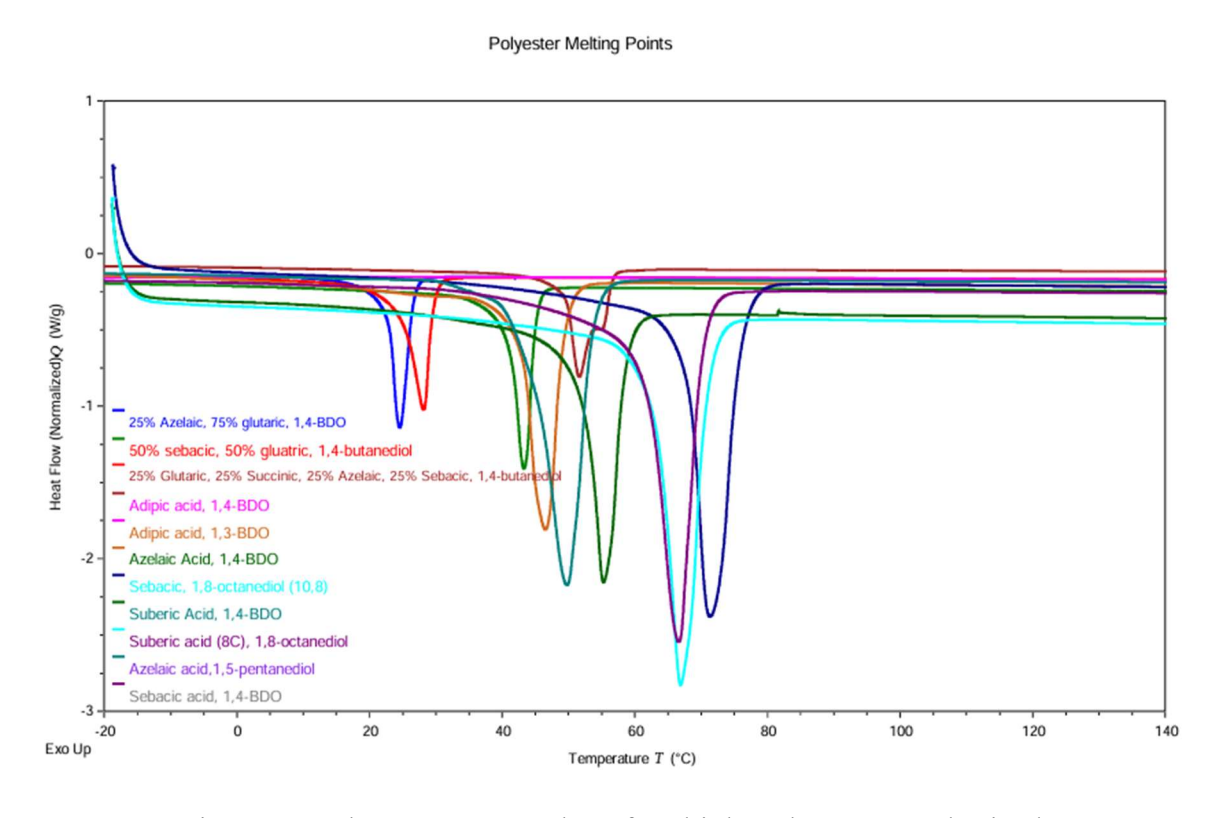


Figure 3.8. Thermogram overlay of multiple polyesters synthesized.

The melting point was increased from  $\sim$ 25 °C to  $\sim$ 72 °C by increasing the number of carbons in the backbone chain of the diacid monomers. Understanding this structure-property relationship is important.

### 3.3.3 Assessing Mechanical Properties

Some of the semi-crystalline polymers were extruded and injection molded in order to obtain dog bones for tensile properties. Similarly, as seen in the previous chapter, the Young's Modulus and strain at break are monitored to observe the mechanical properties. The tensile properties can correspond to crystallinity because high Young's Modulus and low elongation at break indicate high crystallinity. Differential scanning calorimetry is done to further discover information about the crystallinity and transition temperatures. Additionally, DSC is done to determine the effect of aging on crystallinity overtime. As shown in table 3.1 above, the copolyester that is 0.25 mol eq. succinic acid, 0.25 mol eq. glutaric acid, 0.25 mol eq. azelaic acid, 0.25 mol eq. sebacic acid, 1.05 mol eq. 1,4-butanediol, demonstrates a high strain at break of over 1,000%, with very low Young's modulus of 0.05 GPa. Interestingly, when the copolymer ratios are changed to the formulation 0.25 mol eq. azelaic, 0.25 mol eq. sebacic, 0.50 mol eq. glutaric, 1.05 mol eq. 1,4-BDO, the strain at break is reduced by half, or around 500%. There is only one difference between these two polymers, the former has an equal mix of dicarboxylic acids with 4, 5, 9, and 10 carbons, and the latter is missing the 4-carbon monomer, so has 50% of the 5-carbon monomer, and same amounts of 9 and 10-carbons as the first one. This one difference has a drastic effect on the strain at break. Additionally, both copolymers have almost identical thermograms obtained by DSC, but likely the latter copolymer has higher crystallinity as evidenced by the *slightly* higher T<sub>m</sub> and much lower strain at break.



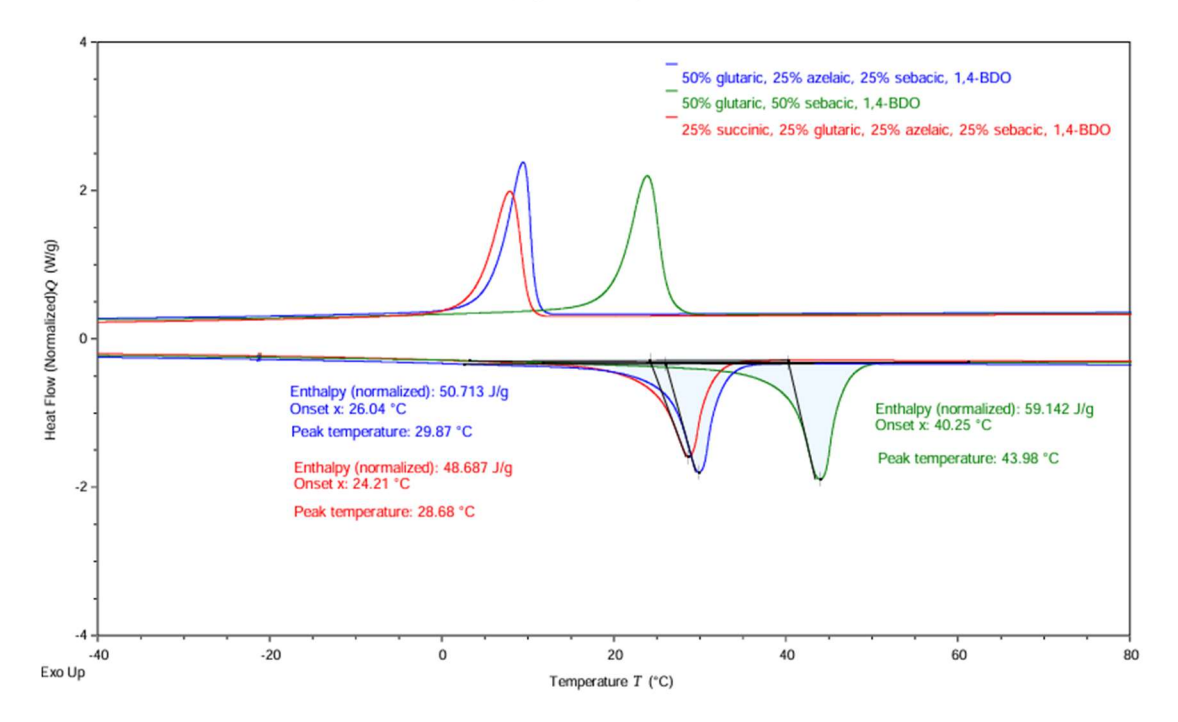


Figure 3.9. Melting and cooling DSC curves for three copolyesters.

Although all three of these copolyesters are composed of similar amounts of even and odd diacids, they display different tensile properties. Specifically focusing on the red and blue curves, these two polymers have almost the same thermogram, similar melting and crystallization temperatures and similar enthalpy. However, the red curve displays a strain at break of 1,000%, while the blue curve only has 500% strain at break. With an elongation at break that is half as long, one would assume that the blue curve would display much higher enthalpy/crystallinity, but this is not what is observed. More work needs to be done to understand the crystal structure and the reasons why such a large difference is seen between the two copolymers.

# 3.3.4 Considerations for biodegradability

It should be noted that although these polyesters are potentially biobased, depending on how the monomers were sourced, it is ideal for them to be biodegradable as well. Polyesters with lower carbons in the backbone (glutaric, succinic, example) have been shown to be

biodegradable (home compostable). Since the mechanism for biodegradation is for the bacteria to consume beginning at the ester groups, polymers with fewer ester bonds for the same molecular weight may have lower biodegradation. Biodegradation studies could be done in the future but is beyond the scope of this current study. These aspects are important factors to consider when designing target polymers.

#### 3.4 Conclusions

In this chapter, structure-property relationships of polyesters were explored by bulk polycondensation of various dicarboxylic acids and dialcohols. These monomers are commercially available, and many of them can potentially be derived from renewable sources. The odd-even and even-even effect was demonstrated by varying the diacid and dialcohol of many polyesters. A library of copolyesters were synthesized and their characteristics were reported, including thermal properties and tensile properties for some. More work needs to be done to understand why certain semi-crystalline copolyesters display more flexibility than others. The polyesters will be utilized as PHA additives in the next chapter.

#### 3.5 References

- (1) Prambauer, M.; Wendeler, C.; Weitzenböck, J.; Burgstaller, C. Biodegradable geotextiles An overview of existing and potential materials. *Geotextiles and Geomembranes* **2019/02/01**, *47* (1). DOI: 10.1016/j.geotexmem.2018.09.006.
- (2) Wang, Y.; Putten, R.-J. v.; Tietema, A.; Parsons, J. R.; Gruter, G.-J. M. Polyester biodegradability: importance and potential for optimisation. *Green Chemistry* **2024 Mar 5**, *26* (7). DOI: 10.1039/d3gc04489k.
- (3) Birkle, M.; Mehringer, H. S.; Nelson, T. F.; Mecking, S. Aliphatic Polyester Materials from Renewable 2,3-Butanediol. *ACS Sustainable Chemistry & Engineering* **February 23, 2024**, *12* (10). DOI: 10.1021/acssuschemeng.3c07665.
- (4) Harwood, H. J. Principles of polymerization(Odian, George). *Journal of Chemical Education* **1971**, *48* (11), A734. DOI: 10.1021/ed048pA734.1.
- (5) Kong, X.; Qi, H.; Curtis, J. M. Synthesis and characterization of high-molecular weight aliphatic polyesters from monomers derived from renewable resources. *Journal of Applied Polymer Science* **2014/08/05**, *131* (15). DOI: 10.1002/app.40579.
- (6) Korshak, V. V.; Vasnev, V. A. Experimental Methods of Solution Polymerization.

  Comprehensive Polymer Science and Supplements 1989/01/01. DOI: 10.1016/B978-0-08-096701-1.00151-8.
- (7) Sokołowska, M.; Molnar, K.; Puskas, J. E.; Fray, M. E. Improving the Sustainability of Enzymatic Synthesis of Poly(butylene adipate)-Based Copolyesters: Polycondensation Reaction in Bulk vs Diphenyl Ether. *ACS Omega* **September 4, 2024**, *9* (37). DOI: 10.1021/acsomega.4c00814.

- (8) Thomsen, L.; Jensen, L. R.; Yue, Y.; Østergaard, M. B. Crystallinity dependence of thermal and mechanical properties of glass-ceramic foams. *Journal of the European Ceramic Society* **2024/10/01**, *44* (13). DOI: 10.1016/j.jeurceramsoc.2024.05.079.
- (9) Pérez-Camargo, R. A.; Torres, J.; Müller, A. J. Understanding even-odd effects in linear semi-crystalline polymers: Polyethers, polycarbonates, polyesters, and polyamides. *Polymer* **2025/04/17**, *324*. DOI: 10.1016/j.polymer.2025.128233.
- (10) Papageorgiou, G. Z.; Bikiaris, D. N.; Achilias, D. S.; Papastergiadis, E.; Docoslis, A. Crystallization and biodegradation of poly(butylene azelate): Comparison with poly(ethylene azelate) and poly(propylene azelate). *Thermochimica Acta* **2011/03/10**, *515* (1-2). DOI: 10.1016/j.tca.2010.12.010.

#### **CHAPTER 4**

# BLENDING AND REACTIVE EXTRUSION OF ALIPHATIC POLYESTERS INTO POLYHYDROXYALKANOATES TO IMPROVE MECHANICAL PROPERTIES

#### 4.1 Introduction

In this chapter, several bio-based amorphous and semi-crystalline polyesters are blended and reactively extruded into PHB-HHx to improve strain at break and decrease aging compared to the control. The same strains of PHB-HHx used in chapter 1 are explored here: PHA6 which consists of ~6% hexanoate content, and PHA8 that consists of ~8% hexanoate content. The increase in hexanoate causes the PHA8 to be more amorphous, resulting in a much higher strain at break and lower Young's Modulus during tensile testing.

# Poly(3-hydroxybutyrate-*co*-3-hydroxyhexanoate)

Figure 4.1. Structure of poly(3-hydroxybutyrate-co-3-hydroxyhexanoate).

Hexanoate content influences the rate of nucleation and crystallization because these more amorphous regions allow for increased chain movements.  $^1$  This means that PHAs with a greater amount of hexanoate tend to have lower  $T_m$  lower glass transition temperature, lower tensile strength, and high elongation at break.  $^{1,2}$  The properties of PHA can be determined through differential scanning calorimetry to find percent crystallinity from the integration of the

melting enthalpy curve as compared to the theoretical 100% crystalline enthalpy value. Please note that this is a theoretical value because a polymer can never be 100% crystalline. Although PHA6 and PHA8 have differences in the amount of amorphous hexanoate copolymer, they have an almost identical T<sub>g</sub> of about 0 °C. However, PHA8 does exhibit a 3 times higher elongation at break.

A library of semi-crystalline and amorphous polyesters was synthesized in chapter 2, and six of these were explored as additives to PHA to make it more flexible. Amorphous polymers have been shown to decrease the crystallinity of a semi-crystalline polymer with blending.<sup>3</sup> However, blending polymers together can pose issues. For example, blending an amorphous polymer into a semi-crystalline polymer such as PHA, is typically immiscible due to the loss of entropy that mixing would cause.<sup>4</sup> Amorphous polymers have high entropy due to little order present in the crystal structure, therefore is it entropically unfavorable for an amorphous polymer to be fully miscible with a semi-crystalline polymer.<sup>4</sup> Take for example polypropylene and polyethylene; although these two polymers are both polyolefins, they are not miscible due it being entropically unfavorable.<sup>4</sup> In additional to thermodynamic considerations, polyolefins can crystallize into different crystal domains.<sup>5</sup> With polymers such as polyesters, hydrogen bonding interactions between two polymers can increase the miscibility, but this interaction must be stronger between the two to overcome self-association.<sup>6,7</sup> One way that miscibility can be measured is by measuring the glass transition temperature. Measuring a single glass transition temperature when two or more polymers are blended indicates miscibility.8

# 4.1.1 Experimental Design

There were a multitude of polyesters synthesized in chapter 2, and many were explored as PHA additives in a small-scale Haake trial, but only 6 were focused on as PHA additives when scaling

up the process 11 trial (these six are reported here in this chapter). The workflow for this experiment begins with the polycondensation of copolyesters, then six that were selected through a small-scale Haake extrusion trial are blended and reactively extruded into PHA using the Process 11. Next, the extrudate is cut and flushed through the Haake extruder and injection molded to form ASTM type V dog bones.

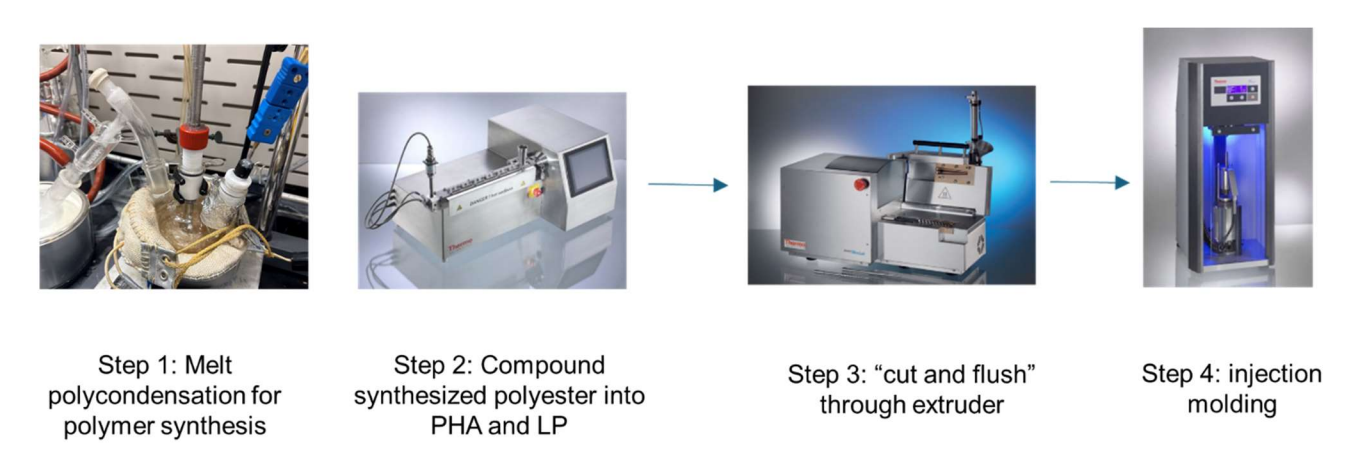


Figure 4.2. The workflow for using biobased long chain polyester as additives in PHA.<sup>9</sup> The six polyesters, named A-F, that were chosen are shown below. Recall that they were synthesized via polycondensation polymerization as described in the previous chapter.

Table 4.1. Six biobased polyesters that are evaluated as PHB-HHx additives.

Polyester	Code	Physical Characterization	T <sub>m</sub> or T <sub>g</sub>	Te	Molecular Weight
0.25 mol eq. succinic acid, 0.25 mol eq. glutaric acid, 0.25 mol eq. azelaic acid, 0.25 mol eq. sebacic acid, 1.05 mol eq. 1,4-butanediol	A	Waxy, semicrystalline	28.16 °C	9.5 °C	120,997
Sebacic acid, 1,4-butanediol	В	Semi-crystalline	66.59 °C	45.83 °C	54,139
Sebacic acid, 1,8-octanediol	C	Semi-crystalline	71.31 °C	54.56 °C	83,000

1 mol eq. azelaic acid, 1 mol eq. lactic acid, 1.05 mol eq. 1,4-butanediol	D	Low-melting semi-crystalline	12.27 °C	-33.13 °C	80,143
0.25 mol eq. sebacic acid, 0.75 mol eq. glutaric acid, 0.5 mol eq. 1,3-propanediol, 0.5 mol eq. 1,4-butanediol	E	Amorphous	-59.77 °C	N/A	68,589
Adipic acid, 1,3-BDO	F	Amorphous	-48.54 °C	N/A	70,000

Each type of polyester has a different purpose. The amorphous polyesters show high compatibility as additives to PHA, especially the PHA8, and they increase the strain at break of PHA8, making the polymer more ductile and less brittle. Additionally, the larger pockets of amorphous polymer between spherulites may help prevent secondary crystallization in PHA8, also known as aging. Aging in PHA is caused by slower secondary crystallization in which the polymer chain stiffens and embrittles overtime. Aging is severely noticed in the first week of processing and extrusion because the strain at break decreases by 30% for PHA6 and 70% for PHA8. Aging can happen due to stiffening of spherulites, as seen in figure 1.4. Aging also happens when the amorphous sections are given enough time to organize entangled chains into a lower energy formation, which may take multiple hours or days at room temperature. This phenomenon can be exacerbated by annealing or prevented by quenching. It has been shown in literature that additives such as PEG that act as plasticizers can slow down secondary crystallization of PHA.

As shown in chapter 2, the strain at break for PHA6, extruded at 150 °C, with a 70 °C mold, is 34% and the Young's modulus is 0.825 GPa. For PHA8, extruded at 150 °C and a 70 °C mold, the strain at break is 119% and the Young's modulus is 0.743 GPa. PHA8 is more amorphous due to the lower modulus and higher strain at break.

#### 4.2 Materials and Methods

#### 4.2.1 Materials

Copolyesters were synthesized through polycondensation polymerization as described previously in chapter 2. Other materials included poly(3-hydroxybutyrate-co-3-hydroxyhexanoate) with 6% hexanoate, named PHA6, and poly(3-hydroxybutyrate-co-3-hydroxyhexanoate) with 8% hexanoate, named PHA8, sourced from the New Materials Institute of the University of Georgia bioreactors. Equipment for extrusion Thermo Scientific Process 11 extruder, Thermo Scientific Haake extruder, Thermo Scientific Minijet injection molder.

#### 4.2.2 Peroxide Masterbatch Preparation

Individual masterbatches were made for each PHA. 10g. of PHA powder was suspended in acetone in a 250 mL round bottom flask. 0.4 g of Luperox P was added to the suspension, sonicated, and the acetone was rotovaped off. The resulting powder was placed under reduced pressure overnight to remove any remaining solvent. The final PHA masterbatch which contained 4 wt% peroxide, ready to be used for extrusion, and stored in the freezer to prevent loss of initiator.

#### 4.2.3 Extrusion Procedure

The Process 11 extruder was heated to 150 °C at all temperature zones, as this is the optimal temperature for PHB-HHX extrusion. The polyester additive was cut into small pieces and weighed out at 10, 20, and 30 wt% loadings. 35 g. of PHA/polyester was weighed out with 0.1 wt% LP, mixed in a coffee grinder, and hand fed into the extruder with screw speed 100 rpm. Samples were then cut up and flushed through the Haake extruder at 150 °C, 100 rpm screw speed into the cylinder of the injection molder at 150 °C, and injected into an ASTM type V dog bone at temperature 70 °C.

# 4.2.4 Mechanical and Thermal Properties

Tensile testing was done on a Shimadzu AGS-X tensile tester where the type V dog bones were pulled at a rate of 10 mm/min. Samples were aged for 1 day prior to testing, and another sample was tested on day 8. Thermal properties, including enthalpy, glass transition temperature, melting temperature, and cold crystallization were collected using a TA instruments Discovery 250 differential scanning calorimeter. Samples were taken from the side of the tensile bar measuring between 4-7 mg. of material, and aluminum reference pans were used. Samples were equilibrated at room temperature, 23 °C, heated to 180 °C at a rate of 10 °C/min, cooled at 10 °C/min to -80 °C to observe glass transition temperature. Lastly, samples were heated once again to 200 °C and cooled to 0 °C to observe any nucleation above that temperature.

# 4.2.5 Soxhlet Extraction for Cell Debris

Soxhlet extraction was done for both PHA samples in which 1 g. of material was weighed into a cellulose thimble and refluxed with chloroform in a Soxhlet condenser for 24 hours. The resulting thimble was dried in a vacuum oven to remove any moisture, and a new mass measurement was obtained. Any mass leftover that did not dissolve into the chloroform is attributed to remaining cell debris. For PHA6, the value was around 1% cell debris, and for PHA8, the value was about 3% cell debris. This amount of cell debris should not affect the thermal and mechanical properties of the two PHAs and can be ruled out as interacting with any additives.

#### 4.3 Results and Discussion:

#### 4.3.1 Mold Temperature Study

As with most extrusion and injection molding projects, an optimal mold temperature should be determined before collecting data. Mold temperature can greatly influence the

crystallization of the polymer and thus dramatically affect the mechanical data. Therefore, a small-scale trial is done to determine if 40 °C of 70 °C mold temperature yields samples with higher strain at break. These two temperatures are used due to previous PHA studies in the Locklin lab.

Table 4.2. The results on different mold temperatures on strain at break.

Polymer Blend	40 °C	70 °C
	Mold	Mold
PHA6 control	16%	27%
10% (25% sebacic, 75% glutaric, 1:1 BDO-PDO)	88%	229%
10% (25% azelaic, 25% sebacic, 50% glutaric, BDO)	49%	145%
10% (25% succinic, 25% glutaric, 25% azelaic, 25% sebacic, BDO)	96%	250%

Consistently across the board, the 70 °C mold temperature yields samples with higher strain at break. Therefore, this temperature is used throughout the study.

# 4.3.2 Additives to PHA6

Initially, a small-scale Haake extrusion and injection molding trial was done to assess how these polyesters and copolyesters act as additives to PHA6 when blended in a 10% loading. The better performing polyesters were then chosen to scale up using the Process 11 in the next step of this project.

Table 4.3. The results from a small-scale extrusion study testing various polyester additives.

Polymer in PHA6	70C mold (2 bars)
PHA6 control	38.5% 0.83 GPa
10% (25% sebacic, 75% glutaric 1,3-PDO), 90% PHA6	201% 0.56 GPa
10% (adipic, 1,4-BDO) 90% PHA6	155% 0.71 GPa
10% (azelaic, 1,4-BDO) 90% PHA6	104% 0.70 GPa
10% (azelaic, 1,3-BDO) 90% PHA6	146% 0.66 GPa
10% (sebacic, 1,4-BDO), 90% PHA6	98% 0.74 GPa
10% (25% azelaic, 25% sebacic, 50% glutaric, 1,4-BDO) PHA6	145% 0.66 GPa
10% (25% sebacic, 75% glutaric, 1:1 BDO:PDO) 90% PHA6	229% 0.63 GPa
10% (50% azelaic, 50% glutaric, 1,4-BDO) 90% PHA6	199% 0.59 GPa
10% (50% azelaic, 50% glutaric, 1,4-BDO) 90% PHA6	178% 0.68 GPa
10% (25% sebacic, 75% glutaric, 1,3-PDO) 90% PHA6	201% 0.56 GPa
10% (adipic, 1,3-BDO), 90% PHA6	133% 0.66 GPa
10% (25% succinic, 25% glutaric, 25% azelaic, 25% sebacic, 1,4-	250% 0.71 GPa
BDO) 90% PHA6	

As demonstrated in the above results, there are several candidates that push the strain at break above 200%, and these are further explored in a Process 11 scale up with the 6 polyesters shown in table 4.1.

# 4.3.3 Process 11 Scale Up

Polyester A, whose composition is 0.25 mol eq. succinic acid, 0.25 mol eq. glutaric acid, 0.25 mol eq. azelaic acid, 0.25 mol eq. sebacic acid, 1.05 mol eq. 1,4-butanediol, with molecular weight of 120 kDa, was evaluated as an additive to PHA6 to increase flexibility.

Figure 4.3. Monomer components of "polyester A."

Polyester A was first explored using 10, 20, and 30 wt% loadings to determine optimal loading.

Table 4.4. Tensile testing results of 10, 20, and 30% polyester A loading into PHA6.

Loading	Strain at Break	Improvement
PHA6-Neat	38.5%	-
5% polyester A	45.4%	-
10% polyester A	220%	5.7 X

20% polyester A	97.0%	2.5 X
30% polyester A	42.1%	-

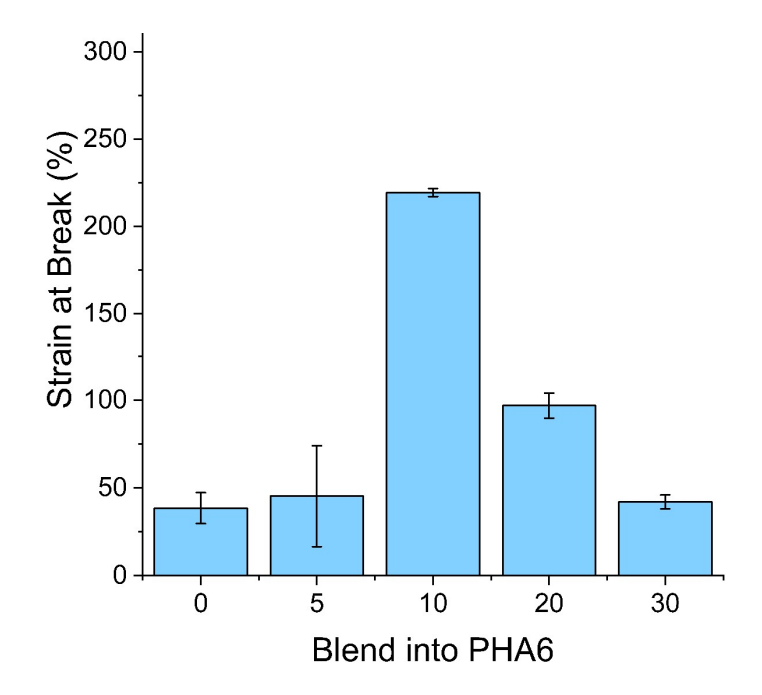


Figure 4.4. Exploring different loadings of polyester A in PHA6.

As seen in the above data, polyester A gives a significant improvement to the strain at break of PHA6 when blended in a 10% abundance, boasting a nearly 6 times increase. The effect severely drops off above the 10% loading. With this data in mind, a new experiment is conducted in which the optimal 10% loading of polyester A in PHA6 is extruded this time in the presence of 0.1 wt% LP to evaluate the effect of reactive extrusion on this blend.

Table 4.5. Tensile testing of blending vs. reactive extrusion of polyester A in PHA6.

Sample	Strain at Break	Improvement
PHA6 Neat	38.5%	-
PHA6 REX	63.4%	1.6 X
10% A Blend	220%	5.7 X
10% A REX	303%	7.9 X

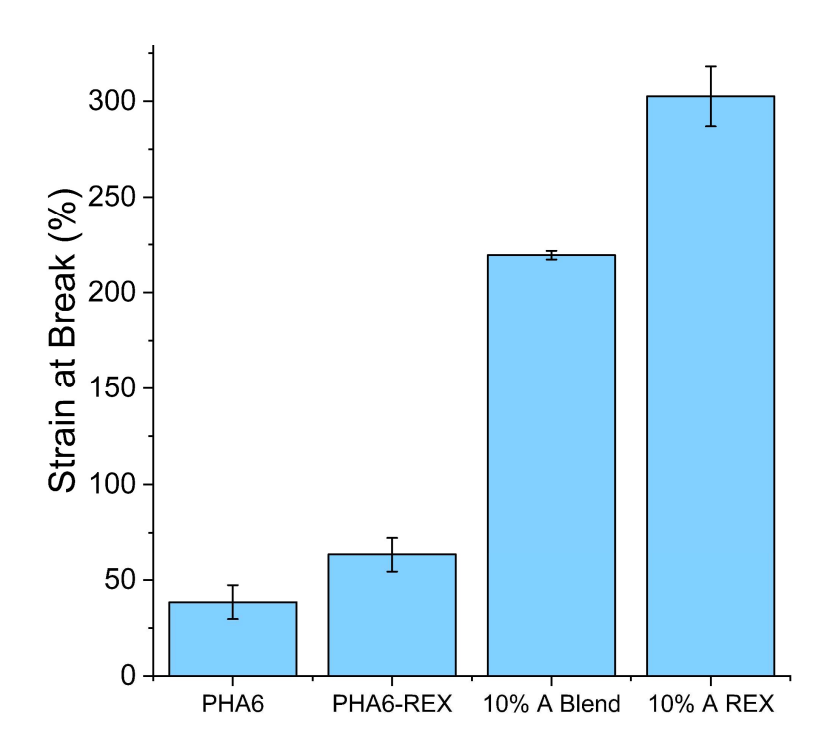


Figure 4.6. Strain at break for polyester A blending and reactive extrusion in PHA6.

The above results indicate an even further improvement to the strain at break when polyester A is incorporated with PHA6 in the presence of the tert-butyl peroxybenzoate. The strain at break of this material is 8 times higher than the PHA6 control sample.

Additionally, the semi-crystalline polyesters B and C, polybutylene sebacate and polyoctylene sebacate respectively, were incorporated into PHA6 by both blending and reactive extrusion.  $T_m \colon 67 \, ^{\circ}C$ 

Figure 4.7. Structural components of polyesters B and C.

The results of blending and reactive extrusion of 10 wt% polyester B and C into PHA6 are shown in the table and bar graph below.

Table 4.6. Tensile results of blending and reactive extrusion of polyester B in PHA6.

Sample	Strain at Break	Improvement
PHA6 Neat	38.5%	-
PHA REX	63.4%	1.6 X
10% B	26.9%	-
10% C	28.6%	-
10% B REX	48.9%	1.3 X
10% C REX	107%	2.8 X

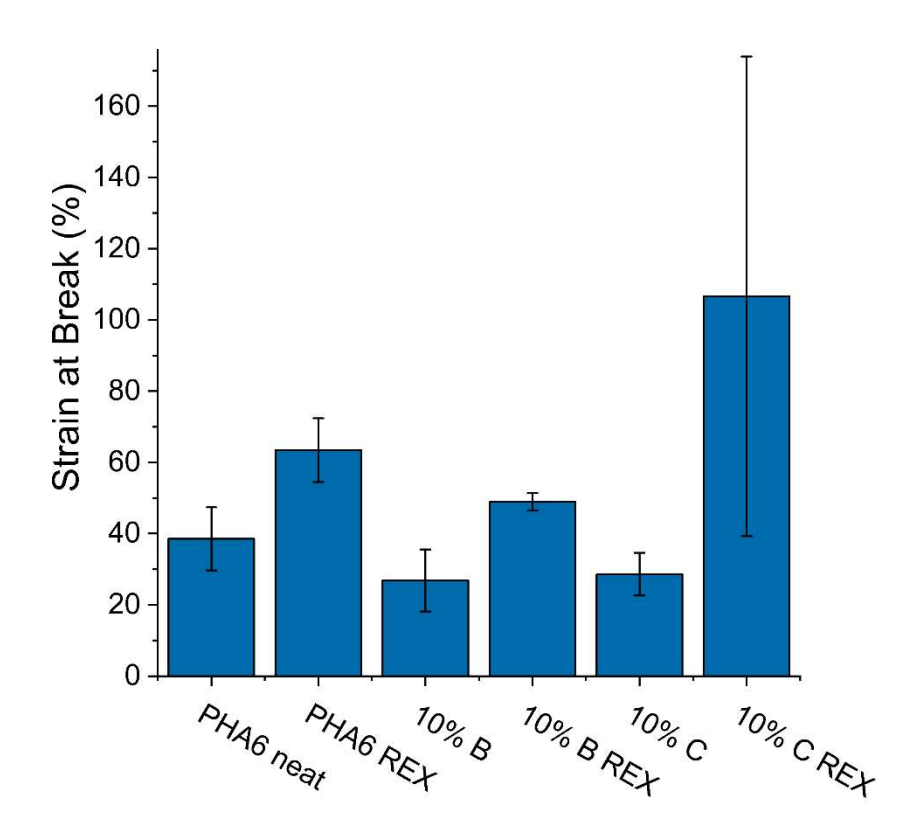


Figure 4.8. Tensile results of blending and reactive extrusion of polyester B in PHA6.

The above data shows that semi-crystalline polyesters B and C have minimal-to-no improvement to the strain at break of PHA6. This may be due to the higher melting point of these polyesters as compared to the copolyester A. Copolyester A has a melting point very close to room temperature, so it may be in the melt during tensile testing, leading to very flexible properties. In chapter 2, copolyester A was tensile tested to assess its properties, and it had over 1,000% strain at break at room temperature. Polyesters B and C have melting temperatures of 67 °C and 71 °C respectively, and therefore are not in the melt at room temperature the same way that polyester A is. Both polyester B and C have very low strain at break when tested on their own, with only 5-7% strain at break for both of them. With this information in mind, it is no surprise that polyester B and C do not drastically improve the strain at break of PHA6 went

blended and reactively extruded in. It is almost surprising that there is not a more drastic decrease in flexibility to the PHA samples.

Next, the low melting polymer D, and amorphous polyesters E and F are assessed as additives to PHA6.

Figure 4.9. The structural components of polyesters D, E, and F.

The results of blending D, E, and F into PHA6 at 10 wt% loading are shown below.

Table 4.7. Tensile results of blending polyester D, E, and F in PHA6.

Sample	Strain at Break	Improvement
PHA6 Neat	38.5%	-
10% D	110%	2.9 X
10% E	124%	3.2 X
10% F	138%	3.6 X

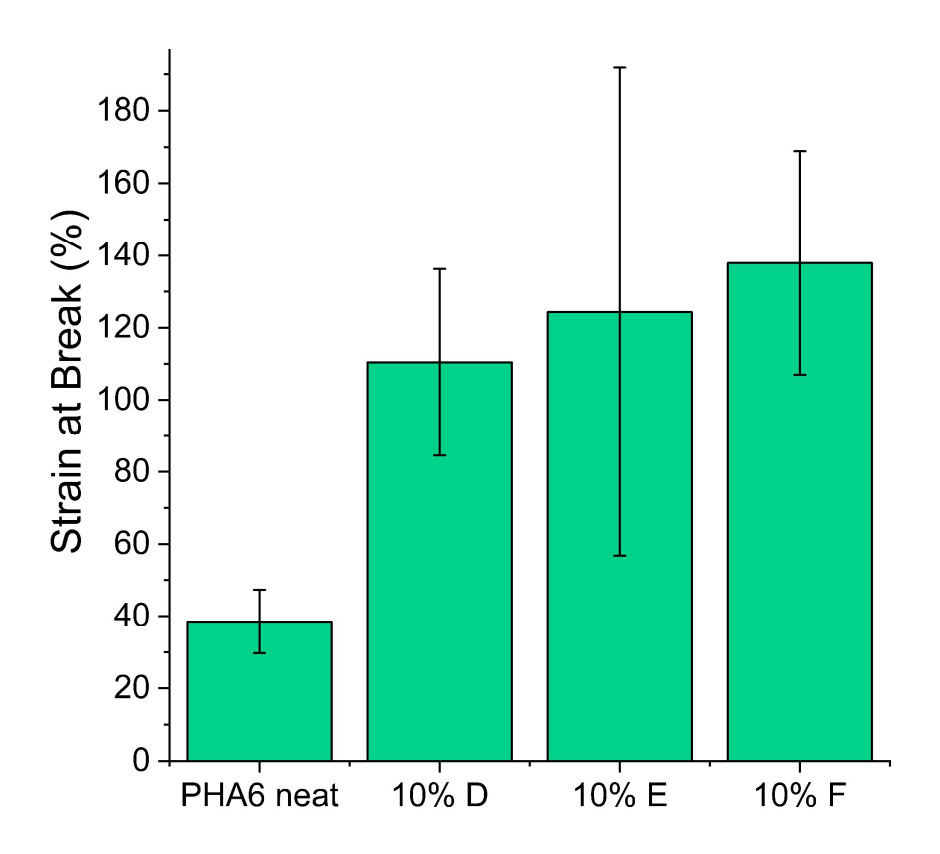


Figure 4.10. Tensile results of blending polyester D, E, and F in PHA6.

The results of blending the low melting and amorphous polyesters into PHA6 show moderate improvement to the strain at break with around 3 to 3.6 times increase. The standard deviation of these three polymer blends is a bit higher than other polymer blends, potentially due to difficulties in mixing. Since these polymers are either molten or completely amorphous at room temperature, they are very sticky, difficult to weigh out, and difficult to mix in the coffee grinder. Once the polymer is completely coated in the PHA powder, it is easier to work with, however it may be less cohesively mixed as compared to polymers that are easier to cut and mix at room temperature.

# 4.3.4 Aging

The polymer blends into PHA6 were assessed for aging (secondary crystallization). This is tested with both tensile testing and DSC to compare the percent crystallinity overtime. As seen in the figure below, the strain at break of PHA6 on day 1 post injection molding is displayed on

the left in blue, and the strain at break of PHA6 on day 8 is displayed on the left in green. This is contrasted on the right with 10% polyester A in PHA6 in the presence of 0.1 wt% LP, day 1 in blue and day 8 in green. In both samples, there is a 30% decrease in the strain at break on day 8 as compared to day 1 post extrusion. Although the addition of polyester A does not prevent aging in the way that was hoped, it should be noted that the strain at break on day 8 after aging is still much higher than the strain at break of PHA6 control on day 1. More research needs to be done in order to find ways to mitigate secondary crystallization and thus mitigate aging of PHA.

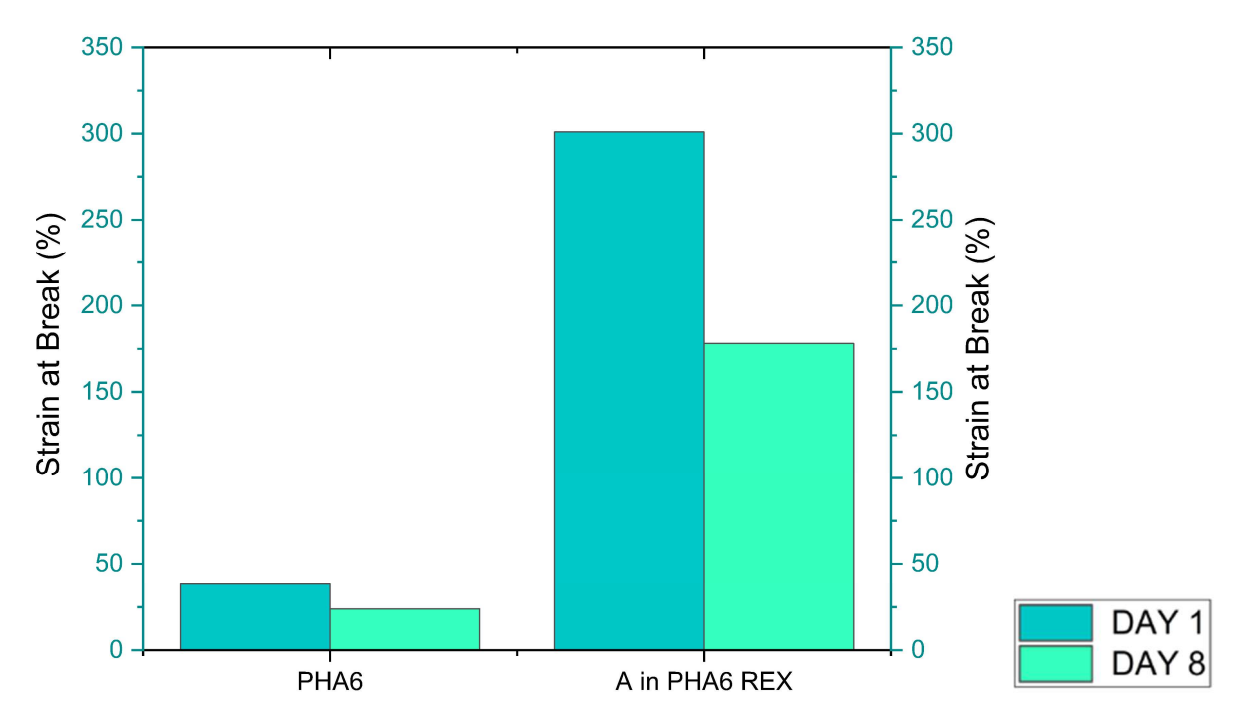


Figure 4.11. The aging of PHA6 compared to the aging of 10% A in PHA6 REX.

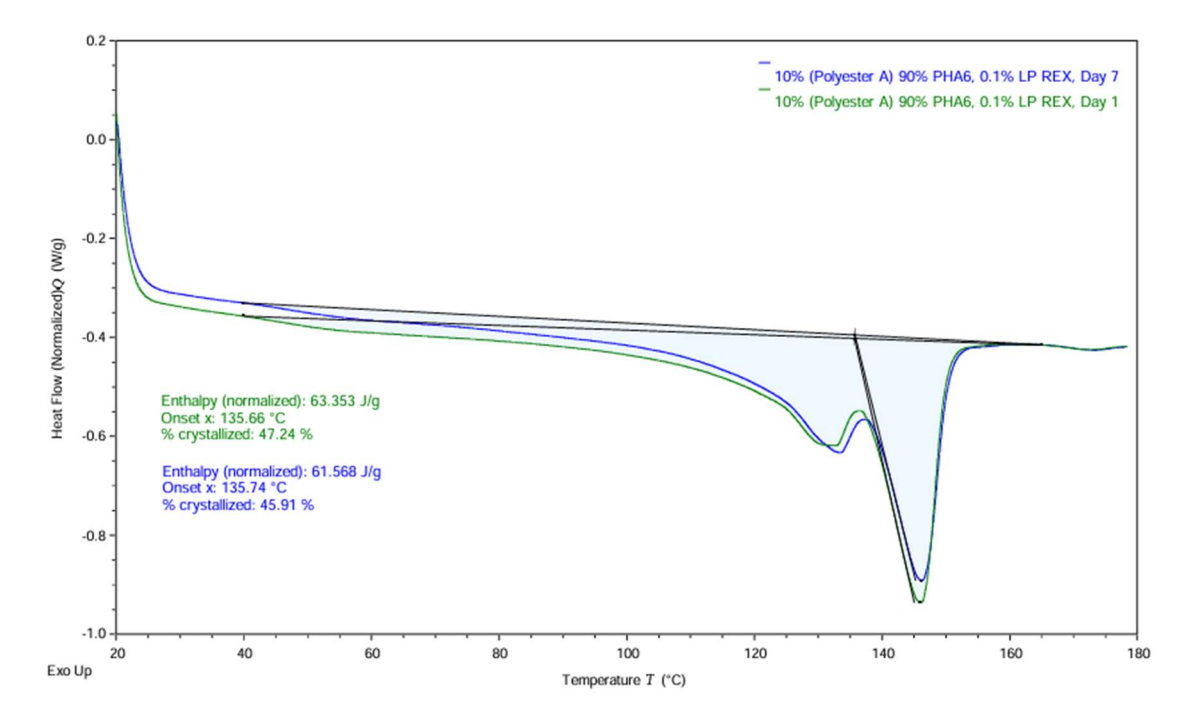


Figure 4.12. DSC thermograms for 10% polyester A in PHA6 on day 1 (blue) and day 4 (green). Interestingly, there is a reduction in crystallinity after aging, while typically there is an increase in crystallinity. This suggests that the addition of polyester A and LP slows down secondary crystallization.

# 4.3.5 Additives to PHA8

Similarly, as the above dataset, polyesters A, B, D, E, and F are tested as additives to PHA8 with the goal of improving strain at break and/or mitigating the effects of secondary crystallization. As before, these extrusions are done by using the Process 11 set to 150 °C and screw speed of 100 rpm to extrude the samples which are then cut and flushed through the Haake and injection molded with the MiniJet injection molder into a mold at temperature 70 °C. Firstly, the table below shows the effects of blending and reactively extruding polyesters A and B into PHA8.

Table 4.8. Tensile data from blending and reactive extrusion of polyesters A and B in PHA8.

Sample	Strain at Break	Improvement
PHA8 Neat	130%	-
PHA8 REX	231%	1.8 X
10% A	256%	2.0 X
10% B	49%	-
10% A REX	266%	2.0 X
10% B REX	82%	-

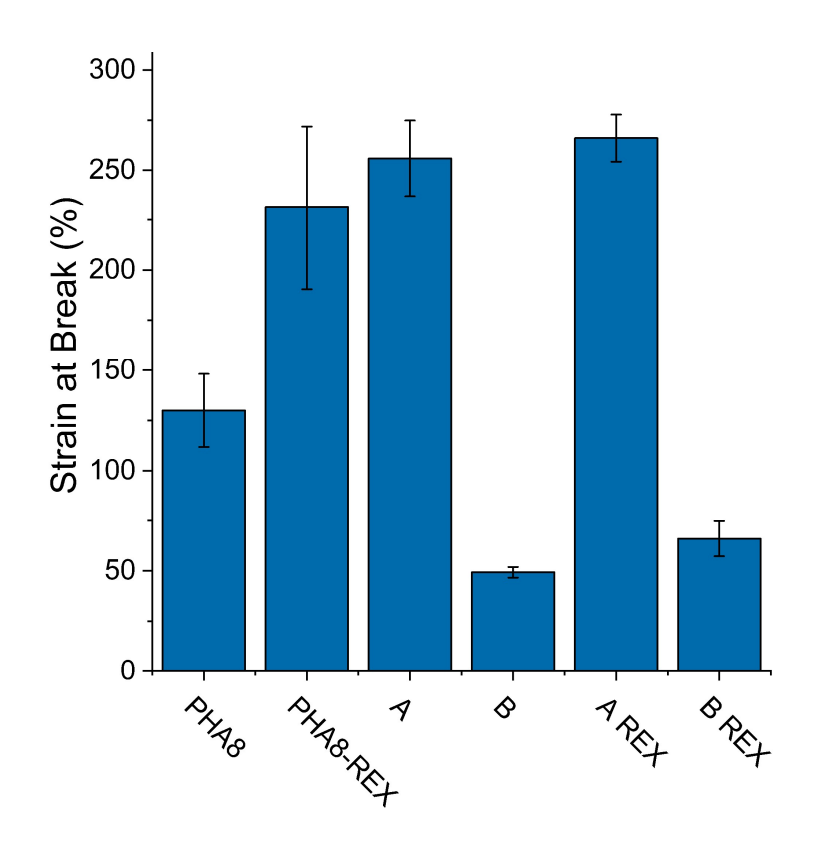


Figure 4.13. Tensile data from blending and reactive extrusion of polyesters A and B in PHA8.

The data above shows that polyester B decreases the strain at break of the PHA8, causing the sample to become brittle, and this is seen both with blending and reactive extrusion with polyester B. On the other hand, polyester A blending and REX yield a strain at break that is twice as high as the PHA8 control. It is noted that this effect is only slightly higher than the results of PHA8 and LP with no polyester A. It is beneficial to increase the strain at break without radical initiator because restrictions could be placed on tert-butyl peroxybenzoate due to its potential toxicity to humans. Therefore, samples formed with Luperox P need to be used in applications that would not put human health at risk.

Next, several loadings of the fully amorphous polyester E are evaluated in PHA8 to discover the optimal loading. 5, 10, 20, and 30 wt% are evaluated for strain at break.

Table 4.9 Tensile results of 10, 20, and 30 wt% loadings of polyester E in PHA8.

Loading	Strain at Break	Improvement
PHA8 Neat	130%	-
5% polyester E	206%	1.6 X
10% polyester E	294%	2.3 X
20% polyester E	165%	1.3 X
30% polyester E	85.2%	-

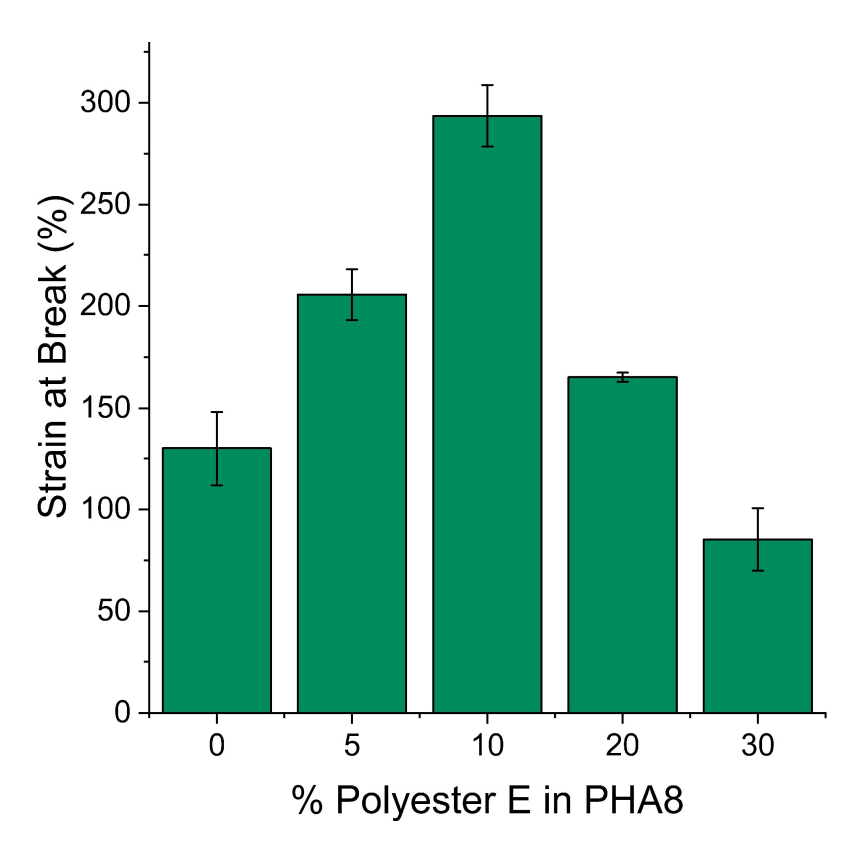


Figure 4.14. Exploring different loadings of polyester E in PHA8.

As with the earlier study with polyester A in PHA6, these results indicate that 10% polyester E is the optimal loading, leading to 2.3 times increase in the strain at break.

With this information in mind, polyesters D, E, and F are blended into PHA8 in 10% loading to evaluate the impact to the strain at break.

Table 4.10 Blending of D, E, and F in PHA8 at 10% loading.

Sample	Strain at Break	Improvement
PHA8 Neat	130%	-
10% D	285%	2.2 X
10% E	294%	2.3 X



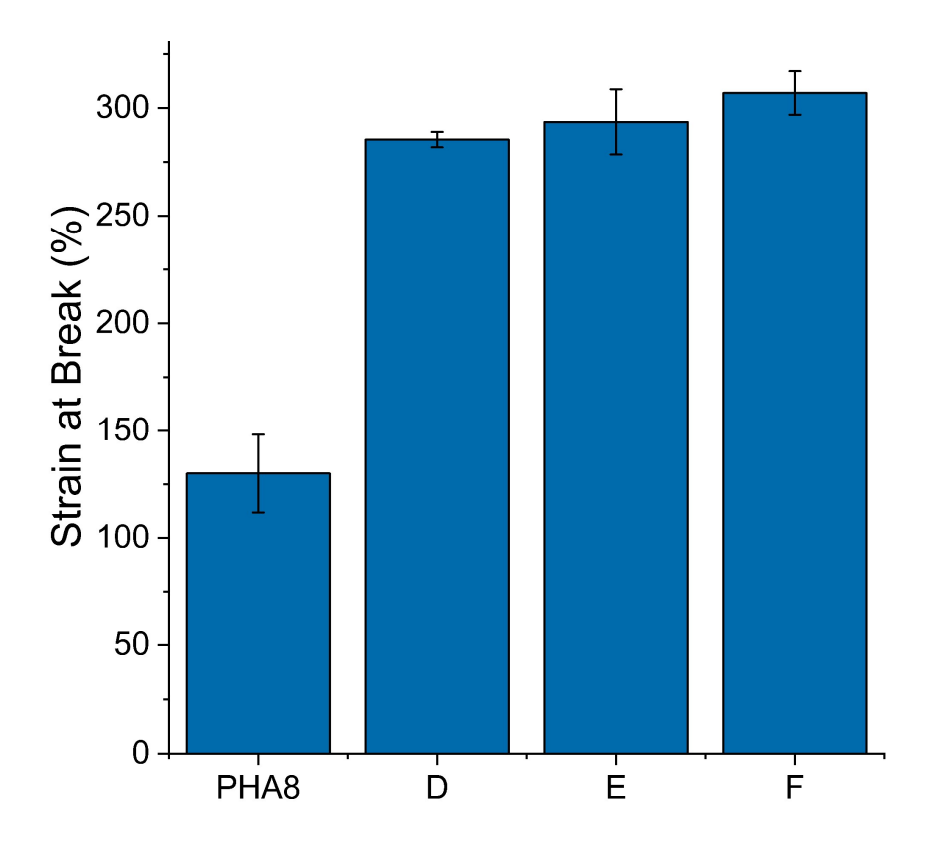


Figure 4.15 Blending of D, E, and F in PHA8 at 10% loading.

As seen in the above data, polymers D, E, and F all increase the strain at break of PHA8 in a similar manner. All increase the strain at break around 2.2-2.4 times the control value.

# 4.3.6 Aging of PHA8

The extent of secondary crystallization is evaluated by tensile testing to determine if the polyester additives decrease the aging effect of PHA8. In the bar graph below, the strain at break of PHA8 on day 1 post injection molding is displayed on the left in blue, and the strain at break of PHA8 on day 8 is displayed on the left in green. In the middle of the graph is PHA8 with 10% polyester E, with day 1 in blue and day 8 in green. On the right is 10% polyester A blended in PHA8—day 1 shown in blue and day 8 in green.

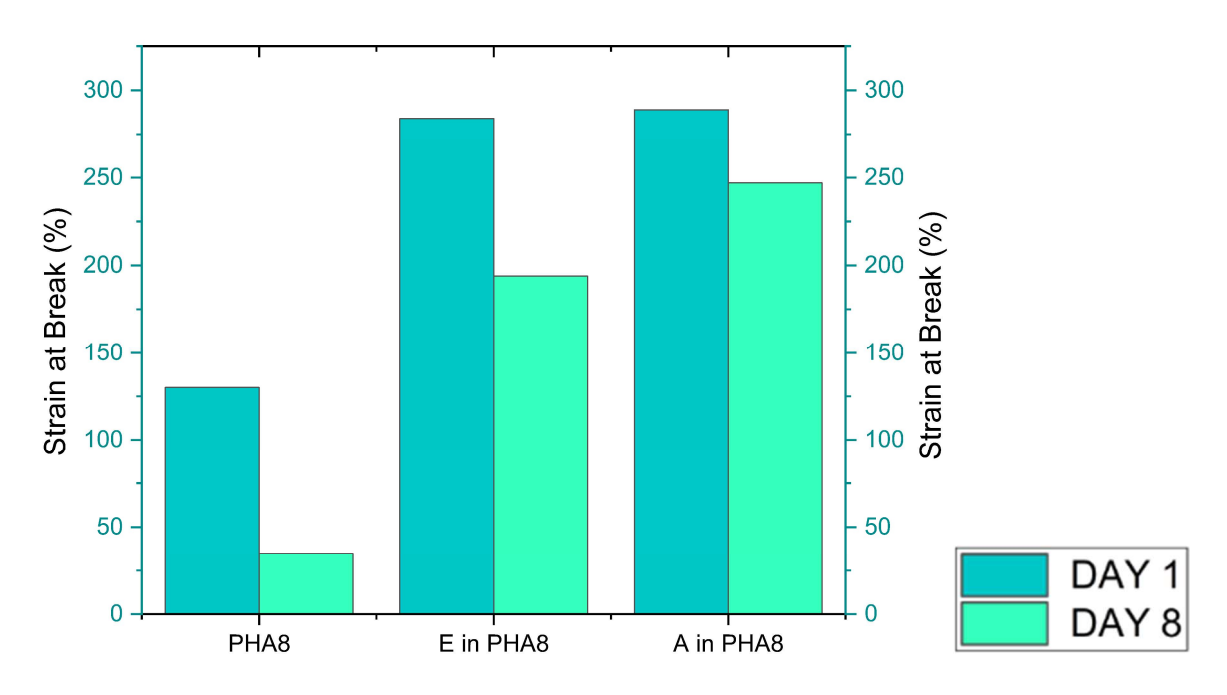


Figure 4.16. Aging data of 10% E and 10% A in PHA8 as compared to the control PHA8.

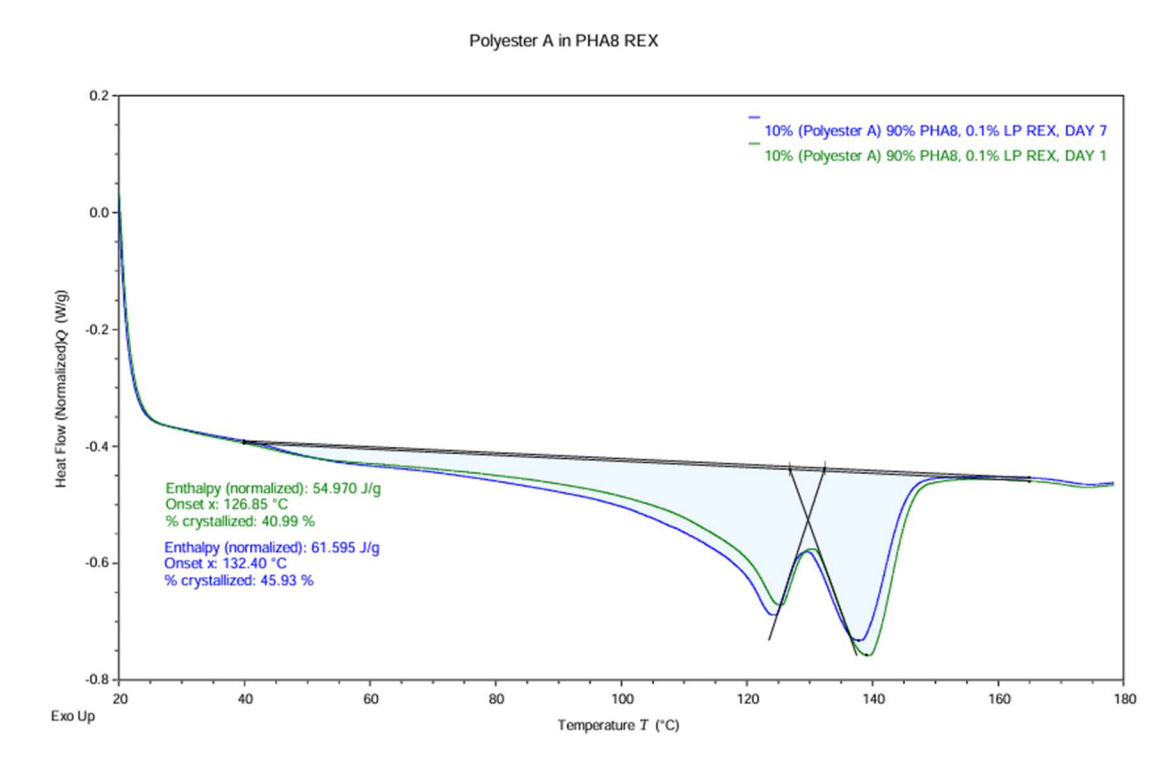


Figure 4.17. DSC thermograms of 10% polyester A in PHA8 REX on day 1 (green) and day 7 (blue).

The percent crystallinity calculated from the integration of the enthalpy peak increases by 5% from day 1 to day 7. It seems that there is an increase in the integration of lower melting species, and a decrease in the higher melting species for the aged sample. This is interesting because the mechanical data showed little aging for this sample, yet the DSC shows a large amount of increase in crystallinity.

When blending polymers, it is important to consider if two polymers will be miscible or not. Usually, two amorphous polymers will be more miscible than an amorphous and a semi-crystalline.<sup>5</sup> Miscibility can be determined by measuring the glass transition temperature, and the distribution of two immiscible polymers could be visualized with SEM.<sup>8</sup> When a polymer is blended into another polymer, they can individually crystallize, creating white streaks in the dog bone shape.

In this chapter, the polyesters that were synthesized in chapter 2 are explored as additives for the two PHA batches used in chapter 1. Although the initial motivation to synthesize the polyesters was to understand structure property relationships, curiosity led to blending these into PHA. These polyesters could be useful as additives if they can increase the strain at break or decreasing aging (ideally both).

#### 4.3.7 Discussion

Overall, amorphous polyesters tend to improve PHA8 much more than they improved PHA6 when blended and reactively extruded in 10% abundance. The low melting and fully amorphous polyesters (D, E, and F) improve the elongation at break more than the semi-crystalline polyesters (A and B) for PHA8 and hovered around a 100% improvement to the strain at break. A marked reduction in aging is seen with the amorphous polyesters, with only a 15%

reduction in strain at break over 1 week as compared to PHA8 control which loses 70% of its elongation at break in the same timeframe.

The opposite trend is observed with PHA6 extruded samples. The near room temperature-melting polyester A improved the elongation at break by over 600% compared to the control when blended. The strain at break further improved to over 700% increase when polyester A was introduced to PHA6 in the presence of 0.1 wt% radical initiator. Contrasting the remarkable improvement of tensile properties due to the addition of polyester A, the low melting and amorphous polyesters (D, E, and F) provide moderate improvement of 100-200%. In addition to a smaller factor of improvement, a larger standard deviation was also noted. This is potentially due to uneven mixing because of the sticky nature of the amorphous polyesters, or there may be a more complicated reason. The same amorphous polyesters yield tight data when incorporated into PHA8, indicating, this is not simply a mixing issue.

To generalize these trends: PHA8 has a higher amount of C6 in the backbone, making it a more amorphous polymer. PHA6 has a lower amount of C6 in the backbone, so it has less interruptions in the crystalline lamella, leading to higher crystallinity and smaller amorphous regions. Therefore, blending an amorphous polyester into PHA6 could be less compatible than blending it into PHA8. The amorphous polyesters could be more compatible with the more amorphous PHA of the two used in this study. It is to be noted that none of the polyesters synthesized and blended are "miscible" with the PHA, since there was no shift in Tg for the PHA. Therefore, the blended polyester and PHA have immiscible domains in both PHA6 and PHA8.

#### 4.4 Conclusions and Future Directions:

The goal of this project was to improve the mechanical properties of polyhydroxyalkanoates by incorporating several biobased polyesters via blending and reactive extrusion. Two PHB-HHx copolymers were used: PHA6 and PHA8, which have 6 and 8% hexanoate respectively. The highest improvement in the strain at break resulted from blending a biobased copolymer into PHA6 at a 10% loading in the presence of 0.1 wt% radical initiator, yielding a 700% increase in the strain at break. Another notable improvement occurred when an amorphous polyester was blended into PHA8 in a 10% abundance, leading to a strain at break that was twice as high as the control. This polymer additive also resulted in a large reduction in the aging of PHA8. More work needs to be done to determine exactly why certain polymers acted as better additives than others.

#### 4.4.1 Future Directions

In the case of PHA6, its properties were drastically improved when polyester A was incorporated during extrusion. This may be because polyester A has a melting temperature just above room temperature and could be partially in the melt during tensile testing. However, in the previous chapter when several biobased polyesters were assessed for tensile strength, a different polyester with very similar melting temperature to polyester A, displayed a strain at break that was half as long (500% as opposed to 1000% for polyester A). This could mean that the interaction between polyester A and PHA6 is more complicated than simply its melting temperature.

Since the Tg of the PHA in the PHA-polyester blends did not change from the value of 0 °C, the polymers are immiscible.<sup>8</sup> Although they are immiscible, there is still significant improvement to the tensile properties by including these polyester additives. This phenomenon

could be explored using DSA. DSA is a method to determine surface energy and can help quantify the energy between the two interfaces of the polymers. If the surface energy at the interfacial boundary is lower is some blends than others, this could help explain why some blends exhibit better properties than others.

In addition to surface energy studies, scanning electron microscopy should be done to understand the distribution of the additive into the polymer. This could shed light on if the polyester additives are equally distributed during the extrusion and injection molding, the size of the pockets of additive, and the regularity of the interfacial boundary. This information could be used to understand why some additives produce much better results than others.

Finally, more biobased copolyesters should be assessed as additives to PHAs. Other additives such as branching agents, nucleating agents, or plasticizers could be incorporated as well to push the boundaries of this research.

#### 4.5 References

- (1) Tang, H. J.; Neoh, S. Z.; Sudesh, K. A review on poly(3-hydroxybutyrate-co-3-hydroxyhexanoate) [P(3HB-co-3HHx)] and genetic modifications that affect its production. *Frontiers in Bioengineering and Biotechnology* **2022 Dec 5**, *10*. DOI: 10.3389/fbioe.2022.1057067.
- (2) VUN, R.; SV, R.; MV, R.; YC, C. Review of the Developments of Bacterial Medium-Chain-Length Polyhydroxyalkanoates (mcl-PHAs) PubMed. *Bioengineering (Basel, Switzerland)* **05/21/2022**, *9* (5). DOI: 10.3390/bioengineering9050225.
- (3) Agarwal, S.; Speyerer, C. Degradable blends of semi-crystalline and amorphous branched poly(caprolactone): Effect of microstructure on blend properties. *Polymer* **2010/03/02**, *51* (5). DOI: 10.1016/j.polymer.2010.01.020.
- (4) Mississippi, U. o. S. *Miscible Polymer Blends*. 2005. <a href="https://www.pslc.ws/mactest/blend.htm">https://www.pslc.ws/mactest/blend.htm</a> (accessed 2025.
- (5) Shanks, R. A.; Li, J.; Yu, L. Miscibility and Co-Continuous Morphology of Polypropylene-Polyethylene Blends. *Imaging and Image Analysis Applications for Plastics* **1999/01/01**. DOI: 10.1016/B978-188420781-5.50009-7.
- (6) Zhuang, H.; Pearce, E. M.; Kwei, T. K. Self-association in poly(styrene-co-4-vinylbenzenephosphonic acid) and miscibility of its blends. *Polymer* **1995/01/01**, *36* (11). DOI: 10.1016/0032-3861(95)95302-H.
- (7) Ziska, J. J.; Barlow, J. W.; Paul, D. R. Miscibility in PVC-polyester blends. *Polymer*1981/07/01, 22 (7). DOI: 10.1016/0032-3861(81)90268-8.

- (8) Tu, W.; Wang, Y.; Li, X.; Zhang, P.; Tian, Y.; Jin, S.; Wang, L.-M.; Tu, W.; Wang, Y.; Li, X.; et al. Unveiling the Dependence of Glass Transitions on Mixing Thermodynamics in Miscible Systems. *Scientific Reports 2015 5:1* **2015-02-17**, *5* (1). DOI: 10.1038/srep08500.
- (9) Fisher, T. <a href="https://www.thermofisher.com/order/catalog/product/567-7600">https://www.thermofisher.com/order/catalog/product/567-7600</a> (accessed.
- (10) Kelly, C. A.; Fitzgerald, A. V. L.; Jenkins, M. J. Control of the secondary crystallisation process in poly(hydroxybutyrate-co-hydroxyvalerate) through the incorporation of poly(ethylene glycol). *Polymer Degradation and Stability* **2018/02/01**, *148*. DOI: 10.1016/j.polymdegradstab.2018.01.003.

#### **CHAPTER 5**

#### CONCLUSIONS AND FUTURE DIRECTIONS

#### **5.1 Conclusions**

In this thesis, blending and reactive extrusion of poly(3-hydroxybutyrate-co-3-hydroxyhexanoate) with various additives including radical peroxide initiators and aliphatic polyesters such as polylactide and novel copolyesters was done to assess the impact on the tensile properties. Strain at break was the main mechanical property evaluated; however, Young's modulus and impact strength was explored in some cases. Differential scanning calorimetry was used to determine thermal characteristics and polymer crystallinity. Secondary crystallization, also known as aging, was decreased by the inclusion of additives that hindered the crystallization of amorphous regions overtime. In the best result, aging was reduced by 80% when copolyester A was extruded into PHA8 at a 10% loading, as compared to the control PHA8. Strain at break was increased by 700% in the case of 10% copolyester A reactively extruded into PHA6 in the presence of 0.1 wt% radical peroxide initiator. A novel analytical method was developed to quantify excess peroxide after REX by using gas chromatography.

The goal of this project was to gain more insight into biobased and biodegradable polyesters to push the boundaries of their mechanical properties. Although PHA, PLA, and the novel copolyesters synthesized can all be produced from renewable sources, there are still many drawbacks including cost, slow crystallization, limited applications, poor mechanical properties, and aging. This thesis aimed to push the field forward by focusing on improving the poor

mechanical properties and minimizing the aging by using polyester additives and peroxide initiator.

The limitations of this project include reactive extrusion having many variables that increase the difficulty of producing tight standard deviations. Small scale extrusion done in an academic lab setting rarely translates to an industrial setting without new optimization. Costs and nucleation were issues that were not addressed in this thesis.

#### **5.2 Future Directions**

This thesis provides a platform for more research to build upon. New copolyesters can be synthesized with branching agents and other additives during the polymerization step to further improve the strain at break that was reported here. Different radical peroxide initiators could be explored to optimize the reactive extrusion step as well as different temperature and screw profiles on the extruder should be optimized. Scanning electron microscopy studies should be done to visualize distribution of immiscible polymers after extrusion to confirm or deny the hypothesis posed in chapter 2 that the pre-compatibilization step stabilizes the interfacial boundary between PHA and PLA. Surface energy studies could be done to assess the energy difference at the interphase between two immiscible polymers to potentially explain why certain immiscible blends possess better properties than others.

#### 5.3 Final Remarks

More work needs to be done in the field of biobased polymers to make them more attractive as alternatives to petroleum-based plastics. After weighing the pros and cons of these types of materials, capitalizing on the fact that they do not produce microplastics is one of their best qualities, and this fact should be advertised more in the future. Microplastics affect all people as it is extremely difficult to remove them from the ecosystem, so I believe that this

impact is the factor that will continue to push this field forward. With more research and break throughs, biobased and renewable polymers could become a viable alternative to some petroleum-based polymers, but likely not all petroleum-based polymers.